AUS DEM LEHRSTUHL
FÜR ORTHOPÄDIE
PROF. DR. J. GRIFKA
DER FAKULTÄT FÜR MEDIZIN
DER UNIVERSITÄT REGENSBURG

**ELUCIDATING THE INFLUENCE OF SENSORY NEUROPEPTIDES
ON INHERENT METABOLIC BEHAVIOR OF MURINE MACROPHAGES
UNDER MECHANICAL LOADING**

Inaugural – Dissertation
zur Erlangung des Doktorgrades
der Medizin

der
Fakultät für Medizin
der Universität Regensburg

vorgelegt von
Anna-Sophie Beiderbeck

2022

AUS DEM LEHRSTUHL
FÜR ORTHOPÄDIE
PROF. DR. J. GRIFKA
DER FAKULTÄT FÜR MEDIZIN
DER UNIVERSITÄT REGENSBURG

ELUCIDATING THE INFLUENCE OF SENSORY NEUROPEPTIDES ON INHERENT METABOLIC BEHAVIOR OF MURINE MACROPHAGES UNDER MECHANICAL LOADING

Inaugural – Dissertation
zur Erlangung des Doktorgrades
der Medizin

der
Fakultät für Medizin
der Universität Regensburg

vorgelegt von
Anna-Sophie Beiderbeck

2022

Dekan: Prof. Dr. Dirk Hellwig

1. Berichterstatter: Prof. Dr. Susanne Grässel

2. Berichterstatter: PD Dr. Agnes Schröder

Tag der mündlichen Prüfung: 18.10.2022

Structure

Zusammenfassung

Als Vorläuferzellen von Osteoklasten spielen Makrophagen während der Osteogenese eine wichtige Rolle. Bei Patienten mit Osteoarthrose (OA) ist der balancierte Prozess aus Knochenaufbau, -umbau und -abbau im betroffenen Gelenk gestört. Mechanorezeption von Zellen ist unabdingbar für Wachstumsprozesse und den Gelenkaufbau, während pathologischer mechanischer Stress Entzündungen und Krankheiten wie OA verursachen kann. Die sensiblen Neuropeptide Substanz P (SP) und α-calcitonin gene-related peptide (αCGRP), die eine hohe Spezifität für den Neurokinin-1 Rezeptor (NK1R) beziehungsweise den calcitonin receptor-like receptor (CRLR)/ receptor activity-modifying protein (RAMP) 1 aufweisen, sind an der Physiologie der Gelenke sowie an mit Arthrose assoziierten, degenerativen Vorgängen beteiligt und regulieren die Osteoklastogenese. SP und NK1R als Teil des Tachykinin-Systems wurden in anderen Zellen, z.B. Tenozyten, bereits als mechanoresponsiv beschrieben. Unter Beachtung dieser Mechanismen war das Thema dieser Arbeit, die Auswirkung der Kombination von mechanischer Belastung und der Stimulation mit Neuropeptiden auf das metabolische Verhalten von murinen Makrophagen zu untersuchen.

Makrophagen der murinen Zelllinie RAW 264.7 wurden zyklischer mechanischer Dehnung ausgesetzt. Die Genexpression der Neuropeptidrezeptoren wurde mittels RT-PCR-Analyse untersucht und die Proteinexpression der Neuropeptide per Western Blot und ELISA analysiert. Das metabolische Verhalten der Makrophagen wurde nach erfolgter mechanischer Belastung anhand von Apoptose, Proliferation und Adhäsion charakterisiert, sowohl mit als auch ohne Neuropeptidstimulation. Die Expression von Makrophagen-Polarisationsmarkern und Genen, assoziiert mit der Osteoklastogenese, wurden nach zyklischer mechanischer Dehnung untersucht. Die Stimulation mittels Neuropeptiden wurde an primären murinen Knochenmarksmakrophagen nach der chirurgischen Induktion von OA wiederholt.

Diese Studie zeigt die Beteiligung der Neuropeptide SP und αCGRP sowie deren Rezeptoren bei der Mechanotransduktion- und regulation von Makrophagen. Die Mechanoregulation über den αCGRP-CRLR/RAMP1-Komplex wurde damit zum ersten Mal nachgewiesen. Unsere Ergebnisse weisen zudem auf die Regulierung von RAMP1 unter mechanischem Stress hin. In Übereinstimmung mit den Ergebnissen

anderer Forschungsgruppen konnten wir eine autokrin vermittelte negative Feedbackschleife des SP/NK1R-Signalweges beobachten.

Des Weiteren zeigten Makrophagen, die mechanischer Belastung ausgesetzt waren, eine erhöhte Caspase 3/7-vermittelte Apoptose und eine reduzierte Adhäsion unter Stimulation mit αCGRP, was auf einen Schutzmechanismus gegenüber schädlichen Entzündungsprozessen in Form von erhöhter Apoptose und reduzierter Migration der Makrophagen hinweisen könnte. Die nach Belastung beobachtete M1-Polarisierung lässt Rückschlüsse auf eine proinflammatorische Aktivität mechanisch belasteter Makrophagen zu. Ob und auf welche Weise dies Makrophagen unter *in vivo*-Bedingungen betrifft, bleibt noch ungeklärt. Zusätzlich konnten wir nach mechanischer Belastung eine erhöhte Genexpression des RANK-Rezeptors beobachten, was die Vermutung nahelegt, dass mechanischer Stress das Osteoklastogenesepotenzial von Makrophagen erhöht.

Weiterführend scheint die experimentelle Induktion von OA die Mechanotransduktion von murinen Knochenmarksmakrophagen (KMM) zu beeinflussen, da wir in KMM acht Wochen nach chirurgischer Arthroseinduktion eine erhöhte Apoptoserate unter mechanischer Belastung im Vergleich zu KMM von Sham-operierten Mäusen nachweisen konnten. Daraus ergibt sich die These, dass OA eine veränderte zelluläre Biomechanik induzieren kann und somit Makrophagenpopulationen beeinflusst. Die zugrundeliegenden Mechanismen sind noch nicht bekannt. Zukünftige Studien könnten dazu beitragen, Regulationsprozesse der veränderten Zellreaktivität unter mechanischem Stress zu identifizieren und damit neue Behandlungsmöglichkeiten bei OA zu entwickeln. Insbesondere pathologische Signalwege der Mechanoregulation im Zusammenspiel mit der Neuropeptidsensitivität von Makrophagen könnten dabei von Bedeutung sein.

1 Introduction

1.1 Mechanosensing and mechanotransduction

In the process of mechanotransduction, mechanical stimuli are converted to electrical or biochemical signals. These stimuli can either be extrinsic (e.g. vibration, touch, pressure, tension, stretch or gravity) or of intrinsic origin (e.g. muscle contraction, body movement). Mechanoreceptors that can detect and process these signals are located on the cell membrane of skin cells, on cells of all organs and tissues. Mechanoreception is indispensable for sensation and regulation of biological processes.

1.1.1 Receptors and signaling pathways

To induce an effect on cells upon application of mechanical loading, mechanoreceptors need to be stimulated. These receptors detect mechanical stimuli (e.g. pressure or stretching), and in a process of mechanoreception and -transmission, transfer this information from the cell membrane directly to the cytoskeleton and the cell organelles [1]. Mechanoreception is not only limited to the binding kinetics between receptor and ligand, but also to the formation and dissociation velocity of the complex that control the frequency parameters of the sensed force. Chen et al. summarised six different modification types of the mechanosensitive domains in response to applied force: 1) deformation of the receptor protein, 2) relative displacement and consecutive channel opening or closure, 3) hinge movements such as in integrins, 4) unfolding or unmasking, 5) translocation and rotation and 6) rearrangement of clustered proteins [2]. By mechanotransduction, the mechanical signal is converted into a nervous impulse or translated into a biochemical or electrical potential, leading to a change in cell behavior [2–4]. This is provided via activation of ion channels sensitive to force or membrane proteins [5]. Various cellular proteins seem to be involved in mechanosensing and -transduction processes, for example cytoskeletal components, such as actin filaments and microtubuli, adaptor and scaffolding proteins, such as talin and vinculin, as well as kinases [2,3,5]. An important role in mechanical signaling pathways play calcium ions. In response to increasing intracellular levels, they bind to calmodulin, where upon calmodulin-dependent kinase II becomes active and regulates cell behavior such as proliferation, migration or apoptosis [6–8]. Apart from protein kinase C (PKC), which follows the same activation pathways as Ca^{2+} via G_q receptors, tyrosine kinases such as Src, mitogen-activated protein kinases (MAPK), c-Jun-N-

terminal kinases (JNK) and focal adhesion kinases (FAK) may contribute to signaling processes induced by the application of mechanical force [2,9]. Furthermore, mechanical cellular stimulation has been demonstrated to result in higher cyclic adenosine monophosphate (cAMP) and inositoltriphosphate (IP$_3$) levels, as well as nuclear factor-kappa-B (NF-κB) nuclear translocation [10,11]. Biomechanical loading and mechanosensing are important for physiological growth and maturation, whereas at pathological dosages inflammation and disease are more likely to occur [5,12–14]. This can be seen in bone metabolism, where loading is an important regulator of bone strength and turnover. Without mechanical stimulation, bone metabolism might be downregulated and result in osteoporosis and fragility fractures. An overload of mechanical stress could also facilitate degeneration, as seen in osteoarthritis (OA) [13–15].

1.1.2 Sensory nerve fibers and neuropeptides as mechanoreceptors

Mechanoreception in peripheral tissues is processed by sensory nerve fibers. A change in the membrane potential in response to physical stress causes a receptor potential and further encodes an action potential that is transferred to the central nervous system. Mammalian mechanoreceptors display a broad morphological complexity, ranging from unbranched nerve endings without any specialization to complex structures like Meissner and Pacinian corpuscles in the skin [16]. Peripheral nerve fibers are critically involved in bone metabolism, vascularization and matrix differentiation as during embryonic limb development, thereby fulfilling a decisive role in modulating musculoskeletal growth, repair and pathophysiology [17,18].

At a cellular level, mechanoreception is mediated via a deformation of the extracellular matrix or a mechanoresponsive system containing neuropeptides and their receptors. Of interest for this work are the two nociceptive neuropeptides associated with sensory nerves: substance P (SP), belonging to the tachykinin family, and alpha-calcitonin gene-related peptide (αCGRP). These neuropeptides are either released from peripheral nerve fibers or secreted by local tissue cells and regulate joint physiology [19]. Several studies indicate that sensory neuropeptides and their receptors allow various cell types to process biomechanical stimuli. Mechanosensing neurokinin-1 receptors (NK1R) that bind SP were detected on human chondrocytes by Millward-Sadler and colleagues [20]. Mechanical stimulation with 0.33 Hz initiated a mechanotransduction process in the cell and is used to measure the effect of SP on

10

chondrocytes. After stimulation with SP, a hyperpolarization of the cell membrane was observed, and this phenomenon was lacking in chondrocytes derived from SP knock-out mice. Blockade with a NK1R antagonist inhibited the cell response to mechanical signals. Additionally, the group observed an elevated SP production following mechanical stimulation. In a consecutive study, the group around Millward-Sadler found an upregulation of the tachykinin 1 gene expression encoding SP in OA chondrocytes [12]. This indicated the involvement of SP in OA, a joint pathology with underlying aberrant biomechanics. Osteocytes, which are the most abundant and main mechanosensing bone cells, were demonstrated to express the NK1R receptor [21,22]. The group of Ytteborg examined atlantic salmon osteocytes and osteoblasts exposed to loading and SP stimulation and suggested an initializing role of SP in mechanically-induced bone formation [22]. Furthermore, Backman et al. detected the expression of NK1R on human tenocytes and observed an increased tenocyte proliferation and metabolic activity after SP stimulation [23]. Capsaicin treatment of mice which leads to a reduced sensory nerve function and therefore a decrease of SP and αCGRP levels, affected the bone adaptation after tibial compression [24]. Additionally, ulnar loading of αCGRP knockout mice resulted in an altered bone turnover compared to controls [25]. Yet, it is still unknown whether the calcitonin receptor-like receptor (CRLR) is able to mediate biomechanical signals resulting in an altered αCGRP response, similar to the effects described for the tachykinin system. There are no studies to date that examine neuropeptide signaling in the context of macrophage mechanoreception and in diseases with altered biomechanics, such as OA.

1.2 Macrophages respond to biomechanical loading and sensory neuropeptide stimulation

Macrophages are highly plastic cells with various tasks and abilities, ranging from immunological functions to providing the osteoclast precursor pool. Their ability to adjust their cell shape and phenotype dependent on endogenous and exogenous factors makes them unique and explains the importance of macrophage functions. Macrophages are regulated by numerous molecules including cytokines, chemokines and neurotransmitters, and they may also react to mechanical forces such as tension or stretch appearing in the bone, lung, heart or vasculature. To perform their eminent task in immune responses, macrophages can acquire a multitude of different

phenotypes. Broken down to a simple classification, there are two main phenotypes: the pro- and the anti-inflammatory macrophages (Fig. 1.1).
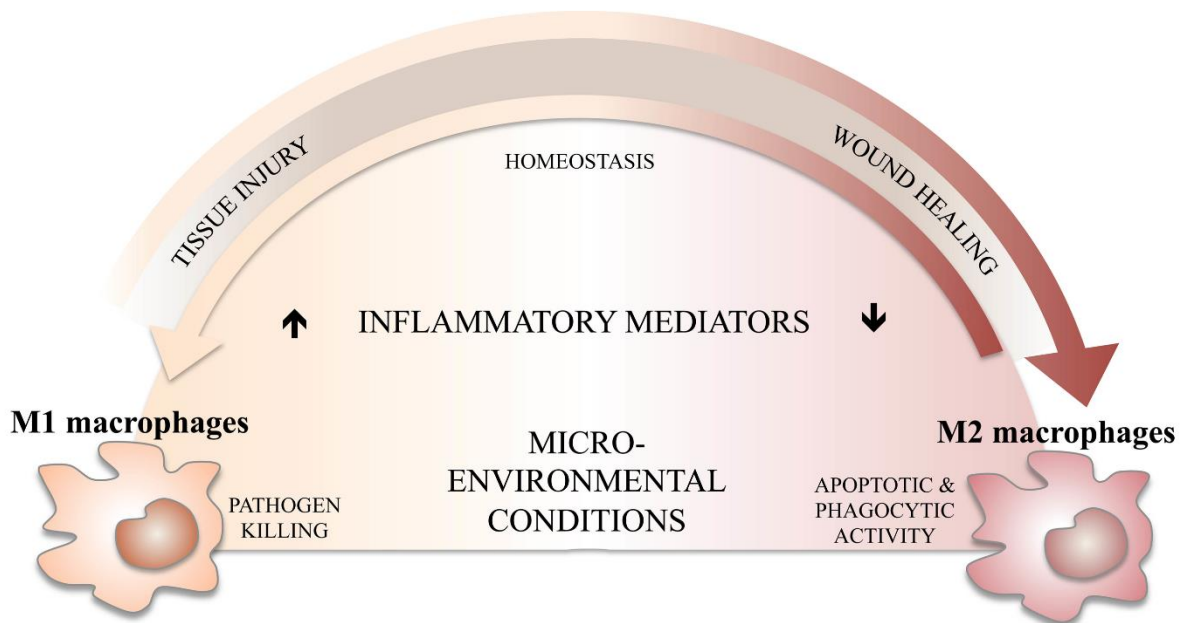
Figure 1.1. Schematic representation of macrophage polarization spectrum. Representation of the M1/M2 polarization states of active macrophages. Proinflammatory M1 macrophages guide acute inflammatory processes such as in tissue injury and act as a defense against intracellular pathogens. M2 macrophages have modulator functions in wound healing and provide an anti-inflammatory immune response. Macrophage phenotypes can be viewed as a continuum between the extreme M1/M2 polarization states, thereby maintaining and optimizing tissue homeostasis. Adopted from [26].

Proinflammatory M1 macrophages are classically activated, e.g. through lipopolysaccharides [27], and they release cytokines like tumor necrosis factor alpha, (TNF-α), interleukin (IL) 6 and inducible nitric oxide synthase (iNOS) and protect the body cells from bacteria, fungi and microbes by phagocytosis [27–30]. Alternatively-activated M2 macrophages produce numerous growth factors and induce the production of extracellular matrix in skin fibroblasts or epithelia for tissue repair and remodeling [27,30–33]. M2 polarized macrophages express cytokines like IL-10, mannose receptor (MRC-1) and krüppel-like factor (KLF) 4. Apart from cytokines, microbes and tissue architecture are able to affect macrophage polarization and phenotype [34].

1.2.1 Mechanoresponsiveness of macrophages

Although the elucidation of mechanical signaling pathways of various cell types is a topic that is frequently dealt with, there are only few experiments concerning mechanical stress on macrophages. An important difference from macrophages to other examined tissue cells is their high motility and migration ability to the sites of

action, where their function is required, e.g. in wound healing or infection. Macrophage mobility is provided by their adhesion to the extracellular matrix which is further mediated by β-integrins and scavenger receptors which has been demonstrated in the murine RAW 264.7 macrophage cell line [27,35]. Additionally, podosomes transduce biomechanical signals to the macrophage cytoskeleton and support macrophage key functions, like migration and invasion by providing a higher dynamic and adaptable stability [27]. Due to their broad exposure and reactivity to mechanical forces, the mechanotransduction chains and subsequent behavioral changes of macrophages are of special research interest. It is known that the formation of osteoclasts, derived from macrophage precursor cells, is modulated by mechanical loading (see 1.2.3). In macrophages derived from human peripheral blood mononuclear cells, Ballotta et al. observed a dose-dependent effect of stretching on the macrophage phenotype: experimental conditions using a high 12 % strain indicated the predominance of pro-inflammatory M1 macrophages, whereas loading with 7 % strain resulted in an elevated anti-inflammatory activity [36]. Experiments like these underline the differential effects of forces ranging from physiological to pathological amplitudes. In general, mechanically loaded macrophages presented a higher cytokine release than unloaded cells [37] and an increased gene expression of iNOS, IL-6 and IL-1β [38].

In addition to mechanical loading, macrophage polarization is likewise determined by environmental factors such as matrix stiffness, surface roughness, porosity and viscosity [39]. A rougher surface increased M2 gene expression of bone marrow-derived macrophages [40]. In particular, stiff substrate surfaces promoted varying macrophage phenotypes [39]. An increased phagocytic activity, indicating a pro-inflammatory polarization, was observed by Rosenson-Schloss et al. by applying shear stress on murine macrophages and by Mattana and colleagues using pressure [41,42]. Furthermore, Mattana et al. demonstrated that uniaxially stretched murine macrophages had less phagocytic activity than unstrained controls [43]. Additionally, mechanical loading results in morphological changes of macrophages, promoting either a vacuolized cell form or elongation, and alters gene expression, protein synthesis and enzyme activity [39].

1.2.2 Macrophages and sensory neuropeptide stimulation

How sensory neuropeptides in combination with mechanical stress affect macrophages has yet to be studied. Experiments display varying results concerning

macrophage polarization induced by neuropeptide treatment. In general, SP and αCGRP treatment increased the release of proinflammatory cytokines from mouse peritoneal macrophages [44]. SP stimulation of RAW 264.7 macrophages activated proinflammatory pathways and increased chemokine production [45]. Moreover, during bacterial corneal and CNS infections, SP induced proinflammatory actions [46–48]. In contrast, SP stimulation caused a shift towards anti-inflammatory M2 macrophages in experiments examining RAW 264.7 macrophages [49] and diabetic rodent wounds [50].

Furthermore, SP stimulation increased reactive oxygen intermediate production by airway macrophages [51]. Experiments of our group revealed an immediate increase in reactive oxygen species (ROS) activity after stretching and SP stimulation, but a ROS decrease after prolonged stimulation [52]. Furthermore, SP stimulation leads to an increased phagocytosis and chemotactic capacity of macrophages, as well as cytokine production [53]. Overall, James and Nijkamp suggest that SP might be involved in a variety of stress-induced responses of macrophages [54].

Stimulation with αCGRP prevented macrophage activation and inhibited hydrogen peroxide production, thereby influencing the macrophage immune response [55]. Yaraee et al. observed a reduced lymphocyte proliferation due to an inhibited macrophage antigen presentation in the presence of CGRP [56]. CGRP stimulation suppressed the DNA synthesis of murine airway macrophages and enhanced cAMP levels in rat alveolar macrophages [57,58]. It further inhibited the phagocytic capacity of RAW 264.7 macrophages [59]. Mapp et al. demonstrated an enhanced endothelial cell proliferation *in vivo* after CGRP injection in rat knee joints [60].

Murine bone marrow macrophages (BMM), the primary cells used in this work, express the SP and CGRP receptors NK1R [61] and CRLR [62] respectively, and the murine macrophage RAW 264.7 cell line is influenced by SP and CGRP stimulation [63,64].

1.2.3 Impact of mechanical loading on macrophages as osteoclast precursors

In the context of bone metabolism and joint physiology, macrophages are of interest as they are not only key effector cells of innate immunity but also provide the precursor pool for osteoclasts, the bone matrix degrading cells.

In the process of bone remodeling, bone formation is achieved through osteoblast matrix production. Bone resorption is mediated by osteoclasts, which differentiate at the bone surface from macrophages, forming a polykaryon (Fig. 1.2). To induce osteoclastogenesis, colony-stimulating factor (CSF) and receptor activator of nuclear factor κ-B ligand (RANKL) are essential, as they induce osteoclast-typical genes encoding for tartrate-resistant acid phosphatase (TRAP), cathepsin K, calcitonin receptor and β3-integrins [65]. Ligand binding to RANK leads to osteoclast activation by rearrangement of the actin cytoskeleton. Tight junctions between the cell membrane and the bone surface form an isolated compartment, the sealing zone, which is stabilized by an actin ring, consisting of specific podosome patterns. The release of hydrogen ions in this vacuole creates acidification, and enzymes like TRAP or cathepsin K increase the lysis of the surrounding osseous tissue. Matrix degradation in the sealing zone causes resorption pits known as Howship's lacunae. The typical ruffled border of the osteoclast develops from intracellular vesicle fusion and supports protease release and bone matrix acidification. Molecular degradation fragments such as minerals and peptides are digested directly in the osteoclast cytoplasm [65–68].
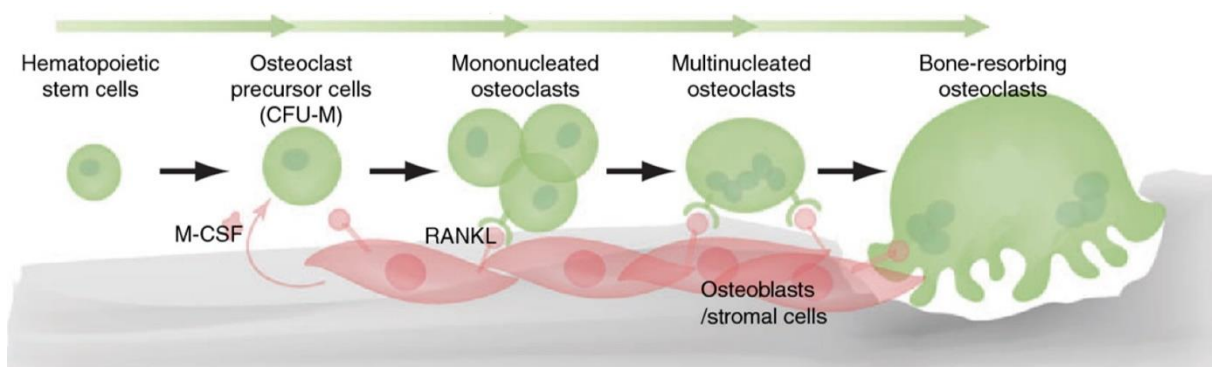
Figure 1.2. Osteoclast differentiation. In the presence of macrophage colony-stimulating factor (M-CSF), the hematopoietic stem cell differentiates to a macrophage colony-forming-unit (CFU-M). Receptor activator of nuclear factor-κB ligand (RANKL) induces the fusion of precursor cells by binding to RANK, thereby activating osteoclasts. Mature bone resorbing osteoclasts form a sealing zone on the bone surface and release hydrogen ions leading to bone lysis. In the picture, the vacuole called Howship's lacuna and the ruffled border of the osteoclast are depicted. Modified from [69].

This study focuses on macrophages, the osteoclast precursor cells, and their reaction to biomechanical stress. It is known that the formation of osteoclasts is modulated by mechanical loading. Yet, the effect of mechanical stress applied to precursor cells and mature osteoclasts seems to vary depending upon the loading mode used to apply mechanical force and loading parameters, such as frequency and duration [70–73]. Ma et al. reviewed direct and indirect effects of fluid shear stress, compressive force

and microgravity on osteoclastogenesis and reported only increasing effects that promoted bone resorption, as a consequence of physical force [74]. Kurata et al. observed that osteoclasts showed a higher mRNA expression rate of TRAP and cathepsin K after stretching. The group hypothesized that a stretch-activated cation channel might be responsible for the increased osteoclastogenesis and subsequent bone resorption. In fact, blockade of this channel abrogated the effects described above. Mechanical stress might affect bone degradation rather by an increase in the number of active osteoclasts than a higher activity of the individual osteoclast [73]. Li et al. studied dynamic knee loading in a osteoarthritic mouse model and, contrary to the previously mentioned studies, they observed a total suppression of osteoclast differentiation and bone resorption in the subchondral bone, leading to a thickening of the subchondral bone plate [75]. Guo and colleagues observed a restrained osteoclastogenic differentiation potential of RAW 264.7 macrophages after loading [76]. Yoo et al. compared the effects of mechanical loading and additional CGRP stimulation and found a similar depressing effect on bone resorption [77]. The group of Xu demonstrated a magnitude-dependent osteoclastogenic regulation of RAW 264.7 macrophages: low-magnitude mechanical loading prevented osteoclast activation and fusion, whereas high-magnitude strain promoted it [78]. Complementary to direct mechanical loading, Shibata et al. also examined osteoclastogenesis after the release of mechanical stress: stress suppressed osteoclastogenesis, whilst unloading induced osteoclast differentiation [79].

Recently, the attention in OA research shifted from the articular cartilage to the subchondral bone, and consequently, the number and diversity of experiments concerning osteoclastogenesis in the osteochondral junction increased. Based on the assumption that osteoclastogenesis might be one of the main contributing processes to histopathology and OA symptoms, the exact mechanisms, pathways and interactions in osteoclast differentiation are currently being elucidated in numerous studies.

1.3 Osteoarthritis: joint degeneration with altered mechanoreception and joint innervation

1.3.1 Etiology and pathology of osteoarthritis

According to the latest white paper of the OARSI (Osteoarthritis Research Society International), *Osteoarthritis. A serious disease* [80], about 240 million people worldwide suffer from OA. From those aged over 70, many persons are affected by OA of either one or more joints [81]. This multifactorial, degenerative disease causes a breakdown of articular cartilage, synovitis and alterations of the subchondral bone among other tissue alterations that are often accompanied by symptoms like inflammation, pain, joint stiffening and movement impairment. Whether the pathological structural changes cause the experienced symptoms or if molecular features of inflammation cause observed radiographic changes, has not been elucidated in detail. Most commonly, the weight-bearing joints of knee and hip as well as the small finger joints are affected. In Europe, more than 70 million people have OA of the knee [82]. Genetics, obesity and traumatic joint injury display the most important risk factors for the disease, further ones being malalignment of the limbs, mechanical stress and gender. A study of the World Health Organization grades hip and knee OA in 11th place of disability causes [82], illustrating the social and economic burden of the disease. The most commonly taken medication against articular pain in Europe are non-steroidal anti-inflammatory drugs (NSAIDs) [83]. Except for total joint replacement, there are no treatment options for OA that either halt or reverse the structural deterioration of the affected joint tissues. Regarding the high prevalence, yet still uncertain etiology and unsatisfying therapy options for OA, further exploration of signaling pathways involved in pathophysiology is necessary. Drugs or regenerative treatments that target pathophysiological processes of OA definitively are of high value.

The main radiographic attributes of OA joint degeneration are joint space narrowing, cartilage degradation, osteophyte formation and subchondral bone alterations such as sclerosis or cysts (Fig. 1.3). In sclerosis, bone mass and density of the subchondral bone are increased, yet demineralized and of minor quality [84,85]. The subchondral bone is an extensively vascularized region [86] from which small blood vessels originate that invade hyaline cartilage during degeneration and carry along small nociceptive nerve fibers [87,88]. Furthermore, the osteochondral junction seems to

17

have nociceptive function, because subchondral bone marrow lesions, as seen on MRI scans appeared to be proportional to pain sensation [89–91]. Nerve fiber infiltration in the cartilage and subchondral bone marrow lesions might be the source of OA pain and therefore subchondral bone is a promising target for pain alleviating treatments.

Formerly, the center of research attention was mainly limited to articular cartilage, but in recent years, subchondral bone and its contribution to OA pathology have gained stronger interest, as it is the source of nutritional and nerve supply for the overlying cartilage. Despite former assumptions that subchondral lesions are the consequence of cartilage damage, they might as well cause it and precede radiological bony changes – a frequently discussed hypothesis [89,92–94]. In the end, the joint is considered as an organ with intense communication between its various tissues [87,92,95,96].
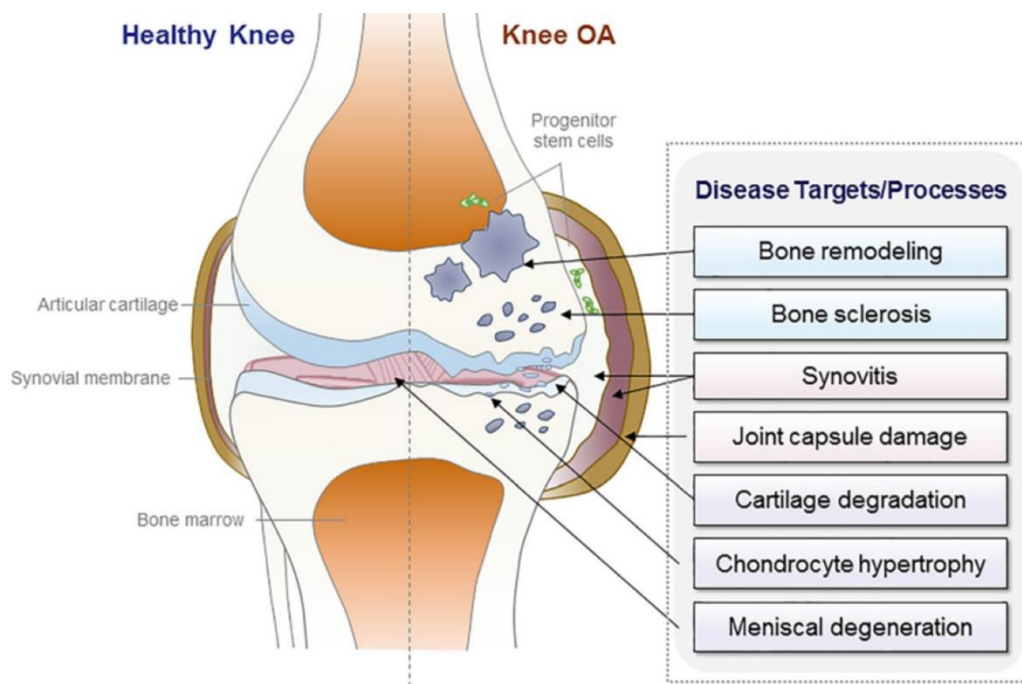
Figure 1.3 Osteoarthritis pathology. Schematic presentation of a healthy knee joint (left) and knee osteoarthritis pathology (right) in frontal plane. Modified from [97].

Following in vitro studies, pre-clinical in vivo studies are necessary for clinical translation. There exist several different animal models for OA that can be distinguished either by spontaneous (either natural or genetically induced) or induced models through chemical or surgical intervention [98,99]. Commonly used animal models for OA research are mouse, rat, rabbit, the guinea pig or horses. Chemical induction in rodents can be achieved by intra-articular injection of (mono)iodacetate, steroids, cytokines or collagenases [98,100]. Surgical OA induction can include

anterior cruciate ligament transection (ACLT), destabilization of the medial meniscus (DMM) or fracture models [98,100]. Advantages of mouse models are the rapid development of OA which allows to study the whole disease progression [99,100] and due to the small joint dimension, histological studies can cover the whole joint [101].

1.3.2 Macrophages in osteoarthritis pathology

Almost all joint tissues house a resident macrophage population (e.g. the synovial membrane, muscle and subchondral bone) with the exceptions being the menisci and cartilage [102–106,106]. Furthermore, macrophages provide the precursor pool for the differentiation of osteoclasts in bone. Besides the macrophage-derived osteoclasts, Chang and colleagues located a non-osteoclastic subgroup of macrophages in bone that is immediately adjacent to osteoblasts, the so-called osteal macrophages or 'osteomacs' [107]. This macrophage subset regulates osteoblast activity and osteoclast function and therefore participates in bone functional dynamics [104,107,108]. Thus, the macrophage lineage is not only a precursor to osteoclasts but due to their redundancy in musculoskeletal tissues might be involved in pathological joint processes including OA.

One aspect that is currently extensively discussed is the contribution of inflammation to OA. Generally, OA is not primarily an inflammatory disease, but there are some aspects that point towards a substantial contribution of innate inflammatory processes to OA pathology and pain. First, a common treatment for OA pain is the intake of anti-inflammatory drugs including NSAIDs [13,83]. Second, in OA joints, levels of prostaglandin E_2 (PGE_2) and nitric oxide (NO), two regulating factors of proinflammatory actions were elevated [13]. Macrophages are a highly important cell type involved in OA inflammatory processes [102]. Activated macrophages were detected in 76 % of knee joints in patients with symptomatic OA [109]. Elevated macrophage numbers in subchondral bone plates of OA joints and high-grade systemic inflammation after macrophage depletion furnish evidence for the involvement of macrophages in bone homeostasis [110–112]. Various authors outline that macrophages a) seem to contribute to osteophyte formation which is associated with pain severity experienced by OA patients, b) may release pro-inflammatory cytokines induced by extracellular matrix proteins in the synovial fluid in already very early disease stages and c) that synovial macrophages might directly influence cartilage damage via the production of tissue-damaging matrix metalloproteinases

(MMPs) [102,113,114]. Regarding the interplay of inflammation and osteoclastogenesis, osteoclast formation from macrophage precursor cells is increased in response to cytokine release during articular inflammation like synovitis, leading to focal erosions of the bone [108]. Additionally, Zhen et al. observed increased angiogenesis and osteoclast numbers in subchondral bone plates after rodent knee injury [115]. Drugs targeting macrophage activity and associated immunological answers might contribute to the inhibition or deceleration of OA [102]. So far, therapeutic attempts to interfere with macrophage pathways have not been successful. Treatment options including the use of methotrexate (MTX) or special cell-mediated gene therapies have been tested in clinical trials. One promising method might be phenotype modulation via inhibition of M1 polarization and promotion of wound-healing M2 macrophages, as seen by treatment with the corticosteroid dexamethasone [102,116].

However, the exact impact of macrophages and macrophage-derived osteoclasts in OA pathology remains unclear and further elucidation of their contribution could provide a better understanding of the disease.

1.3.3 Pathological biomechanical loading in osteoarthritis

In general, there is a strong indication that abnormal mechanical strain, leading to structural joint changes, is central for OA pathophysiology [14]. Obesity, joint malalignment, trauma or instability, all associated with altered biomechanical loading patterns, are important risk factors for the incidence of OA [82,117–119].

Biomechanical loading within a physiological range is important for maintaining bone and cartilage structure, integrity and function [9,120–122]. Loading above the physiological range can occur during high intensity physical exercise or due to the abnormal weight increase of obese patients. Micro-damage of the articular cartilage, as a consequence of excessive chronic mechanical loading, might initiate matrix degradation [14]. Sanchez-Adams et al. suggest that the mechanotransduction ability of chondrocytes is altered in response to mechanical strain and that chondrocytes partly lose their capacity to respond physiologically to biomechanical strain, all resulting in degenerative processes [123]. The group of Thompson observed a disassembly of chondrocyte primary cilia at high loading strains, thereby reducing mechanosensitive signaling and providing a chondroprotective mechanism to prevent

OA progression [124]. Catabolic proteins such as MMPs and A disintegrin- and metalloproteinases with thrombospondin-like motifs (ADAMTS) are increased in OA cartilage, leading to a degradation of cartilage extracellular matrix [93,125,126]. Griffin and Guilak summarize that mechanical stress on chondrocytes may activate cyclooxygenase (COX) 2 and nitric oxide synthase (NOS) 2, inducing inflammation and cartilage damage [13]. Furthermore, induction of hypoxia-inducible factor 2α (HIF-2α) and inhibition of transforming growth factor β (TGF-β) signaling are molecular cytokine pathways involved in aberrant mechanical stress responses [115,127–129]. Intracellular calcium levels which are modulated by mechanical signals might be important for chondrocyte metabolism [14]. Inhibition of the transient receptor potential vanilloid 4 (TRPV4) calcium channel during dynamic loading suppressed the expression of certain cartilage-protective genes [130].

Thickening of the calcified cartilage facilitates transfer of mechanical stress to the deeper cartilage zones [15]. Impaired cartilage integrity might induce subchondral bone lesions as a consequence of altered mechanotransduction [127], as demonstrated in early OA, whereby microfractures of the subchondral bone are formed [131]. Vice versa, a disturbed subchondral bone structure modifies stress distribution to the articular cartilage and might evoke cartilage damage [127,132]. Balanced bone resorption and formation in the subchondral bone provide damage repair after mechanical loading, a mechanism that is impaired with excessive mechanical stress. Due to microfractures, fissuring or complete loss of articular cartilage, synovial fluid and its cytokines can access the subchondral bone and affect all local cells [127]. Early OA signs detectable in MRI are bone marrow lesions (former bone marrow edema). These lesions can potentially heal, but when exposed to chronic abnormal loading, non-union of the bone appears, contributing to subchondral bone sclerosis [127]. Subchondral thickening may go along with blood vessel infiltration of the articular cartilage and invasion of sensory nerve fibers, thereby altering subchondral bone remodeling [110,127]. Berenbaum points out that mechanical stress might evoke immune responses by inducing inflammatory mediators like prostaglandins or cytokines, in chondrocytes and subchondral bone cells, leading to inflammatory-driven OA progression and pain [113]. OA-associated pathological processes in the subchondral bone are thickening of the subchondral bone plate, as well as development of cysts and osteophytes, leading to joint incongruity and further adverse

biomechanical joint strain. TGF-β and bone morphogenetic protein 2 (BMP2) seem to play a crucial role in osteophyte formation, since signaling pathway inhibition of these growth factors led to reduced osteophyte development [133]. Furthermore, Zheng and Cao outlined that high levels of active TGFβ in the subchondral bone might cause disturbed joint homeostasis and integrity [115,132]. Weber et al. supposed that high TGF-β levels, released from areas of subchondral bone microfractures after mechanical overloading, might activate the adaptive immune system. The interplay of inflammatory cells and cytokines may result in prolonged or insufficient healing of microcracks, leading to typical subchondral bone changes and disease chronicity [110].

Overall, mechanical loading might affect all cell types within the joint. That includes not only chondrocytes and bone cells like osteoclasts and osteoblasts, but also macrophages residing in the synovium, bone marrow and in all the surrounding tissues.

1.3.4 Sensory innervation of joints and its alterations in osteoarthritis

In the joint, sensory nerve fibers are located mostly in the synovia, in the outer, vascularized parts of the menisci, the periosteum, the bone marrow and the epiphyseal growth plates [134–136]. During OA progression, modifications of the local peripheral nervous system and joint innervation have been reported. Pathological change in patients with OA displays, for example, altered density of peripheral SP and CGRP fibers. OA disease state or tissue specificity might have an impact on nerve fiber distribution. So far, studies show varying results ranging from lost or unaltered to increased nerve fiber density. Eitner et al. examined synovia of human OA knees from total knee replacement surgeries and observed a significant decrease of CGRP positive nerve fibers in tissue depths close to the synovial lining [137]. After OA induction by collagenase injection, CGRP and SP fibers disappeared after a few weeks [138]. In a similar model, CGRP fibers decreased after only one week [139]. SP- and CGRP nerve fibers were reduced in the synovium of patients with rheumatoid arthritis (RA) [140]. In contrast, there was a higher sensory nerve fiber density in human knee synovia, knee menisci and hips with OA pathology [135,141,142]. Increased levels of SP and αCGRP in the synovial fluid were detected by several research groups and may contribute to intensified pain perception and tissue degradation like articular cartilage damage [19,143–145]. High pain levels experienced by patients with knee

OA were associated with tibial osteophytes. Suri et al. detected sensory nerve innervation in the cavities of these osteophytes as well as αCGRP- and SP-positive nerve fibers in the osteochondral junction [88]. To summarize, thin nerve fibers invading joint structures and growing along vascular channels have been seen in proceeding OA [19], whereby articular components that are normally not innervated, become pain sources [81,136]. Angiogenesis and neovascularization, accompanied by nerve fiber growth, are highly associated with increased local expression of the nerve growth factor (NGF). Targeting OA pain by inhibition of NGF yielded promising results [146,147] but several clinical trials had to be stopped due to severe adverse side effects and an overall increased need of joint replacement in the NGF patient group [148].

The main neuropeptides of the sensory nervous system are SP, a member of the tachykinin family, and αCGRP. Both peptides have been studied with respect to nociceptive function in OA but both possess additional functions in e.g. regulation of bone cell and chondrocyte behavior.

1.3.4.1 Substance P (SP)

SP is an undecapeptide from the tachykinin family (Fig. 1.4), produced by alternative splicing from the tachykinin (TAC1) 1 gene that also encodes neurokinin A and B [149,150]. In general, SP is involved in vasodilation, pain perception, nausea and vomiting and has proinflammatory properties. Regarding pain perception, an increased mRNA expression of the TAC1 gene and its receptor [151] and a high SP release [152,153] were demonstrated after the exposure to nociceptive stimuli or neurogenic inflammation. In numerous inflammatory conditions, SP acts as a mediator, e.g. in lung, visceral organs, skin or migraine [151]. Furthermore, it supports macrophage-associated proinflammatory immune responses by activating macrophages to produce cytokines, chemokines and free radicals [45]. The characteristic and prominent vasodilating capacity of SP induces a strong plasma extravasation [154].

Figure 1.4. Amino acid sequence of the neuropeptide Substance P (SP). Arg.: Arginine, Pro: Proline, Lys: Lysine, Glu: Glutamine, Phe: Phenylalanine, Gly: Glycine, Leu: Leucine, Met: Methionine.

Whether SP acts as an anabolic or catabolic compound in bone and cartilage metabolism, is unclear. In chondrocytes, SP acts not only in its classical neuropeptide manner, but also as a trophic and anabolic factor in physiology and differentiation, since it promoted the proliferation of growth plate chondrocytes [17,19]. However, during degenerative pathologies such as OA arising from developmental hip dysplasia, higher levels of SP and also αCGRP were reported in the synovium and the synovial fluid, which might point towards catabolic properties of the neuropeptides [144]. On the other hand, high levels of neuropeptides could occur as a consecutive repair mechanism of the body and thus emphasize their anabolic function. The SP receptor NK1R is a 7-transmembrane receptor that is coupled with a G_s-protein. After ligand binding, phospholipase C and IP_3 and the pathway via adenylyl cyclase and cAMP are activated, both resulting in cytosolic Ca^{2+} increase leading to protein phosphorylation and cellular responses [46]. Additionally, NK1R activation stimulates the formation of a scaffolding complex containing β-arrestin and extracellular signal-regulated kinases 1 and 2 (ERK1/2), which are members of the mitogen-activated protein kinase (MAPK) cascade. The scaffolding complex seems to be responsible for the commonly observed proliferative [23,155–157] and anti-apoptotic effects of SP [158,159]. Macrophages express the naturally occurring variant of a truncated NK1R that might react differently to SP stimulation than other cells of the musculoskeletal tissues, such as chondrocytes or osteocytes expressing the full-length receptor variant [160].

The NK1R has been detected on numerous bone cells, for example, osteocytes [21], osteoclasts [161,162] and bone marrow macrophages (BMM) [61]. BMM also secrete SP [61]. In in vitro osteoclastogenesis experiments, stimulation with SP led to an increased bone resorption [163]. By adding a SP antagonist, Mori et al. consistently observed a reduction of bone resorption [164]. After SP stimulation of rabbit osteoclasts, the group detected elevated intracellular calcium levels which might cause increased bone turnover. Shih and colleagues observed dose-dependent osteogenic effects of SP [165]. Wang et al. examined that SP increased osteoclastogenesis specifically in RAW 264.7 cells [166]. SP also promoted the M2 subtype of macrophage polarization [167,168], demonstrated likewise in RAW 264.7 macrophages [49].

1.3.4.2 Alpha-calcitonin gene-related peptide (αCGRP)

αCGRP is a 37-amino acid peptide deriving from calcitonin by alternative splicing. In general, it evokes vasodilation [169], is involved in pain transmission [141,170–172] and capable to induce anti-inflammatory processes [63]. αCGRP is released from type C nerve fibers in response to activation of TRPV1 [173]. Many cell types residing in the joint including chondrocytes, osteoblasts, osteoclasts and their precursors, the BMM express the heterodimeric receptor for αCGRP consisting of the CRLR and RAMP1 [19,62,174,175]. Of the two existing forms, βCGRP is mainly present in the intestines, whereas αCGRP, the isotype discussed in this work, is extensively expressed in the central and peripheral nervous system [176]. CGRP-containing unmyelinated type C and Aδ nerve fibers mostly run along blood vessels [177]. During OA, CGRP in the joint might affect inflammatory processes and afferent sensitization [81].

To effectively bind αCGRP, the 7-transmembrane CRLR needs to interact with RAMP1, a single pass transmembrane protein (Fig. 1.5). This type of receptor is referred to as a two-domain class B G-protein coupled receptor (GPCR) [178]. Characteristic for the binding process of this receptor is the interaction of the peptide C-terminal and the extracellular receptor N-terminal that supports affinity and selectivity of the molecule complex. Meanwhile, the peptide region carrying the N-terminal activates the receptor by binding to the transmembrane domain with its extracellular loops [179]. It is assumed that small variations and specific interactions between the extracellular receptor, N-terminal and the binding RAMPs can alter the receptor function. Specifically, RAMPs seem to provide accessibility to the special peptide binding site on the CRLR N-terminal [180]. A 16 kDa receptor component protein (RCP) provides the intracellular G-protein-coupled signaling and is likely to additionally modulate αCGRP-mediated effects [181]. Subsequently, G_S-protein pathways are activated, leading to an increase of cAMP and intracellular Ca^{2+} [182].
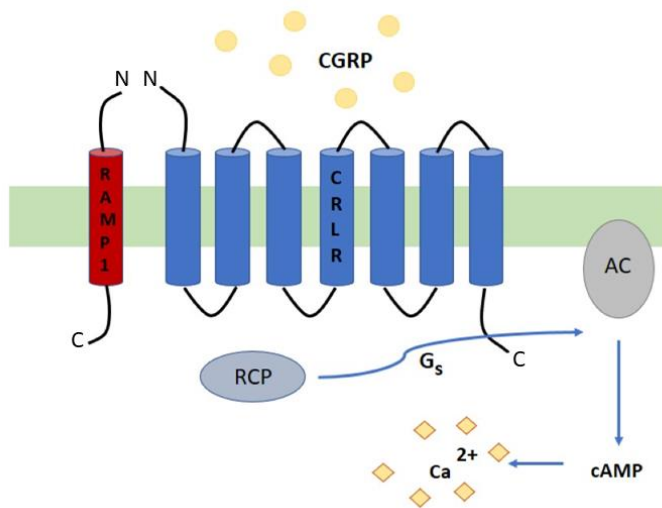
Figure 1.5. Schematic structure of the αCGRP receptor. The single transmembrane protein (red) is the receptor activity-modifying protein 1 (RAMP1), the seven transmembrane proteins of the calcitonin receptor-like receptor (CRLR) are depicted in blue. Extracellularly, their N-terminal chains form the extracellular domain of the receptor where αCGRP binds. Interaction of the GPCR with the receptor component protein (RCP) activates adenylate cyclase (AC), which leads to an increase of cyclic adenosinmonophosphate (cAMP) and the intracellular release of Ca^{2+}.

Regarding bone metabolism, αCGRP is known to decrease osteoclast formation [183–185]. Cornish et al. observed a similar effect in a dose-dependent manner in mouse bone marrow macrophages [186], while Yoo et al. found a stimulating effect of αCGRP on osteoclastogenesis similar to mechanical loading [77]. Another group suggests that αCGRP regulates bone metabolism by increasing osteoblast formation and indirectly reducing bone resorption by inhibition of osteoclastogenesis [187]. The osteogenic effect of αCGRP is supported by experiments that protected ovariectomized rats from bone loss using αCGRP injections [188]. Furthermore, αCGRP knock-out mice demonstrated low bone mass and development of osteopenia [25,175].

2   Objective of the study

The aim of the project was to examine the influence of sensory neuropeptides on metabolic cell parameters of murine macrophages in the context of mechanical stress application. Therefore, we studied the impact of neuropeptide stimulation together with mechanical stress on gene and protein expression of the sensory neuropeptides and their receptors, as well as proliferation, adhesion, apoptosis and osteoclastogenesis in the murine RAW 264.7 macrophage cell line. SP and αCGRP, the sensory neuropeptides, were selected for this study due to their ability to regulate macrophage and bone cell behavior in vitro and in vivo. αCGRP effects in bone were described to be mainly anabolic. αCGRP stimulation inhibited osteoclast formation in mouse BMM cultures in a dose-dependent manner [186] and was shown to suppress bone resorption similar to the effect of mechanical loading [77], resulting in an anabolic effect. Instead, addition of SP increased osteoclastogenesis of RAW 264.7 cells [166], acting as a catabolic mediator. It has been previously demonstrated that the NK1R senses and processes mechanical signals of cells exposed to mechanical loading, e.g. tenocytes, chondrocytes and osteocytes [20,21,23,161,162]. Whether the dimeric αCGRP receptor CRLR/RAMP1 mediates similar effects in response to αCGRP binding has not been elucidated so far.

How the combination of mechanical loading and simultaneous neuropeptide stimulation influences the metabolism and osteoclastogenic differentiation potential of murine macrophages is not known so far and is the aim of this project. New insights into mechanotransduction pathways and the interplay of mechanical stress and sensory neuropeptides could help elucidate if and how sensory neuropeptides and their receptors might participate in loading-related pathophysiology mechanisms of OA and might offer new ideas for therapeutic targets. The following questions were addressed in this work:

- Does mechanical loading of macrophages cause changes in the expression of NK1R and CRLR/ RAMP1 and affect the endogenous production of SP and αCGRP by murine macrophages?
- How does mechanical loading modulate the influence of SP and αCGRP on metabolic parameters such as proliferation, adhesion and apoptosis in murine macrophages and their osteoclastogenic differentiation?

- Does induction of experimental OA cause changes in the mechanotransduction of BMM and alter the impact of SP and αCGRP on proliferation, apoptosis and osteoclastogenesis of BMM?

To test these hypotheses, the experiments were performed in the murine macrophage cell line RAW 264.7 and in primary BMM from mice with surgical-induced OA via destabilization of the medial meniscus (DMM).

3 Material and Methods

3.1 Cell Culture

3.1.1 RAW 264.7 cell culture

The murine RAW 264.7 monocyte/ macrophage cell line (ATCC-Nr. TIB-71) was a kind gift from the group of Prof. Anita Ignatius from the University of Ulm. Manipulated with an Abelson murine leukemia virus-induced tumor, it belongs to the S2 organisms, according to the biological agents regulation. As a consequence, waste was collected separately and products were only used once. 1×10^6 cells in passage 9 were thawed, resuspended in 10 ml RAW medium (Table 3.1) and centrifuged at 130 xg for 5 min (Hettich Universal 320, Tuttlingen, Germany). The supernatant was discarded and the pellet was resuspended in 10 ml medium before it was transferred into a 75 cm² culture flask (Corning, NY, USA). RAW 264.7 cells were cultured at 37 °C and 5 % CO_2 in RAW 264.7 expansion medium that was changed twice a week. Experiments were performed with cells from passages 8 to 15. The cell line was used to establish the loading scheme and to examine the impact of loading on receptor and neuropeptide expression, metabolic parameters, as well as for gene expression analysis.

Table 3.1. Composition of the RAW 264.7 expansion medium

RAW 264.7 medium:	
500 ml	Dulbecco's Minimum Essential Medium (Gibco, Thermo Fisher Scientific, Waltham, MA, USA)
10 %	fetal calf serum (Sigma-Aldrich, St. Louis, MO, USA)
1 %	antibiotics/ antimycotics (Sigma)
1 %	Glutamax (Gibco, Thermo Fischer Scientific, Waltham, MA, USA)

For further experiments, the cultured cells were washed with 5 ml PBS (Sigma-Aldrich, St. Louis, MO, USA) and detached in 5 ml RAW 264.7 expansion medium using a police rubberman (Sarstedt, Nürnbrecht, Germany). Samples were centrifuged and the supernatant was discarded. RAW 264.7 cells tend to form aggregates and thorough resuspension was necessary. The best resuspension was achieved using a total volume of 10 ml medium and different pipette volume sizes. Cell numbers were determined using the CEDEX XS Cell Analyzer (Roche Innovatis Ag, Basel, CH).

3.1.2 Isolation and culture of primary bone marrow-derived macrophages (BMM)

Male, 12-week-old C57Bl6J mice were either subjected to surgical OA induction by DMM or Sham surgery. For the induction of OA, 10-week-old male C57Bl/6J wildtype

mice were purchased from Charles River Laboratories (Sulzfeld, Germany) and were adapted to standard housing conditions under a 12 h dark/light cycle until the age of 12 weeks. The mice had access to food and water ad libitum. All animal experiments were approved by the ethical committee of the local authorities (Regierung Unterfranken, AZ 55.2-2531-2-289, date of approval 27th July 2016). All surgeries were performed by Dr. Dominique Muschter from the Experimental Orthopedics group of Prof. Dr. Susanne Grässel. OA was induced following a method described by Glasson et al. [62]. Briefly, after intraperitoneal applied anesthesia solution composed of fentanyl, medetomidin and midazolam, a 3 mm skin incision was made between the distal patella and the proximal tibia plateau of the right leg, exposing the knee joint. The joint capsule was opened with a 1–2 mm incision medial to the patellar tendon. For induction of OA, the medial meniscotibial ligament was dissected carefully after visualization using microscissors. Sham surgery was performed in the right knee of a separate control group with visualization of the ligament only. The joint capsule and skin were closed and animals received analgesia (buprenorphine in 0.9 % NaCl solution, 0.1 mg/g body weight). Dissection of the medial meniscal ligament causes joint instability and leads to development of moderate OA, resembling human post-traumatic OA. Immediately after surgery, animals were allowed to move freely and recover from the surgery. After 2 and 8 weeks, animals were asphyxiated with CO_2 followed by cervical dislocation and the bone marrow was isolated.
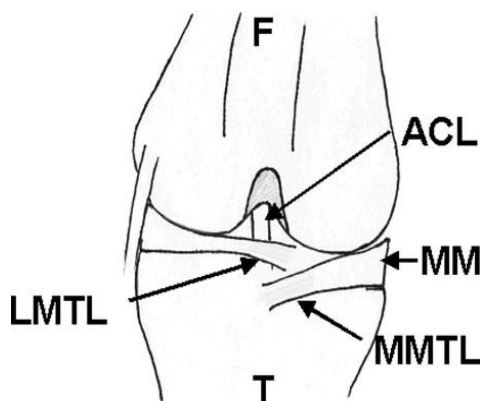
Figure 3.1. Dorsal view of the knee joint. For surgical induction of OA by destabilization of the medial meniscus (DMM), the medial meniscal tear ligament (MMTL) is cut, which leads to joint instability and results in the development and progression of OA symptoms.

F – Femur, T – Tibia, ACL – Anterior Cruciate Ligament, MM – Medial Meniscus, MMTL – Medial Meniscotibial Ligament, LMTL – Lateral Meniscotibial Ligament.

Picture from Glasson et al., Osteoarthritis and Cartilage (2007) 15, 1061-1069

Bone marrow (BM) was isolated under sterile conditions from femur and tibia of the operated right leg, 2 and 8 weeks after surgery. Therefore, the bones were prepared roughly at the bench top and remaining muscle and ligaments were carefully removed under a laminar flow. Bones of femur and tibia were cut open at the distal ends and the BM was rinsed out with 5 ml BMM medium (Table 3.2) using a 27G needle (BD, Franklin Lakes, NJ, USA) that was inserted into the bone. Cell aggregates were

separated and impurities were retained using a 40 µm cell strainer (Greiner bio-one, Kremsmünster, AUT). The cell solution was centrifuged at 130 xg for 5 min (Hettich), and the supernatant was discarded. The bone marrow was depleted of red blood cells by hypotonic shock using 4.5 ml ice cold, sterile aqua bidest. and the before red pellet dissolved into a white-yellowish solution. To stop further lysis, 500 µl of 10x PBS was added quickly after resuspension. Following centrifugation at 130 xg and 5 min, the remaining cells were seeded in petri dishes used for bacterial culture (Greiner bio-one) in 10 ml BMM medium containing 20 ng/ml murine macrophage colony-stimulating-factor (M-CSF) (#315-02, Peprotech, Rocky Hill, NJ, USA). Cells were cultured in an incubator set to 37 °C and 5 % CO_2.

Table 3.2. Composition of the BMM medium

BMM medium:	
500 ml	α-minimum essential medium (Sigma, St. Louis, MO, USA)
10 %	fetal calf serum (Sigma-Aldrich, St. Louis, MO, USA)
1 %	antibiotics/ antimycotics (Sigma)
2 %	Glutamax (gibco, Thermo Fischer Scientific, Waltham, MA, USA)

After three days, adherent BMM were harvested and subjected to subsequent mechanical loading. Therefore, 5 ml of 0,02 % EDTA (ethylene diamine tetraacetic acid, Roth, Karlsruhe, Germany) was added per plate and cooled on ice for 5 min, followed by one 1 min at -20°C. Gentle, but thorough lifting was achieved with a cell lifter (Corning, NY, USA). The plates were rinsed two times with 5 ml BMM medium. If necessary, lifting was repeated. After centrifugation at 130 xg for 5 min, the supernatant was aspirated and 1 ml medium was added for resuspension. The cell number, viability and aggregate formation was determined using an automated cell counter (Cedex).

Depending on the absolute cell number harvested after pre-culture, up to $1.2x10^6$ BMMs were seeded in flexible six-well-plates (#BF-3001U, FlexCell, Burlington, NC, USA) in BMM medium and 20 ng/ml M-CSF (Peprotech) was added. The BMMs were allowed to recover overnight and loaded for 2 consecutive days, 4 h each, before performing various assays.

3.1.3 In vitro osteoclastogenesis of bone marrow-derived macrophages

BMM from DMM- or Sham-mice were seeded punctiform to flexible-bottom six-well-plates (FlexCell), after 25.000 cells had been resuspended in 100 µl BMM medium containing 20 ng/ml M-CSF (Peprotech) and 10 ng/ml RANKL (#462-TEC, R&D,

Minneapolis, MN, USA). Cells were allowed to adhere for 10 min, then medium was added to a final volume of 2 ml/ well. M-CSF was used as a survival and growth factor, while RANKL as the ligand to the RANK receptor (receptor activator of NF-kB) is necessary for the induction of osteoclast differentiation. Before application of mechanical stress, αCGRP and SP at a concentration of 10^{-8} M per well were added to all the plates (see 3.1.5). Cells were loaded for 4 h per day on 5 consecutive days. Medium including the stimulations was changed after 3 days. Osteoclasts were quantified using tartrate-resistant acid phosphatase (TRAP) staining (see 3.3.8.1).

3.1.4 In vitro osteoclastogenesis of RAW 264.7 cells

Osteoclast differentiation of RAW 264.7 cells on Flexcell plates appeared to be difficult due to reduced adherence to the plate surface. Coating with rat-tail collagen I (Gibco) did not lead to any improvement in attachment. After purchase of collagen I-coated plates (#BF-3001C, Flexcell), adherence and differentiation were improved. The best result was achieved seeding 10.000 cells punctiform in 500 µl BMM medium. Following 10 min for cell adherence, medium containing 20 ng/ml M-CSF (Peprotech) and 50 ng/ml RANKL (#462-TEC, R&D, Minneapolis, MN, USA) was added to a final volume of 2 ml/well. Before application of mechanical stress, 10^{-8} M αCGRP and SP per well were added (see 3.1.5). Cells were loaded for 4 h per day on 5 consecutive days. Medium including RANKL/ M-CSF and neuropeptide stimulations was exchanged after 3 days. Osteoclasts were detected after 7 days of differentiation and quantified after TRAP staining (see 3.3.8.1).

3.1.5 Neuropeptides and specific receptor antagonists

To study the influence of sensory neuropeptides on different metabolic cell parameters, we used the sensory neuropeptides αCGRP (#H-2265, Bachem, Bubendorf, CH) and SP (#S6883, Sigma, St. Louis, MO, USA), as well as their specific receptor antagonists CGRP$_{8-37}$ (αCGRP receptor antagonist, #1169, Tocris Bioscience, Bristol, UK), L733,060 (NK1R receptor antagonist, #1145, Tocris Bioscience) and a combination of the specific agonist and antagonist. The 10^{-5} M neuropeptide stock solution was diluted to the final concentration of 10^{-8} M. The final concentration of 10^{-10} M was prepared by a predilution of the stock to 10^{-7} M in phosphate-buffered saline (PBS). Stock solutions of both antagonists (10^{-3} M) were prediluted in PBS to 10^{-4} M and used at a final concentration of 10^{-7} M concentration.

3.1.6 Application of mechanical load

Mechanical stress was induced by exposing the cells to stretching. In cooperation with the Department of Orthodontics, we used a self-built machine similar to the tension systems offered by FlexCell International Corporations®. This system uses a stamp that is pushed against a flexible membrane and causes a stretch that extends to the cells seeded onto the membrane. The system used for this project was built in cooperation with the Department of Physics from the University of Regensburg. Control measurements assured that equal stretching occurred all over the membrane, except for the outer margin.

For all experiments, cells were seeded on 6-well-plates with a flexible bottom membrane (Flexcell). Depending upon the experiment, $5x10^5$ to $1.2x10^6$ cells were seeded into each well and allowed to adhere overnight. Cells were stretched with a frequency of 1 Hz and an amplitude of 28, equaling a stretching of 10 %.
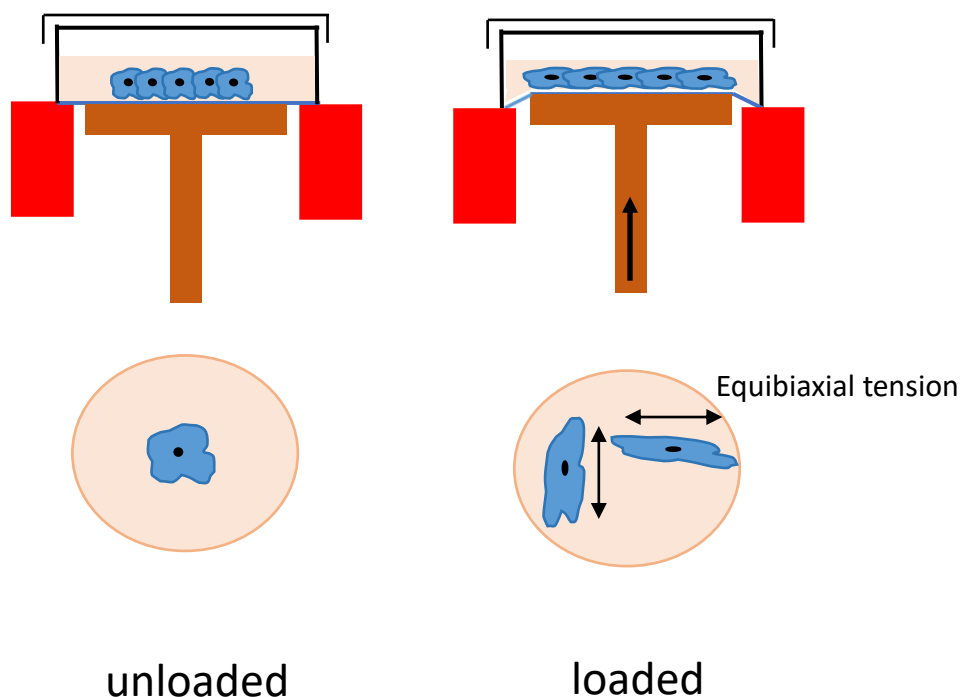
Figure 3.2. Schematic representation of the cell stretching. Depicted is a vertical and a horizontal view on the cell culture plate, on loaded and unloaded cells. In the loading position, the stamp pushes against the flexible membrane the cells were seeded onto and causes an equibiaxial tension.

Pretension was set to 110 µC. For smooth sliding and optimal contact of the machine stamps, the membranes of the six-well-plates were thinly coated with a silicon paste on the outer surface (Bayer, Leverkusen, Germany). Cells were stretched for 240 min for 2 to 5 consecutive days, depending on the experiment.

3.2 Molecular Biology

3.2.1 RNA Isolation and quantification

For RNA analysis, 1×10^6 cells per well were seeded in an uncoated 6-well-plate (Flexcell) and loaded for 4 h on 2 consecutive days. Cells were lifted in medium with a police rubberman, centrifuged at 130 xg for 5 min (Hettich), the supernatant was aspirated and the cell pellet was stored at -80 °C.

RNA was isolated using the Absolutely RNA Miniprep Kit (Agilent Technologies, CA, USA) including the use of pre-filter spin cups and a lysis buffer containing β-mercaptoethanol (β-ME). The buffer also contains guanidine thiocyanate, a very strong protein denaturant that protects from RNase-driven RNA degradation. Generally, working steps were carried out according to the manufacturer's instructions. Samples were mixed with 350 µl of lysis buffer and vortexed for 1 min to optimize lysis. Use of the pre-filter cleared the sample from possible cell fragments and contaminations. After addition of 350 µl of 70 % ethanol (Roth, Karlsruhe, Germany), RNA was bound to a matrix in the RNA-binding spin column and separated from contaminants by several subsequent washing steps. 55 µl DNase incubation for 15 min at 37 °C was used to digest remaining DNA impurities. Highly purified RNA was eluted in 30 µl elution buffer. The elution step was repeated twice to ensure complete recovery of RNA from the column.

The RNA concentration and purity were measured using the Nanodrop 1000 spectrometer (Thermo Scientific, Waltham, MA, USA).

3.2.2 RNA quality assessment

To determine the quality of the RNA, samples were tested with the RNA 6000 nano kit using the 2100 Bioanalyzer from Agilent Technologies (Santa Clara, CA, USA). The assay separates RNA by its size using a microcapillary electrophoresis system. The purity is given as RIN (RNA Integrity Number), with a range from 10 to 1 representing completely intact to degraded RNA. Initially, the purity was tested exemplarily, resulting in RINs of 9 and higher for RNA of RAW macrophages.

3.2.3 cDNA synthesis

The isolated RNA was transcribed to single-stranded cDNA using the AffinityScript qPCR cDNA Synthesis Kit from Agilent (Santa Clara, CA, USA). The kit contains the reverse transcriptase enzyme responsible for the transcription, the buffer containing

MgCl$_2$ and dNTPs (deoxyribonucleotide triphosphates) as well as oligo and random primers.

The RNA sample was premixed with the nuclease-free water and subsequently added to the prepared reaction. The synthesis reaction (Table 3.3) was carried out in a T3000 Thermocycler (Biometra, Göttingen, Germany) following a three-step protocol: primer annealing for 5 min at 25 °C, synthesis reaction for 15 min at 42 °C and termination of the reaction for 5 min at 95 °C.

Table 3.3. Components of the cDNA reaction

25 µl (total volume)	component
10 µl	First strand master mix (2x)
1.5 µl	Oligo (dT) primers
1.5 µl	Random primers
1 µl	AffinityScript RT/ RNase Block enzyme mixture
2.2 µl	RNA (used concentration: 30 ng/ml)
Final volume 25 µl	Add nuclease-free PCR-grade water to final volume

3.2.4 Polymerase Chain Reaction (PCR)

cDNA or DNA can be amplified using a DNA polymerase enzyme. Each product synthesized at one step will be used as template for the next amplification step, thereby enabling the yield of a high amount of cDNA from small initial amounts.

3.2.4.1 Quantitative real-time PCR

The qRT-PCR is a method to determine specific gene expression rates. A gene of interest is amplified using specific primers (Table 3.4) and expression rates are normalized to the expression of a constitutive "household" gene (endogenous control) and calibrated against the expression of the gene of interest in control cells (unloaded/ unstimulated cells, calibrator).

PCR was performed using the Mx3005P QPCR System from Agilent Technologies and the Brilliant II SYBR Green QPCR Master Mix with ROX (Agilent Technologies, Santa Clara, CA, USA). The SYBR Green I Dye emits fluorescence when bound to double-stranded DNA. When cDNA is amplified using specific primers the fluorescence intensity of each cycle becomes more intense with increasing amounts of double-

Table 3.4. Primer used for qualitative and quantitative PCR

GENE	PRIMER SEQUENCE (5'→ 3')	TM (°C)	AMPLICON SIZE (BP)	ACC.NR.
ENDOGENOUS CONTROL GENE				
GAPDH	Fwd: AACTTTGGCATTGTGGAAGG	59,97	223	-
	Rev: ACACATTGGGGGTAGGAACA	60,09		
NEUROPEPTIDES AND NEUROPEPTIDE RECEPTOR GENES				
NK1R	Fwd: ATTGAGTGGCCAGAACATCC	57,9	135	NM_009313
	Rev: ACTGGCCCACAGTGTAATCC	59,7		
CRLR	Fwd: GCCAATAACCAGGCCTTAGTG	59,0	77	NM_018782
	Rev: GCCCATCAGGTAGAGATGGAT	58,7		
RAMP1	Fwd: CCTGACTATGGGACTCTCATCC	59,1	139	NM_016894
	Rev: CGTGCTTGGTGCAGTAAGTG	59,8		
SP	Fwd: GATGAAGGAGCTGTCCAAGC	58,6	102	NM_009311
	Rev: GCACAGGAGTCTCTGCTTCC	60,4		
CGRP	Fwd: TGCAGGACTATATGCAGATGAAA	57,7	91	NM_007587
	Rev: GGATCTCTTCTGAGCAGTGACA	59,5		
OSTEOCLAST MARKER GENES				
c-FMS	Fwd: CAGAAGACCCACCTTCCAAC	59,0	93	NM_001037859
	Rev: CTGCTTGGCAGGTTAGCATA	59,0		
RANK	Fwd: GCTCCTGAAATGTGGACCAT	57,9	241	NM_009399
	Rev: CACGATGATGTCACCCTTGA	57,6		
M1 POLARITY GENES				
NFkB	Fwd: GGCAGCTCTTCTCAAAGCAG	60,0	107	NM_008689
	Rev: CCACTCCCTCATCTTCTCCA	60,0		
TNF-α	Fwd: GACAGTGACCTGGACTGTGG	59,9	132	NM_013693
	Rev: GAGACAGAGGCAACCTGACC	60,0		
IL-6	Fwd: CCGGAGAGGAGACTTCACAG	59,2	134	NM_031168
	Rev: CAGAATTGCCATTGCACAAC	56,5		
iNOS	Fwd: CAAGCACCTTGGAAGAGGAG	58,2	149	NM_010927
	Rev: AAGGCCAAACACAGCATACC	58,7		
M2 POLARITY GENES				
MRC-1	Fwd: AGAAAATGCACAAGAGCAAGC	59,0	101	NM_008625
	Rev: GGAACATGTGTTCTGCGTTG	60,0		
IL-10	Fwd: CCAAGCCTTATCGGAAATGA	55,5	162	NM_010548
	Rev: TTTTCACAGGGGAGAAATCG	55,7		
KLF4	Fwd: CCGTCCTTCTCCACGTTC	59,0	93	NM_010637
	Rev: GAGTTCCTCACGCCAACG	60,0		

stranded DNA. Therefore, the increase of the fluorescence signal is proportional to the amplification of PCR products and enables gene expression quantification. Relative gene expression rates were determined using the ΔΔCt method.

The cDNA was diluted in nuclease-free water and subsequently added to the prepared reaction (Table 3.5). Samples were pipetted as duplicates into a 96 well plate (4titude, Wotton, Surrey, UK), centrifuged briefly (Multifuge 3S-R, Heraeus, Hanau, Germany) and covered with a plate sealer (4titude). Samples were denatured at 95 °C for 15 min followed by 40 cycles with an initial denaturation step at 95 °C for 10 sec and an annealing step at 60 °C for 30 sec. 1 min at 95°C, 30 sec at 55 °C and 30 sec at 95 °C terminated the reaction. This fast, two-step cycling protocol was chosen due to the length of the reaction products of less than 150 base pairs.

Table 3.5. Reaction mix of the qRT-PCR reaction

25 µl (total volume)	components
12,5 µl	2x Brilliant II SYBR Green QPCR master mix
0,5 µl	Forward primer (200 mM)
0,5 µl	Reverse primer (200 mM)
0,45 µl	cDNA (concentration 50 ng/ml)
11,05 µl	nuclease-free PCR-grade water

To describe the gene expression alterations, the ΔΔCt method as a relative quantification (RQ) method was used.

$$\Delta Ct = Ct_{\text{target gene}} - Ct_{\text{endogenous control}}$$

$$\Delta\Delta Ct = \Delta Ct_{\text{sample}} - \Delta Ct_{\text{control}}$$

$$RQ = \text{relative quantification} = 2^{-\Delta\Delta Ct}$$

It describes the activity of the gene of interest normalized to an endogenous control gene (GAPDH). Loaded samples and samples stimulated with the neuropeptides and/ or receptor antagonist are related to unloaded / unstimulated control cells (calibrator). A RQ higher than 1 indicates an upregulation of the gene expression, whereas below 1 gene expression was downregulated. Providing optimized experimental conditions, RT-qPCR effectiveness ranges from 1.5 to 2.0 [189]. Some genes (RAMP1/ αCGRP) were not expressed in unloaded cells and only induced by loading. Therefore, results

were expressed as ΔCt where the gene of interest is referred to the expression of the endogenous control gene.

3.2.4.2 Qualitative endpoint PCR

The aim of performing a qualitative PCR is to prove the presence or absence of a specific mRNA.

The qualitative PCR was run for the amplified RAMP1 gene due to its low expression after qRT-PCR. The polymerase used was from the Brilliant II SYBR Green QPCR Master Mix with ROX from Agilent (Santa Clara, CA, USA), as described in 3.2.4.1. The amplified cDNA was run in agarose gel electrophoresis (see 3.2.5) and compared to a size marker.

3.2.5 Agarose Gel Electrophoresis

A 2 % agarose gel (Biozym LE Agarose, Hessisch-Oldendorf, Germany) containing RotiSafe dye (Roth, Karlsruhe, Germany) at a 1:20.000 dilution for detection of PCR products was prepared. Samples were mixed with a 6x loading dye (New England Biolabs, Ipswich, MA, USA) and loaded onto the gel in Tris-acetate-EDTA (TAE) buffer. The pore size and the electrical field (80 V, ca. 60 min) induce a separation of the cDNA fragments according to their size. Gels were photographed in the BioRad Gel Doc EZ Imager (Hercules, CA, USA). The fragment size was compared to a 50-base pair ladder marker (New England Biolabs, Ipswich, MA, USA).

Table 3.6. Components of the TAE buffer

TAE buffer 50x (pH=7,8) → dilute to 1x using Aqua dest.		
242 g/L	Tris	AppliChem
57,1 ml	Acetate Acid	Roth
100 ml	0,5 M EDTA	Roth

3.3 Protein biochemistry

3.3.1 Proliferation Assay

Proliferation was determined using the colorimetric BrdU cell proliferation enzyme-linked immunosorbent assay (ELISA) from Roche (Basel, CH). The assay detects the quantitative integration of the thymidine analog 5-bromo-2'-deoxyuridine (BrdU) into newly synthetized DNA using a specific anti-BrdU antibody. The incorporated amount

of BrdU is proportional to the amount of synthetized DNA and allows the comparison of proliferative activity between different conditions.

After 2 days of loading, 10.000 cells in 100 µl medium per well were seeded into a 96-well plate (Corning, NY, USA) and were allowed to adhere overnight. For the BMM, 20 ng/ml M-CSF (Peprotech) was added. Cells were starved from FCS to synchronize the cells. After 24 h, medium containing FCS as well as BrdU labeling reagent and the respective neuropeptides/ inhibitors were added and cultivated for 48 h. After incubation, cells were processed in accordance to the manufacturers' instructions. For fixation, 200 µl Fix&Denat solution was added per well and incubated for 30 min. Plates were tilted and tapped. 100 µl of anti-BrdU-working solution (1:100 dilution from the stock) was added and incubated for 60 min at room temperature. Washing was done 3 times with 200 µl washing buffer or PBS per well. In the experiments with RAW 264.7 cells, the final blue staining appeared rapidly after the addition of 100 µl substrate solution per well. The reaction was stopped after 2 min by adding 25 µl H_2SO_4 per well. The reaction of the BMMs took more time and was stopped after 3-5 min. The absorption was measured at 450 nm (reference wavelength of 690 nm) using a microplate reader (Tecan Genios, Männedorf, CH).

3.3.2 Apoptosis assay

Apoptosis was analyzed with the Apo-ONE® Homogenous Caspase-3/7 Assay (Promega, Fitchburg, USA). The assay system utilizes the release of fluorescent Rhodamin-110 from the non-fluorescent substrate (Z-DEVD-110) by active caspase 3/7 (Fig. 3.2).
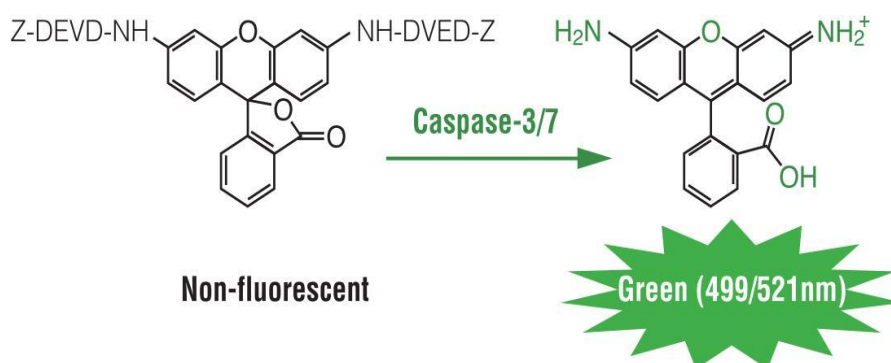

Figure 3.2. Caspases split the non-fluorescent Z-DEVD-R110 substrate, Rhodamin 110 is released and the fluorescence can be detected in a photometer. Picture rights belong to Promega®.

Following a loading period of 2 days, 30.000 cells/ well were seeded in black 96-well plates with a clear bottom (Falcon by Corning, NY, USA) in 50 µl of medium with/ without sensory neuropeptides and receptor antagonists. The caspase substrate was diluted 1:100 in buffer and 50 µl was added into each well containing the seeded cells. Due to the light sensitivity of the caspase reagent and to avoid scattered light at the measurement, black plates were used. Apoptosis activity was measured after 2, 6 and 24 h at 485 nm using a microplate reader (Tecan).

3.3.3 Adhesion assay

Cells that underwent loading for 2 days were harvested and 30.000 cells were seeded in 100 µl per well in a 96-well plate (Corning, NY, USA) in the presence of SP, αCGRP, the respective receptor antagonists and the combination of agonist and antagonist.

After incubation for 30 min at 37 °C and 5 % CO_2, the cells were washed with 200 µl PBS and fixed with 100 µl 1 % glutaraldehyde solution per well (Merck, Darmstadt, Germany) for 30 min. The plate was again washed with 200 µl PBS per well. For staining, 150 µl of 0.02 % crystal violet solution (Roth, Karlsruhe, GER) was added for 15 mi. Afterwards, plates were washed thoroughly until the blue staining vanished. The amount of crystal violet dye incorporated into the cells is considered to be proportional to the number of cells attached in each well. Incubation in 150 µl 70 % ethanol/ well for 1 h on an orbital shaker, covered with a plate sealer (4titude, Surrey, UK), dissolved crystal violet out of the cells. Absorbance of ethanol-dissolved crystal violet dye was measured using a microplate reader (Tecan) at 595 nm. Differences in absorbance values were correlated with differences in adhesion capacity of cells.

3.3.4 Protein isolation and concentration measurement

For western blot analysis, proteins were harvested directly from the respective cell culture vessel. Cells were lysed in radioimmunoprecipitation assay (RIPA) buffer (Thermo Fisher Scientific, Waltham, USA) containing a protease inhibitor mix (Complete Mini, Roche, Basel, CH). Cells were lysed in 50 µl RIPA buffer and transferred into a reaction cup.

Cells were homogenized by sonification with a Sonopuls HD 2070 ultrasound homogenizer (Bandelin, Berlin, Germany), twice for 20 sec, 3 cycles and at a power of 40 %. Samples were centrifuged for 10 min at 14.000 xg and 4 °C (3K30, Sigma, Osterode am Harz, Germany) and the collected supernatant was used for further

analysis. Protein amount of the supernatant was measured using the BCA kit from Pierce (bicinchoninic acid, Thermo Fisher Scientific, Waltham, USA) and a standard curve with known concentrations of bovine serum albumin (BSA). Results were calculated from duplicate values. The samples were diluted 1:50 in Aqua $_{dest.}$ and 10 µl were transferred into a 96-well plate (Greiner, Kremsmünster, AUT) in triplicates. Per well, 200 µl of Working Reagent were added. The plate was incubated for 30 min at 37 °C. The underlying mechanism is the reaction of Biuret during which Cu^{++} is reduced to Cu^+ and forms a lilac complex with the bicinchoninic acid (BCA). The absorption of the colored complex was measured in the Tecan Genios spectrometer (Tecan Group, Männedorf, CH) at 595 nm and the referring protein amount was calculated from the standard curve.

3.3.5 SDS gel electrophoresis

For comparison of the neuropeptide receptor expression, protein samples were separated via sodium-dodecyl sulfate polyacrylamide gel electrophoresis (SDS-PAGE). Therefore, 40 µg of protein from cell lysates were mixed with the appropriate 5x loading buffer (Table 3.8) and denatured for 5 min at 95 °C (ThermoMixer C, Eppendorf, Hamburg, Germany) before loading onto a 12 % polyacrylamide gel (Table 3.7). As a size marker, the Precision Plus Protein Dual Color Standards from BioRad (Hercules, CA, USA) was used. Gel electrophoresis ran at 120 V for 110 to 120 min, using a tank blot chamber (Mini-PROTEAN Tetra, Bio-Rad) and running buffer (Table 3.8).

Table 3.7. Reaction of the separating and stacking gel for electrophoresis

Separating gel, 12 %	[ml]	Stacking gel	[ml]	
H_2O	6,6	H_2O	2,78	
30 % acrylamide mix	8,0	30 % acrylamide mix	0,83	Roth, Karlsruhe, Germany
1,5 M Tris pH 8,8	5,0	0,5 M Tris pH 6,8	1,25	AppliChem, Darmstadt, Germany
10 % SDS	0,2	10 % SDS	0,05	Roth
10 % ammonium persulfate (APS)	0,2	10 % ammonium persulfate (APS)	0,05	Serva, Heidelberg, Germany
TEMED	0,008	TEMED	0,005	Roth
Σ	20 ml	Σ	5 ml	

3.3.6 Western Blot

After SDS-PAGE, gels were equilibrated in Western Blot transfer buffer to remove salt supernatants from the running buffer that might disturb the blotting procedure and bulge the gel.

The separated proteins were transferred onto a 0.45 µm nitrocellulose membrane (GE Healthcare Life Sciences, Little Chalfont, UK) by tank blotting for 90 min at 120 mA on ice. SDS-Gel was stained using Coomassie-Blue (incubation for 30 min on a vertical shaker), first color remover (30 min, on a vertical shaker) and second color remover (incubation overnight on a shaker) (see Table 3.5). Gels were dried using glycerol solution (Table 3.5.), applied two times for 30 min. Ponceau red solution staining of the membrane (Sigma-Aldrich, St. Louis, MO, USA) was used to control if the blotting procedure was successful. Unspecific binding sites were blocked using 5 % dry milk (Carl Roth, Karlsruhe, Germany), dissolved in Tris-buffered-saline with Tween 20 (T-TBS) for 1 h at room temperature on a vertical shaker (Duomax 1030, Heidolph, Schwabach, Germany). The primary antibody (directed against the protein of interest, listed in table 3.9), dissolved in 5 % dry milk, was added and incubated overnight at 4 °C on a shaker. Afterwards, the membrane was washed three times for 10 min with T-TBS, followed by incubation with the secondary antibody for 1 h at room temperature and subsequent washing as described above. Parallel detection of endogenous β-actin served as the loading control.

Table 3.8. Components of the solutions used during gel electrophoresis and Western Blot

Running buffer 10x (pH=8,3):		
Glycin (192 mM)	144 g/L	AppliChem, Darmstadt, GER
Tris (25 mM)	30,3 g/L	AppliChem
SDS (0,1 %)	10 g/L	Roth, Karlsruhe, GER
Transfer buffer 10x (pH=8,3):		
Glycin (192 mM)	144 g/L	AppliChem
Tris (25 mM)	30,3 g/L	Roth
Transfer buffer 1x:		
Aqua dest.	800 ml	
Transfer buffer 10x	100 ml	
Methanol	100 ml	
SDS loading buffer 5x:		
Aqua dest.		
Tris/ HCl pH 6,8	1 M	AppliChem
SDS	10 %	Roth
DTT	0,5 M	AppliChem, #A1101
Glycerin	50 %	Roth

Bromphenole blue, dissolved in H20	0,01 %	Sigma
TBS-T 20x (pH=7,6):		
Tris (20 mM)	48,4 g/L	AppliChem
NaCl (140 mM)	160 g/L	Roth
Tween 20 (0,1 %)	20 ml/L	Sigma, St. Louis, MO, USA
Coomassie Blue Solution		
Coomassie Blue	2,5 g/L	Roth
2-propanol	250 ml/L	Merck, Darmstadt, GER
Acetic acid	200 ml/L	Roth
1st color remover		
Methanol	50 %	Merck
Acetic acid	10 %	Roth
2nd color remover		
Methanol	5 %	Merck
Acetic acid	7,5 %	Roth
Glycerole solution		
Glycerine	2 %	Roth
Ethanol	25 %	Fischar, Saarbrücken, GER

Membranes were developed using the "Pierce ECL Western Blotting Substrate" (Thermo Scientific, Waltham, MA, USA). Therefore, ECL substrate solutions were mixed 1:2 and the membrane was incubated for 1 min. Chemiluminescence was measured at 1, 3, 5, 10, 15 and 45 min in the Chemi smart 500 chemiluminescence lamp (PeqLab, Erlangen, Germany). Membranes for detection of the RAMP1 protein were developed in the GelDoc Imager (Biorad).

Table 3.9. Antibodies used for Western Blotting

ANTIBODY	ANTIGEN	FUNCTION	IG	DILUTION	PRODUCT INFORMATION
CRLR	α-CGRP	Primary AB	polyclonal	1: 500	Bioss #bs-1860R
NK1R	SP	Primary AB	monoclonal	1: 20.000	Abcam #183713
β-actin	β-actin	Primary AB	monoclonal	1: 5.000	Abcam #ab8227
Donkey anti-rabbit		Secondary AB		1: 10.000	Jackson Immuno Research #711-036-152

For a more sensitive detection of the CRLR protein, the "Pierce SuperSignal West femto" (Thermo Scientific, Waltham, MA, USA) was used for development. 650 µl of solution A and B were put on the membrane, incubated for 5 min in the dark and developed at 10 and 30 sec, 1, 3, 5, 10 and 15 min.

3.3.7 Enzyme-linked immunosorbent assay (ELISA)

In a 6-well Flexcell plate (Burlington, NC, USA), 1×10^6, 7.5×10^5 and 5×10^5 RAW 264.7 cells were seeded, incubated for 1 night and loaded for 1, 2 or 3 consecutive days. Before the respective last loading time point, medium was exchanged for FCS-free RAW medium. Afterwards, 200 µl proteinase-inhibitor (Complete Mini, Roche) was added to the medium and the supernatant was collected and stored at -80 °C until ELISA analysis.

3.3.7.1 Calcitonin gene-related peptide ELISA

To detect the αCGRP peptide in the supernatants of loaded and control samples, the rat/ mouse "Enzyme Immunoassay Kit" from Phoenix Pharmaceutical Inc. ('EK-015-09, Burlinghame, CA, USA) was used according to the manufacturers' instructions. The assay principle is based on the competition of biotinylated αCGRP contained in the kit with endogenous αCGRP of the samples for the binding site of the primary antibody. The Fc part of the primary antibody binds to the immobilized secondary antibody. Added streptavidin-horseradish peroxidase (SA-HRP) forms a complex with the biotinylated peptide and HRP catalyzes the substrate solution. The developing blue color is directly proportional to the amount of SA-HRP-biotinylated peptide complex and inversely proportional to the amount of peptide in the samples. The reaction is stopped by addition of 2NHCl inducing a colour shift to yellow. Absorption was measured at 450 nm. The unknown concentration of αCGRP was extrapolated from the standard curve.

3.3.7.2 Substance P ELISA

For detection of endogenous SP in the supernatants the "Substance P ELISA kit" from Enzo Life Sciences Inc. (Farmingdale, NJ, USA) was used according to the manufacturers' instructions. The assay principle is similar to the αCGRP enzyme immunoassay principle described before.

3.3.8 Histology

3.3.8.1 Tartrate-resistant acid phosphatase staining

To identify osteoclasts differentiated either from BMM or RAW 264.7 macrophages, cells were fixed and stained with the "Acid Phosphatase, Leukocyte (TRAP)" kit from Sigma-Aldrich (#A387, Taufkirchen, Germany) for detection of the osteoclast marker TRAP.

Following differentiation, medium was aspirated and cells were fixed for 30 sec (Table 3.10), washed three times with Aqua dest. and incubated with the coloring solution (Table 3.11) for 60 min at 37 °C. TRAP hydrolyzes the esters of naphthol AS-BI phosphate acid, which forms a complex of low solubility with the diazotized Fast Garnet GBC salt. Counterstaining with hematoxylin was not performed to avoid overstaining. Osteoclasts and BMMs with active TRAP appear red-violet to red-brownish. The plates were scanned using the Tissue Faxs microscope system (TissueGnostics, Vienna) and the pictures were evaluated using Adobe Photoshop CS4 (Adobe Inc., CA, USA). Cells with three and more nuclei were graded and counted as osteoclasts.

Table 3.10. Fixation solution

1 ml (total volume/ well)	Components	
255 µl	Citrate	Kit: Sigma-Aldrich
663 µl	Acetone	Sigma
82 µl	37 % Formaldehyde	AppliChem, Darmstadt, Germany

Table 3.11. Staining solution

1 ml (total volume/ well)	Components (all Sigma-Aldrich)
20 µl (10 µl + 10 µl)	diazotized Fast Garnet GBC: (Fast Garnet GBC Salt Solution + Sodium Nitrite Solution)
900 µl	Aqua dest. at 37 °C
10 µl	Naphtol-AS-BI Phosphate
40 µl	Acetate
20 µl	Tartrate

3.4 Statistical Analysis

Statistical data analysis was performed using Microsoft Office Excel 2011 (Redmont, WA, USA) and the GraphPad Prism 5 and 6 software (San Diego, CA, USA). Data are presented as boxplots showing the median and inter-quartile ranges. Whiskers show the range from minimum to maximum. The percentage graphs illustrate the influence of the neuropeptides with respect to the unstimulated control. The Wilcoxon Signed-Rank Test was used to analyze statistically significant differences between samples and control (set to 100 %) or for evaluation of gene expression. The comparison between the loaded controls and the unloaded controls was evaluated using the non-parametric Mann-Whitney U-Test. Significance level was $p < 0.05$ for all test results.

4 Results

4.1 Impact of mechanical loading on the expression of SP and α-CGRP and their receptors NK1R and CRLR/ RAMP1 in RAW 264.7 murine macrophages

The premise for a stimulation experiment must be the expression of the respective receptors on the examined cells. We analyzed timely changes in neuropeptide and receptor protein expression after 1, 2 and 3 days of loading. The receptor protein expression of the NK1R, binding SP, as well as CRLR and RAMP1, interacting with αCGRP, was determined by western blot (Fig. 4.1). Each lane was referred to the respective expression of β-actin in the sample. Protein expression of SP and αCGRP was measured by ELISA in cell culture supernatants. Furthermore, expression of each protein was further evaluated on mRNA level after 2 days of loading.

Regarding the neuropeptide receptor expression, the gene expression of NK1R (Fig. 4.2, A) and CRLR (Fig. 4.3, A) as well as their receptor protein expression were significantly enhanced through loading. Both receptor proteins were significantly higher expressed after three days of loading (Fig. 4.2, B) with the CRLR receptor protein also significantly upregulated after one day of loading (Fig. 4.3, B).
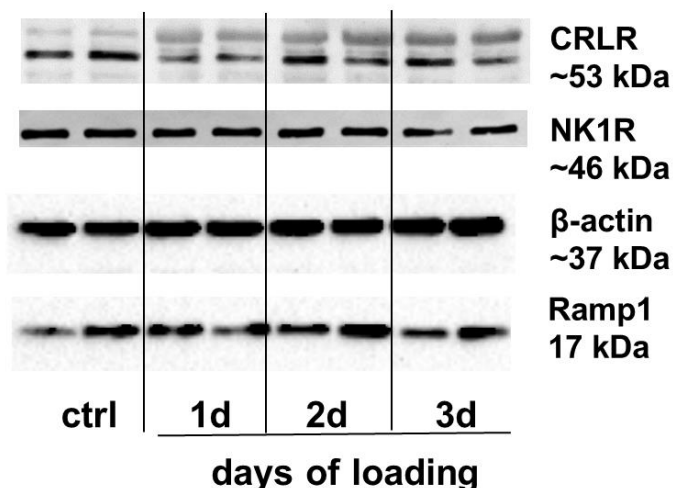

Fig. 4.1. Western Blot. Representative Western Blot pictures for 4 independent replicates of the CRLR (53 kDa), the NK1R (46 kDa), RAMP1 (17 kDa) and β-actin (43 kDa, endogenous control) of control cells and cells loaded for 1, 2 and 3 consecutive days (presenting 2 lanes for each condition).
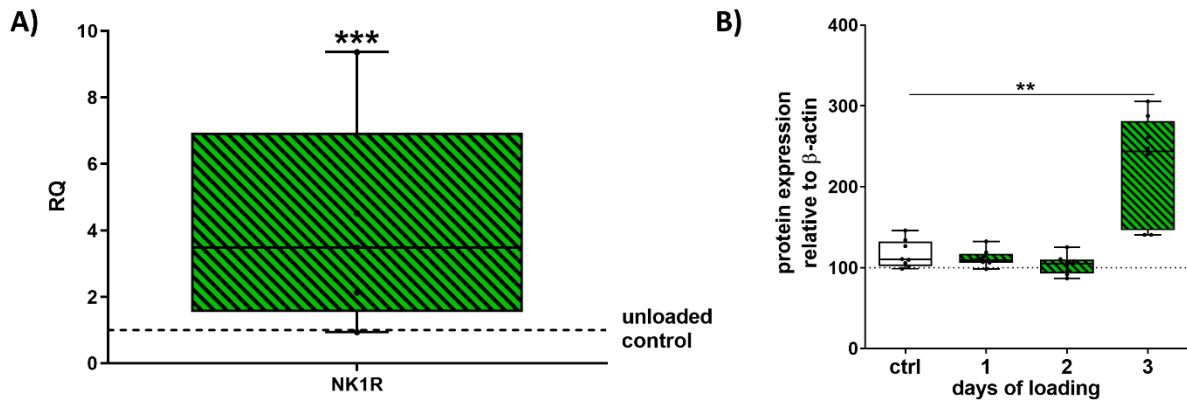
Fig. 4.2. Influence of loading on the expression of neurokinin receptor 1 (NK1R).
A) Gene expression of NK1R after 2 days of loading is depicted as relative quantification (RQ). The gene of interest was referred to the endogenous control gene, GAPDH, and the loaded samples to the unloaded controls (calibrator). Wilcoxon-signed rank test. *** $p<0.001$. qPCR was performed in duplicates. n=15. B) Densitometric evaluation of NK1R protein expression of unloaded controls and samples after 1, 2 and 3 days of loading by Western Blot. Respective boxplots were referred to the β-actin lane (=100 % line) and are depicted as relative percentages. Comparison of loaded samples to unloaded controls was tested with Mann-Whitney test. ** $p<0.01$. n=7-8. Boxplots represent median, whiskers cover minimum to maximum. The blank box represents controls, striped boxes depict loaded samples.
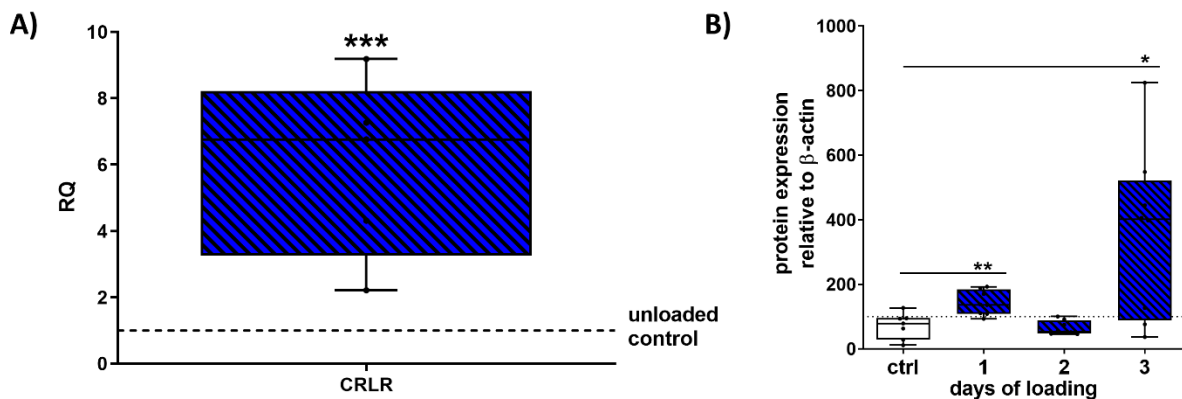

Fig. 4.3. Influence of loading on the expression of calcitonin receptor-like receptor (CRLR).
A) Gene expression of CRLR after 2 days of loading is depicted as relative quantification (RQ). The gene of interest was referred to the endogenous control gene, GAPDH, and the loaded samples to the unloaded controls (calibrator). Wilcoxon-signed rank test. *** $p<0.001$. qPCR was performed in duplicates. n=15. B) Densitometric evaluation of the CRLR protein expression of unloaded controls and samples after 1, 2 and 3 days by Western Blot. Respective boxplots were referred to the β-actin lane (=100 % line) and are expressed as relative percentages. Comparison of loaded samples to unloaded controls was tested with Mann-Whitney test. * $p<0.05$, ** $p<0.01$. n=7-8. Boxplots represent median, whiskers cover minimum to maximum. The blank box represents controls, striped boxes depict loaded samples.

Results of the qPCR analysis showed that RAMP1 mRNA was expressed, yet in low concentrations and not detectable in all samples (Fig. 4.4, A). Therefore gene expression can only be depicted as ΔCt. Mechanical stress did not alter RAMP1 mRNA expression. RAMP1 receptor protein expression was not significantly affected by loading, there was a tendency for reduced expression in loaded samples relative to controls (Fig. 4.4, B).
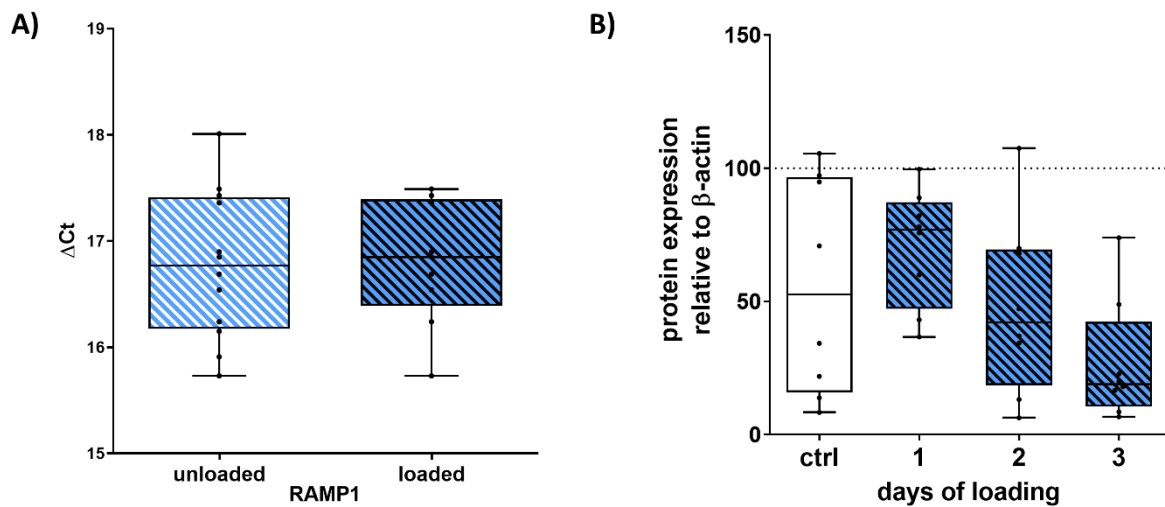
Fig. 4.4. Influence of loading on the expression of receptor activity-modifying protein 1 (RAMP1). A) Gene expression of RAMP1 in RAW 264.7 cells, loaded for 2 days, is depicted as Δct, the gene of interest referred to the endogenous control gene, GAPDH. qPCR was performed in duplicates. n=15. B) Densitometric evaluation of the RAMP1 protein expression of unloaded controls and samples after 1, 2 and 3 days of loading by Western Blot. Respective boxplots were referred to the β-actin lane (=100% line) and are expressed as relative percentages. Comparison of loaded samples to unloaded controls was tested with Mann-Whitney test. n=7-8. The blank box represents controls, striped boxes depict loaded samples. Boxplots represent median, whiskers cover minimum to maximum.

For both neuropeptides, SP and αCGRP, loading had no significant influence on the protein expression (Fig. 4.5, C and D). The gene expression of SP was significantly downregulated by cyclic stretching (Fig. 4.5, A). αCGRP gene expression was only detectable in loaded samples and not in control cells (Fig. 4.5, B).
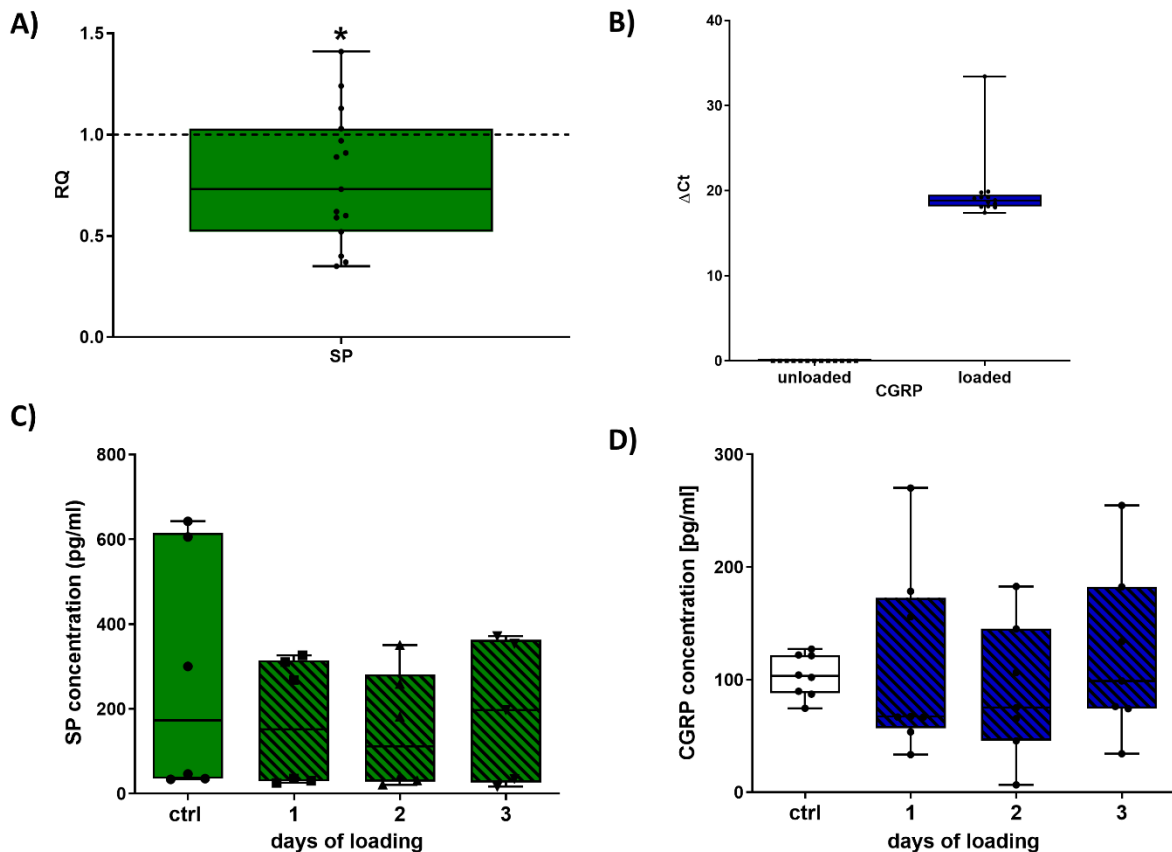
Fig. 4.5. Influence of loading on the expression of neuropeptides substance P (SP) and α-calcitonin gene-related peptide (αCGRP). A) Gene expression of SP after 2 days of loading is depicted as relative quantification (RQ). The gene of interest was referred to the endogenous control gene, GAPDH, and the loaded samples to the unloaded controls (calibrator). Wilcoxon-signed rank test. * $p < 0.05$. B) Gene expression of αCGRP after 2 days of loading is depicted as Δct, the gene of interest referred to the endogenous control gene, GAPDH. qPCR was performed in duplicates. n=15. C) and D) depict the protein expression of SP (C) and αCGRP (D) measured by ELISA in cell culture supernatants of unloaded controls and samples loaded for 1, 2 or 3 days. Comparison of loaded samples to unloaded controls was tested with Mann-Whitney test. n=7-8. Boxplots represent median, whiskers cover minimum to maximum. The blank box represents controls, striped boxes depict loaded samples.

4.2 Impact of mechanical loading and sensory neuropeptide stimulation on inherent metabolic behavior of RAW 264.7 cells

Based on the mechanotransduction hypothesis, a signal from a mechanical stimulus is converted further to a biochemical signal that modulates cell behavior. Referring to this thesis, the influence of mechanical loading on the metabolic parameters proliferation, apoptosis and adhesion was tested in RAW 264.7 macrophages, as well as in BMMs isolated from mice after DMM or Sham surgery.

4.2.1 Proliferation

To study the proliferation of RAW 264.7 cells, the BrdU Incorporation assay was performed. There was a tendency for reduced proliferation in loaded cells compared to unloaded controls (Fig. 4.6).

Fig. 4.6. Influence of loading on 2 consecutive days on proliferation of RAW 264.7 cells. The figure shows the unloaded, unstimulated cells, set to 100 %, and in relation the loaded, unstimulated cells, depicted as respective percentage. Boxplots represent median and the whiskers cover minimum to maximum. Mann-Whitney test, p<0.05. Assay was performed in triplicates. n=6.

Stimulation with 10^{-8} M SP and 10^{-7} M NK1R receptor antagonist L733,060 decreased the proliferation rate in unloaded cells, whereas the combination of both reduced proliferation in loaded cells (Fig. 4.7, A). Stimulation with 10^{-10} M αCGRP significantly decreased proliferation in unloaded samples (Fig. 4.7, B).

Fig. 4.7. Influence of sensory neuropeptide stimulation on proliferation of loaded and unloaded RAW 264.7 cells. The unloaded and loaded cells (loading on 2 consecutive days) without stimulation were set to 100 % (continuous line) and the results for the stimulation are depicted as respective percentage. A) shows the results for stimulation with SP, the neurokinin receptor 1 antagonist L733,060 as well as both in combination. B) shows the results for stimulation with αCGRP, the receptor antagonist CGRP$_{8-37}$ as well as the combination of both. Boxplots represent median and the whiskers cover minimum to maximum. Comparison of differences to control (100 %): Wilcoxon-signed rank test (asterix directly above box), comparison of stimulations between loaded and unloaded cells: Mann-Whitney test. * $p < 0.05$. Assay was performed in triplicates. n=7.

51

4.2.2 Adhesion

Crystal-violet staining was used to analyze the adhesion ability of unloaded and loaded cells to the cell culture plastic surface. Mechanical loading increased adhesion (Fig. 4.8) of RAW 264.7 cells.
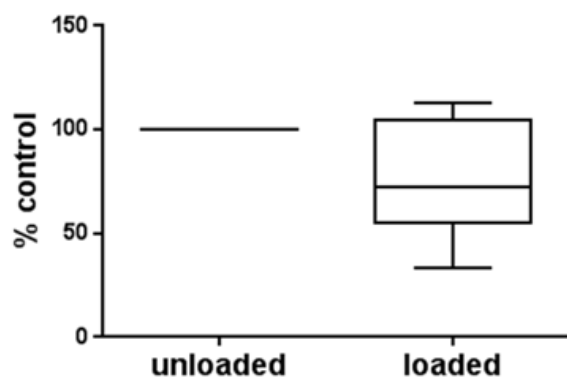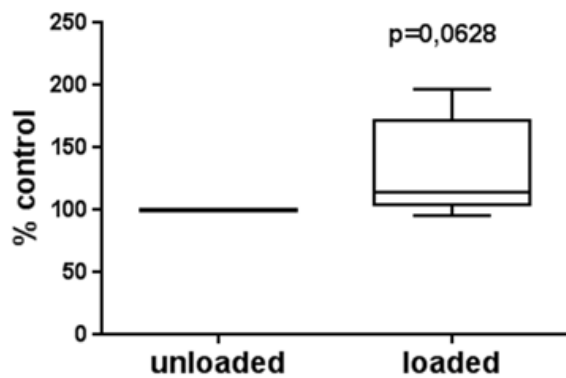

Fig. 4.8. Influence of loading on 2 consecutive days on adhesion of RAW 264.7 cells. The figure shows the unloaded, unstimulated cells, set to 100 %, and in relation the loaded, unstimulated cells, depicted as respective percentage. Boxplots represent median and the whiskers cover minimum to maximum. Comparison between loaded and unloaded cells: Mann-Whitney test. $p < 0.05$. Assay was performed in triplicates. n=7.

Stimulation with 10^{-8} M SP significantly reduced adhesion of unloaded RAW cells (Fig. 4.9, A). Additionally, stimulation effects of 10^{-10} M SP differed significantly in unloaded and loaded samples. Adhesion of unloaded controls stimulated with 10^{-10} M SP was significantly higher compared to respective loaded RAW 264.7 macrophages.

In loaded RAW macrophages, stimulation with 10^{-10} M αCGRP, 10^{-7} M CGRP$_{8-37}$ and the combination of αCGRP and CGRP$_{8-37}$ significantly reduced adhesion compared to unstimulated and loaded cells (Fig. 4.9, B). Additionally, stimulation with the CGRP receptor antagonist, CGRP$_{8-37}$ alone, resulted in significantly opposite effects on adhesion in loaded and unloaded RAW 264.7.
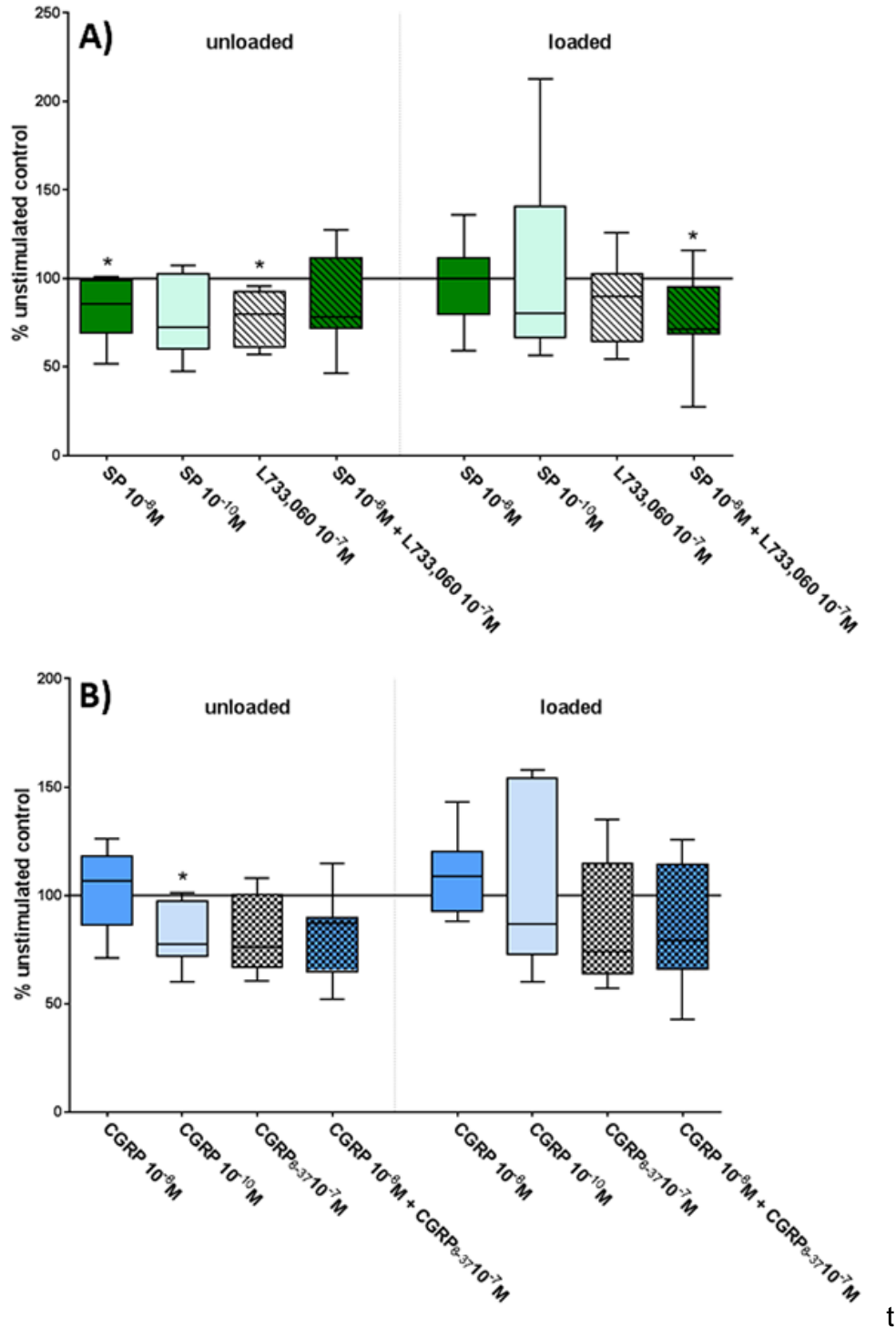
Fig. 4.9. Influence of sensory neuropeptide stimulation on adhesion of loaded and unloaded RAW 264.7 cells. The unloaded and loaded cells (loading on 2 consecutive days) without stimulation were set to 100 % (continuous line) and the results for the stimulation are depicted as respective percentage. A) shows the results for stimulation with SP, the neurokinin receptor 1 antagonist L733,060 as well as both in combination. B) shows the results for stimulation with αCGRP, the receptor antagonist $CGRP_{8-37}$ as well as the combination of both. Boxplots represent median and the whiskers cover minimum to maximum. Comparison of differences to control (100 %): Wilcoxon-signed rank test (asterix directly above box), comparison of stimulations between loaded and unloaded: Mann-Whitney test. * p<0.05. Assay was performed in triplicates. n=7.

53

4.2.3 Apoptosis

The apoptosis of RAW 264.7 macrophages was analyzed by measuring caspase 3/7 activity.

Apoptosis rate was increased in loaded cells in relation to respective unloaded control cells (Fig. 4.10). The effect was significant after 6 and 24 h.
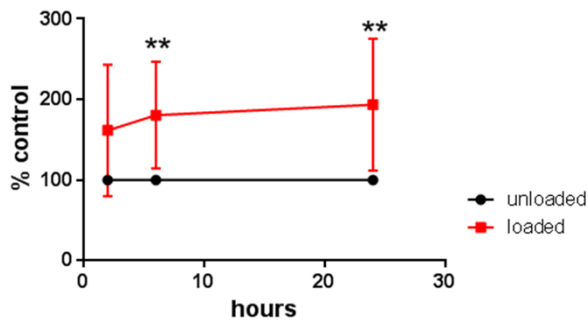
Fig. 4.10. Influence of loading on 2 consecutive days on apoptosis of RAW 264.7 cells. The figure shows the caspase 3/7 activity after 2, 6 and 24 h of unloaded, unstimulated cells, set to 100 % (black), and in relation of the loaded, unstimulated cells, depicted as respective percentages (red). Error bars show standard deviation. Comparison between loaded and unloaded cells: Mann-Whitney test. ** $p<0.01$. The assay was performed in triplicates. n=5.

Apoptosis of RAW macrophages at different time points was not affected by neuropeptide or receptor antagonist stimulation (Fig. 4.11).

2 hours

A)

B)

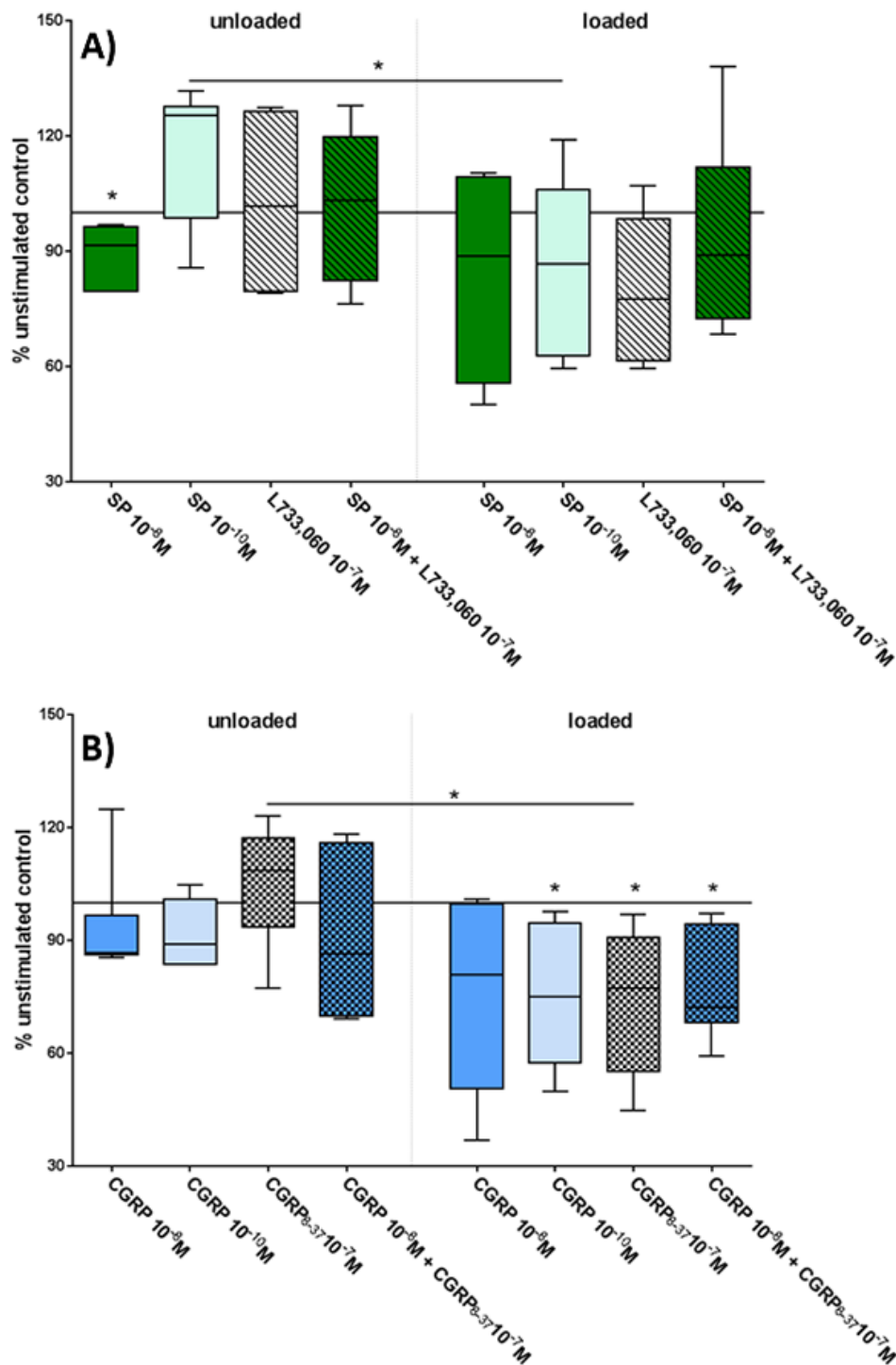**6 hours**

C)

D)

24 hours

E)

F)
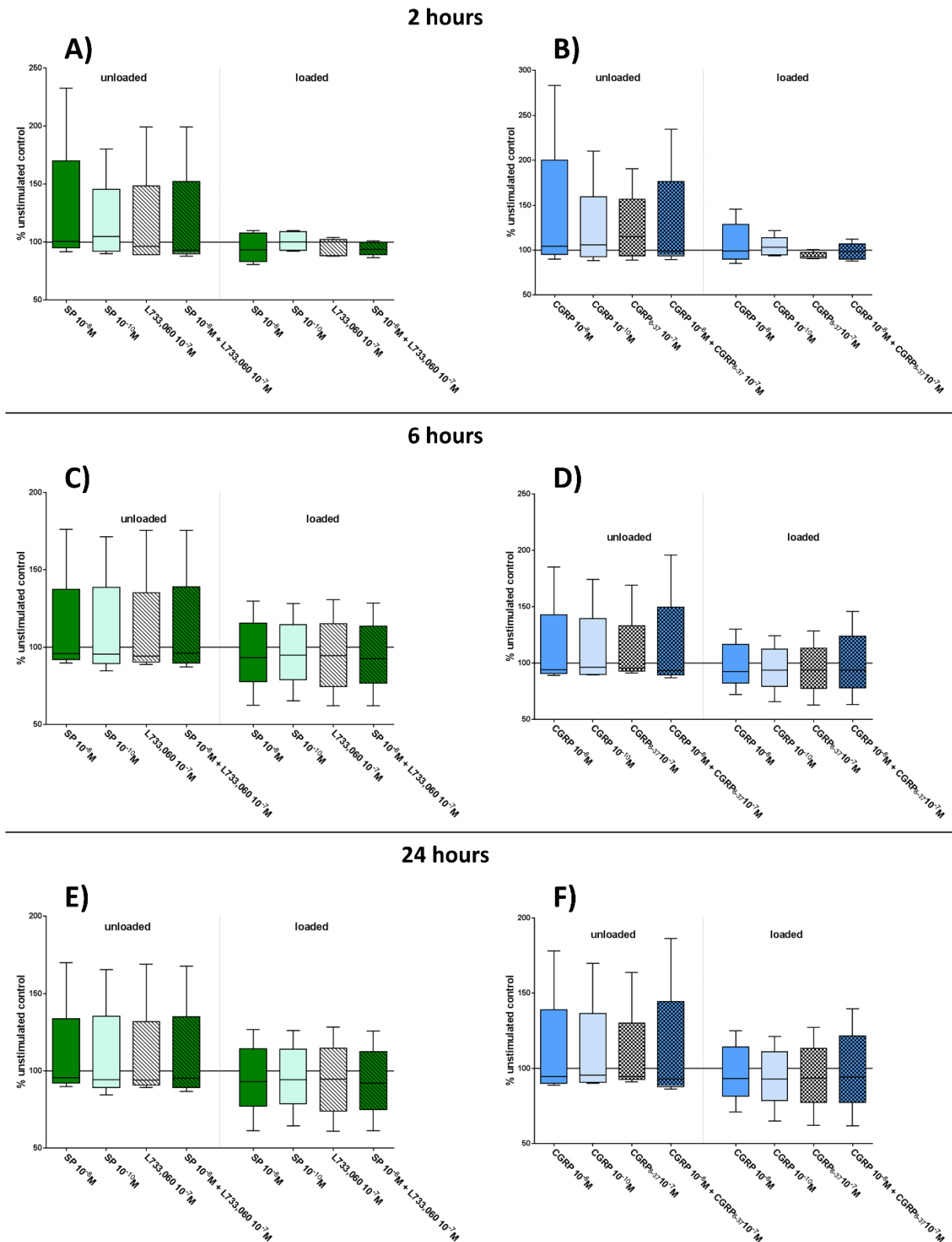
Fig. 4.11. Influence of sensory neuropeptide stimulation on apoptosis of loaded and unloaded RAW 264.7 cells. The unloaded and loaded cells (loading on 2 consecutive days) without stimulation were set to 100 % (continuous line) and the results for the stimulation are depicted as respective percentage. A), C) and E) show the results for stimulation with SP, the neurokinin receptor 1 antagonist L733,060 as well as both in combination after 2, 6 and 24 h respectively. B), D) and F) show the results for stimulation with αCGRP, the receptor antagonist CGRP$_{8-37}$ as well as the combination of both. Boxplots represent median and the whiskers cover minimum to maximum. Assay was performed in triplicates. n=5.

55

4.2.4 Osteoclastogenesis

Establishing the osteoclastogenesis procedure of RAW 264.7 macrophages appeared to be difficult. Cell adhesion and differentiation on normal plastic 6-well-plates was possible, but adhesion and differentiation on the silicone membrane of the FlexCell plates was a challenge. Collagen-I-coated plates improved the outcome, yet the results were highly variable. During the last set of experiments, osteoclastogenesis of RAW 264.7 macrophages was evaluated after 7 days of differentiation. Neither culture of controls nor loaded cells showed an appropriate number of osteoclasts (results not shown). As a consequence, neuropeptide stimulation did not show any effects. Overall, osteoclastogenesis of RAW 264.7 macrophages on flexible membrane plates requires further establishment.

4.3 Impact of mechanical loading on gene expression of marker genes related to osteoclastogenesis in RAW 264.7 macrophages

Colony-stimulating factor 1 receptor (c-FMS/ CSF1R) and receptor activator of NF-kB receptor (RANK) are the receptors for the major osteoclast differentiation factors M-CSF (macrophage colony-stimulating factor) and RANK ligand (RANKL). The purpose of this experiment was to determine the impact of mechanical loading on gene expression of marker genes related to osteoclastogenesis. The gene expression analysis of the two receptors showed an increase in c-FMS and a significant upregulation of RANK after loading (Fig. 4.12).

Fig. 4.12. Influence of loading on 2 consecutive days on gene expression of osteoclast differentiation markers in RAW 264.7 cells. Gene expression is depicted as relative quantification (RQ). The gene of interest was referred to the endogenous control gene, GAPDH, and the loaded samples to the unloaded controls (calibrator). The figure depicts the effect of loading on osteoclast differentiation marker genes c-FMS (colony-stimulating factor-1 receptor gene) and RANK receptor (receptor-activator of NF-κB). Wilcoxon-signed rank test. *** $p < 0.001$. qPCR was performed in duplicates. n=15.

4.4 Impact of mechanical loading on gene expression of markers for macrophage polarization in RAW 264.7 macrophages

To test whether loading might polarize RAW 264.7 macrophages towards the pro-inflammatory M1 or the anti-inflammatory M2 phenotype, a panel of respective marker genes was analyzed by qPCR. Loading induced a significant upregulation of proinflammatory M1-associated genes (Fig. 4.13). Gene expression of IL-6, iNOS (inducible nitric oxide-synthase), NFkB (nuclear factor kappa-b) and TNF-α (tumor necrosis factor-α) was upregulated after exposure to mechanical stress. Expression of M2-associated genes such as IL-10, MRC-1 (mannose receptor) and KLF4 (krüppel-like factor) was not affected by loading.
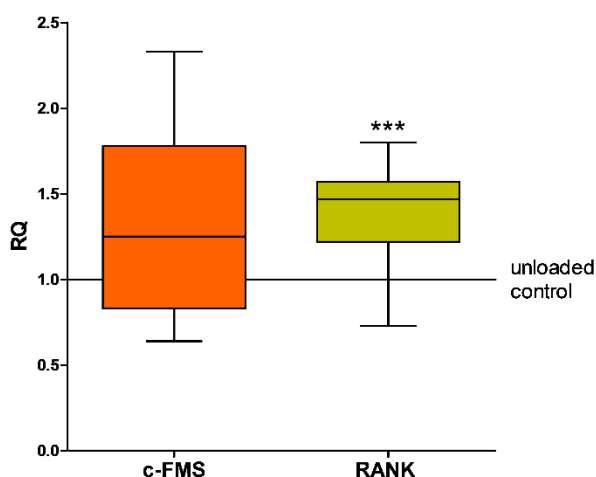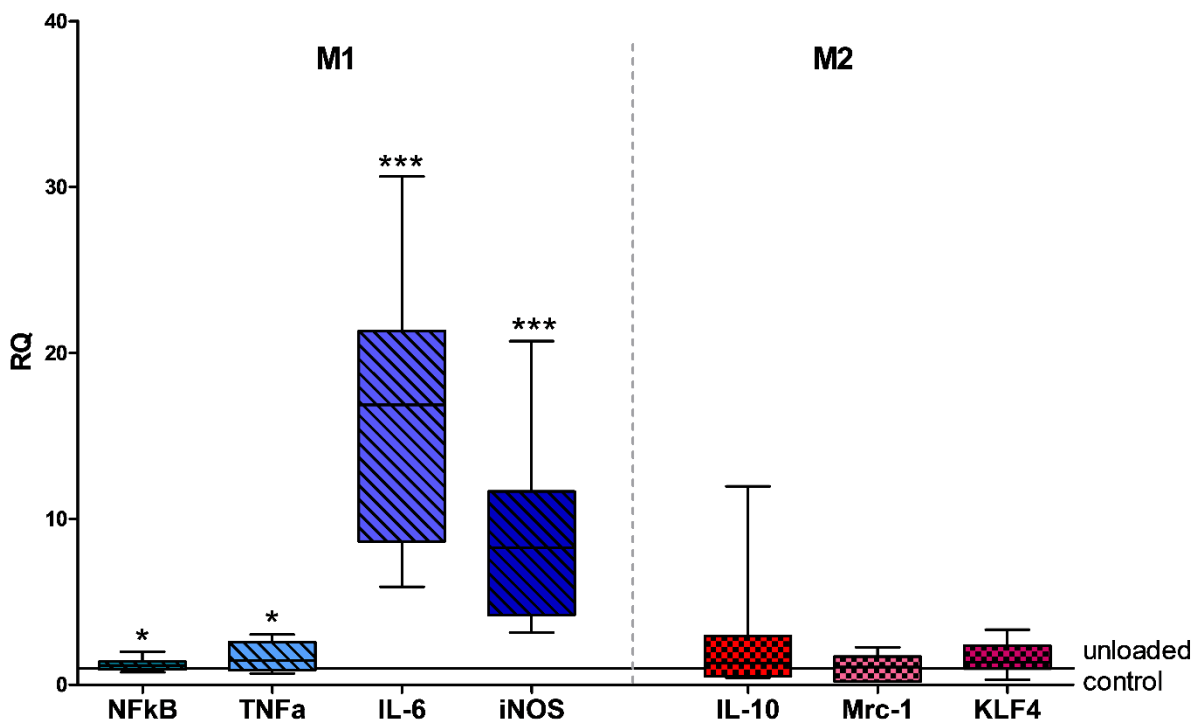

Fig. 4.13. Influence of loading on 2 consecutive days on gene expression of macrophage polarization markers in RAW 264.7 cells. Gene expression is depicted as relative quantification (RQ). The gene of interest was referred to the endogenous control gene GAPDH, and the loaded samples to the unloaded controls (calibrator). The figure shows the influence of loading on genes characterizing macrophage polarization. M1 markers included NFκB (nuclear factor κB), TNF-α (tumor necrosis-factor), IL-6 (interleukin 6) and iNOS (inducible nitric oxide-synthase), M2 markers included IL-10 (interleukin 10), MRC-1 (mannose receptor) and KLF4 (kruppel-like-factor). Wilcoxon-signed rank test. * p<0.05, *** p<0.001. qPCR was performed in duplicates. n=15.

4.5 Impact of mechanical loading and sensory neuropeptide stimulation on inherent metabolic activities of primary BMM from DMM and Sham mice

4.5.1 Proliferation

The impact of mechanical loading on the proliferative activity of primary BMM was compared between BMM isolated from mice 2 and 8 weeks after either DMM or Sham surgery to analyze whether OA induction could alter mechanosensation/responsiveness in the context of sensory neuropeptide stimulation. Mechanical strain on BMM derived from DMM mice increased the proliferation rate at 2 weeks (Fig. 4.14, A) and significantly after 8 weeks (Fig. 4.14, B) in relation to respective unloaded BMM control. The effect seemed to be less obvious in Sham-BMM. Neither SP nor αCGRP appeared to have an additive effect on proliferation of loaded and unloaded BMM (Figure 4.15) isolated from either DMM or Sham mice, but interpretation of the results is difficult due to low sample number and high variability of the data.

Fig. 4.14. Influence of loading on 2 consecutive days on proliferation of bone marrow-derived macrophages, 2 and 8 weeks after induction of OA. Each figure shows the unloaded, unstimulated DMM/ Sham cells, set to 100 %, and in relation the respective 2-day-loaded, unstimulated cells, depicted as respective percentages 2 weeks (A) and 8 weeks (B) after surgery. Boxplots represent median and the whiskers cover minimum to maximum. Comparison between loaded and unloaded cells: Mann-Whitney test. * p<0,05. Assays were performed in triplicates. n=3-4.
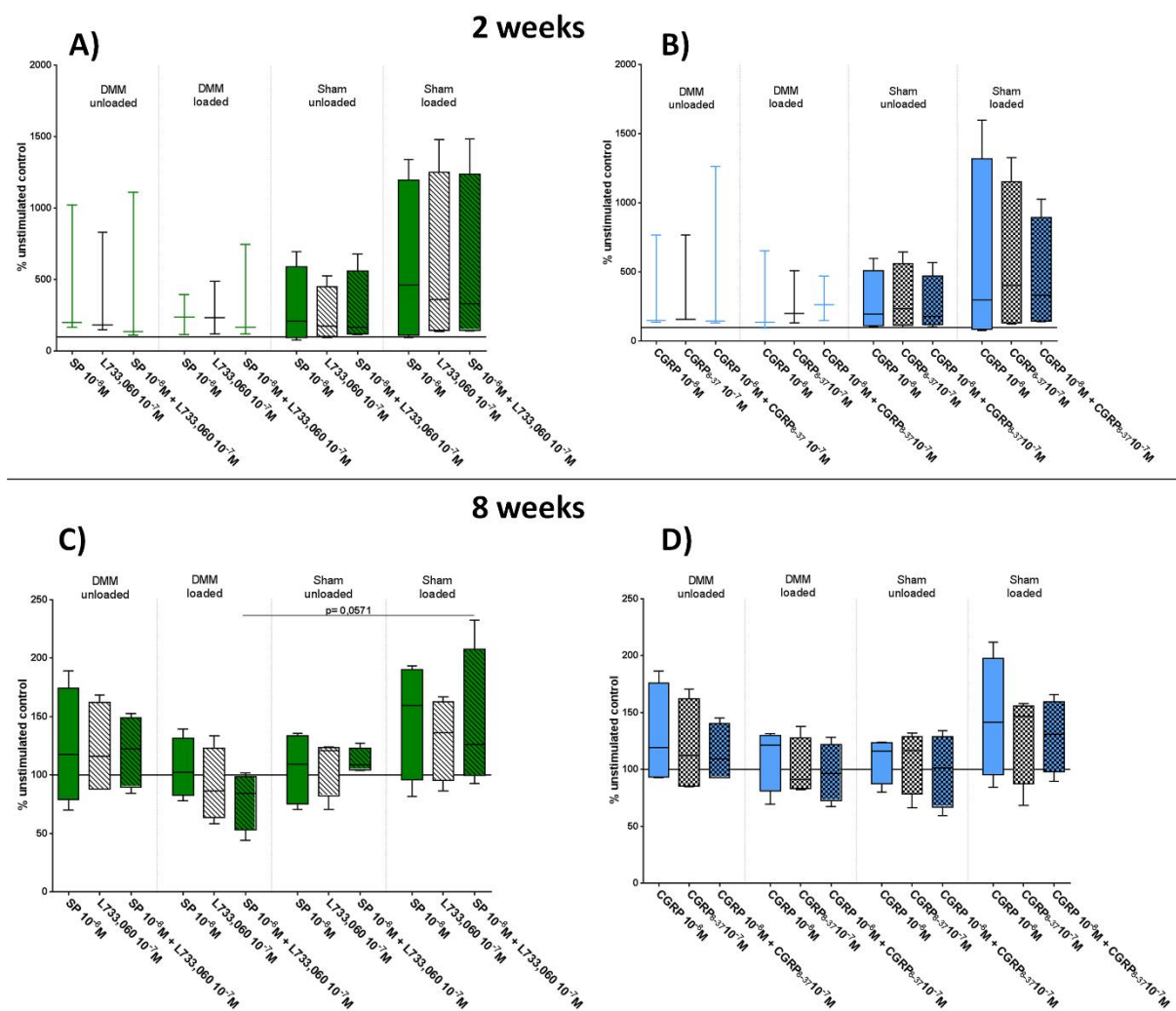
Fig. 4.15. Influence of sensory neuropeptide stimulation on proliferation of bone marrow-derived macrophages. The unloaded and loaded cells (loading on 2 consecutive days) without stimulation were set to 100 % (continuous line) and the results for the stimulation are depicted as respective percentage. A) and C) show the results for stimulation with SP, the neurokinin receptor 1 antagonist L733,060 as well as both in combination 2 and 8 weeks after surgery, respectively. B) and D) show the results for stimulation with αCGRP, the receptor antagonist CGRP$_{8-37}$ as well as the combination, 2 and 8 weeks after surgery, respectively. Boxplots represent median and the whiskers cover minimum to maximum. Comparison of stimulations between loaded and unloaded: Mann-Whitney test. Assay was performed in triplicates. n=3-4.

4.5.2 Apoptosis

The impact of mechanical loading on apoptosis of primary BMM was compared between BMM isolated from mice 2 and 8 weeks after either DMM or Sham surgery to analyze whether OA induction could alter mechanosensation/responsiveness in the context of sensory neuropeptide stimulation. The caspase 3/7 activity after 2, 6 and 24 h was correlated to the apoptosis rate of stressed cells and controls. Apoptosis rate was unaffected in BMM, 2 weeks after the surgical OA induction (Fig. 4.16, A). A higher

apoptosis rate was observed in loaded BMM, isolated 8 weeks after either Sham or DMM surgery induced a higher apoptosis rate (Fig. 4.16, B). The caspase 3/7 activity was significantly increased in DMM-BMM after 2,6 and 24 h whereas the caspase 3/7 activity of Sham-BMM increased with delay after 6 and 24 h.
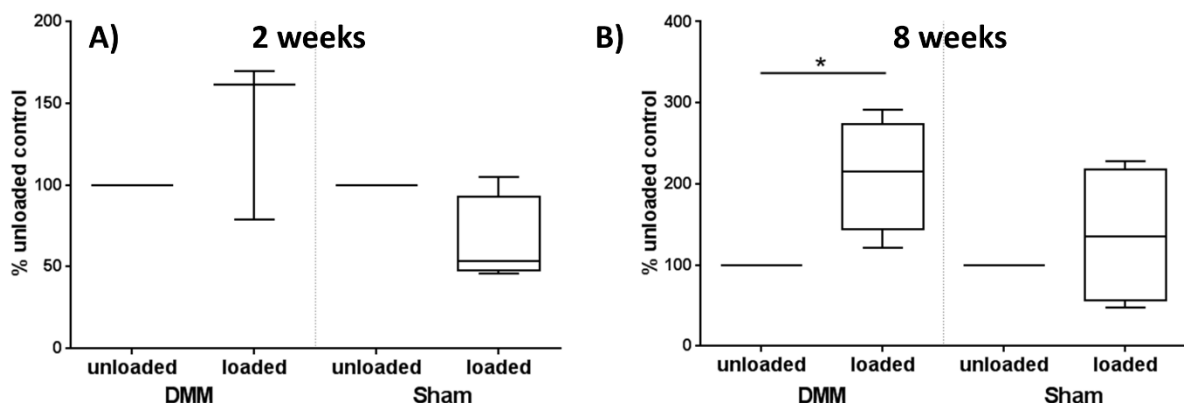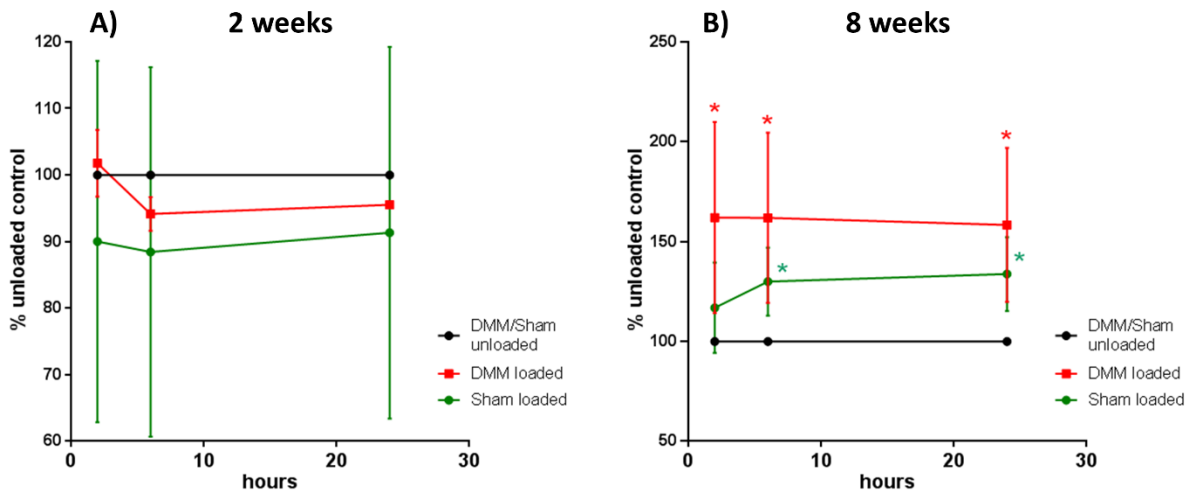

Fig. 4.16. Influence of loading on 2 consecutive days on apoptosis of bone marrow-derived macrophages, 2 and 8 weeks after induction of OA. The graphs show repeated measurements (2,6, 24 h) of caspase 3/7-mediated apoptotic activity of loaded, unstimulated BMM (red: DMM, green: Sham) 2 (A) and 8 (B) weeks after surgery in relation to the unloaded, unstimulated DMM/Sham cells, set to 100 % (black). Error bars show standard deviation. Comparison between loaded and unloaded cells: Mann-Whitney test, * p<0,05. Assays were performed in triplicates. n=3-4.

Stimulation with SP, αCGRP, their receptor antagonists and the combination of both in BMM 2 weeks after OA induction did not have significant effects on the apoptosis rate (Fig. 4.17).

In BMM at 8 weeks after OA induction, results did not differ highly, but some significant effects were measurable (Fig. 4.18). Stimulation of BMM with 10^{-8} M SP and 10^{-8} M CGRP had significantly different effects on loaded DMM- and Sham BMM. Loaded Sham-BMM had a higher apoptosis rate compared to loaded DMM-BMM (6 h after loading). The same effect was detectable for the combination of 10^{-8} M SP and 10^{-8} M CGRP and their respective receptor antagonists (Fig. 4.18, C and D).
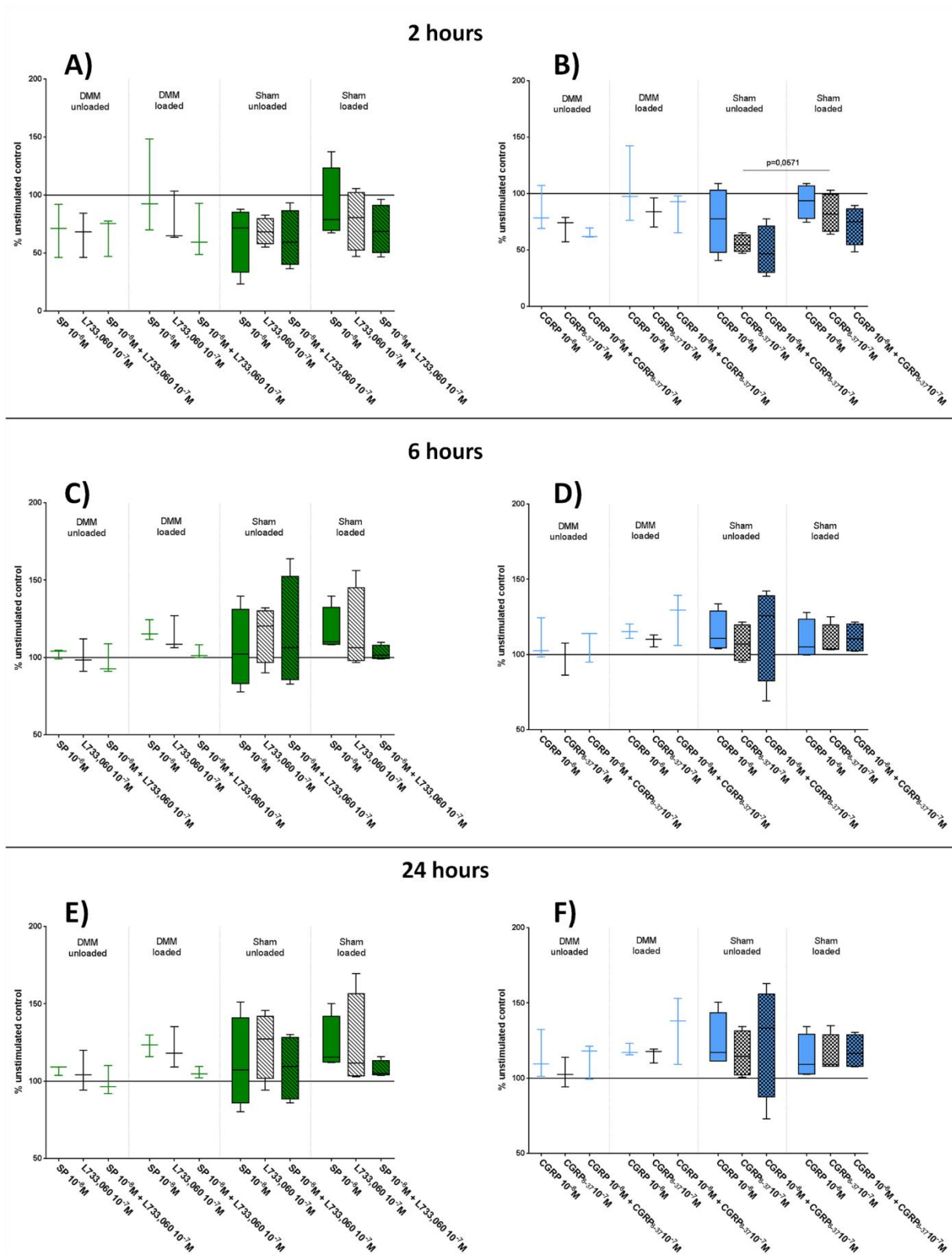
Fig. 4.17. Influence of sensory neuropeptide stimulation on apoptosis of bone marrow-derived macrophages, 2 weeks after the induction of OA. The unloaded and loaded cells (loading on 2 consecutive days) without stimulation were set to 100 % (continuous line) and the results for the stimulation are depicted as respective percentage. A), C) and E) show the results for stimulation with SP, the neurokinin receptor 1 antagonist L733,060 as well as both in combination. B), D) and F) show the results for stimulation with αCGRP, the receptor antagonist CGRP$_{8-37}$ as well as the combination. Boxplots represent median and the whiskers cover minimum to maximum. Comparison of differences

Fig. 4.18. Influence of sensory neuropeptide stimulation on apoptosis of bone marrow-derived macrophages, 8 weeks after the induction of OA. The unloaded and loaded cells (loading on 2 consecutive days) without stimulation were set to 100 % (continuous line) and the results for the stimulation are depicted as respective percentage. A), C) and E) show the results for stimulation with SP, the neurokinin receptor 1 antagonist L733,060 as well as both in combination. B), D) and F) show

the results for stimulation with α-CGRP, the receptor antagonist $CGRP_{8-37}$ as well as the combination. Boxplots represent median and the whiskers cover minimum to maximum. Comparison of differences to control (100 %): Wilcoxon signed rank test (asterix directly above box), comparison of stimulations between loaded and unloaded: Mann-Whitney test. * $p < 0.05$. Assays were performed in triplicates. n=4.

4.5.3 Osteoclastogenesis

Similar to RAW 264.7 macrophages, osteoclastogenesis turned out to be challenging when cells were seeded onto the silicone membrane of the FlexCell plates due to incomplete adhesion. Collagen-I-coated FlexCell plates improved the outcome, yet the results remained highly variable. After osteoclast counting using Adobe Photoshop, it seemed that loading reduced the osteoclast numbers per well, also in combination with neuropeptide stimulation (Fig. 4.19). Primary BMMs derived from either DMM or Sham mice did not affect this result. Due to the described methodological difficulties, differentiation and osteoclast numbers were highly variable throughout the experiments and valid comparisons were not possible. Overall, osteoclastogenesis of the primary BMM groups did not show any significant differences that would allow further conclusions.
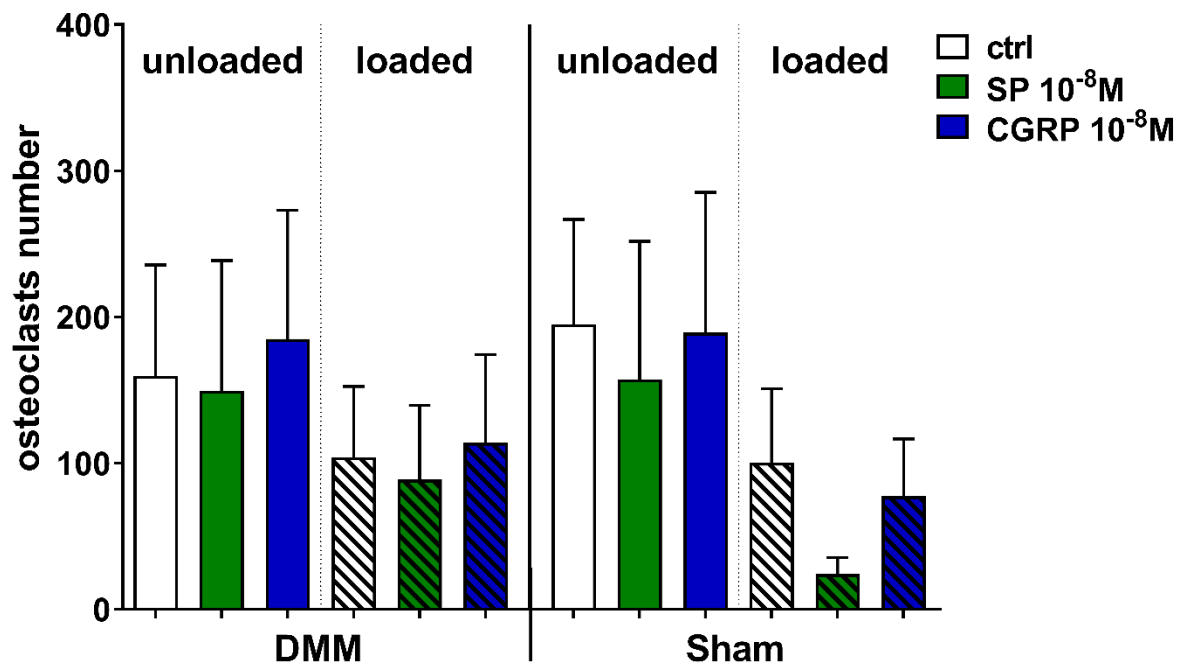
Fig. 4.19. Influence of mechanical loading and neuropeptide stimulation on osteoclastogenesis of BMM isolated 8 weeks after DMM or Sham surgery. BMM were isolated 8 weeks after DMM or Sham surgery and subjected to osteoclastogenesis under loading. The graph shows absolute osteoclast numbers per well of unstimulated BMM and BMM stimulated with 10-8 M SP or 10-8 M CGRP. Wells remained unloaded or were loaded for 4 h per day on 5 consecutive days. n= 5-6.

5 Discussion

5.1 Methodological discussion

5.1.1 Cyclic stretch as a mode of mechanical force

Since cell stress evoked by mechanical forces is known to modulate the function of various cells in a physiological and pathophysiological fashion, many studies have tried to elucidate mechanisms and pathways of mechanotransduction. Different types of mechanical stimulation were used in these experiments, such as cyclic or static strain or tension [23,190,191], 3-point- or 4-point-bending [192,193], compressive [194] or tensile force, hydrostatic or -dynamic pressure, fluid shear stress [77] or microgravity. In this study, we used cyclic stretch, a frequently used method in the field of mechanobiology [72,73,195–202]. Stretch is applied by seeding cells on a flexible membrane which transfers the material stretch to the cells seeded on top. In vitro macrophage cultures were performed in 2D in literature and hence, we chose the 2D approach. This allowed culture of macrophages at a sufficient number needed for the gene and protein expression analysis performed after loading. Initially, we considered performing the experiments using hydrostatic pressure, but 3D cultivation of macrophages requires more advanced techniques and allows analysis of only low numbers of cells at a time. Additionally, the hydrostatic equipment did not perform as reliable as we would have needed. Yet, 3D experiments on macrophages become more popular, since it was shown that cell parameters like migration and cytokine expression, as well as cell morphology changed significantly in 3D-cultured macrophages compared to 2D cultures [27,203].

5.1.2 Loading parameters

The comparison of studies using cyclic stretch is difficult due to the high variation in the parameters used to apply mechanical load including the frequency, strain of the flexible membrane and the duration of the experiment.

According to a variety of studies, a frequency of 1 Hz, indicating one stretch per second, was chosen for the force protocol. This physical value of mechanical input is consistent with parameters described in various experiments using rabbit osteoclasts, mouse osteoblasts, human tenocytes, synoviocytes, mesenchymal stem cells and RAW 264.7 macrophages [23,73,76,77,199,200].

The amplitude, equaling the percent of stretch applied to the membrane, is another parameter that has a critical impact on the outcome of the experiments. Translating tissue strain into experimental studies is challenging and the true physiological value is hardly ever achieved. After extensive research of the literature, we decided to use a 10% stretch that was commonly used in a number of published studies. The group of Backman et al. stretched human tendon cells with a 10 % strain [23], also Kameyama et al. stretched RAW 264.7 cells with this amplitude, inducing osteoclastogenesis under mechanical loading [72]. After applying 10 % elongation and 0.5 Hz for 48 h, Shibata et al. measured the effect of force release on osteoclastogenesis [79]. Furthermore, human mesenchymal stem cells were tensioned with a 10 % elongation [200].

Membrane stretch can either be produced by application of a vacuum or by mechanical means, like a stamp that is pressed against a membrane. The disadvantage of machines that cause a stretch through inducing a vacuum traction is the production of a strain that highly exceeds physiological values perceived in bone tissue and joints [204]. Stretch can be measured in micro-strain (change of length divided through initial length); by definition a strain of 1000 µε equals a cellular deformation of 0.1 % [73,76]. Based on this calculation, the 10 % stretch used in the present study equals 100.000 µε and lies far above the physiological bone strain ranging from 5 to 3000 µε [205–208]. In contrast, it has been demonstrated that single bone cells require a 20 to 100 fold higher loading rate and deformation than the whole bone itself [209]. Wall et al. observed that tenocytes experienced only 37±8 % of the equi-biaxial strain on the cellular level compared to the applied strain magnitude [190]. Agarwal et al. state that during physiological movement, the strain on articular chondrocytes in vivo is 15 %, causing a 5 % elongation of the cells [10]. The 10% strain in our experiments, induced by stretching using a mechanical stamp, might comply best to the actual physiological stress. In general, physiological and non-physiological stress, that was observed in joint tissue cells in OA, is hard to reproduce in an experimental setting and this needs to be considered when interpreting the results of this study. Ultimately, extensive pre-studies would have been required to elucidate which parameters would be best to evoke physiological and non-physiological responses in specific cell types. Using data from the literature, only allows for comparison of experimental outcomes to previous studies and does not necessarily reflect the actual in vivo situation.

65

Loading times described in the literature range from 2 h [23,72] up to 48 h [79]. Times might vary as some tissues usually might experience constant loading (e.g. heart, lung), whereas musculoskeletal tissues experience alternating periods of rest and loading. For example, Sumanasinghe et al. stretched human mesenchymal stem cells for 4 h per day, lasting up to 14 days [200]. Another study exposed rat fibroblasts to 2, 4 and 6 h of compressive loading [194]. Hence, our choice of 4 h-loading cycles is defensible and resembles time periods used in other studies.

A shortcoming of this study might be the varying loading times of the experiments for the gene and protein expression. Gene expression was measured after 2 days of mechanical loading, whereas the protein expression was examined after 3 consecutive days of loading. The initial NK1R western blot showed a significant increase of the NK1R protein after 2 days of loading, therefore we defined a 2-day loading regime for the experiments. Repeating the western blot experiments shifted the increase in NK1R expression from 2 to 3 days, however, we kept the 2-day loading protocol for the gene expression studies, as gene expression changes precede protein expression.

5.1.3 Culture material

Adlerz et al. demonstrated that human macrophages regulate their behavior in response to the substrate property: apart from an increased cell volume and higher migration speed, they could observe a higher proliferation rate of macrophages cultured on stiff substrates compared to soft ones [210]. Plastic and glass are materials that macrophages can successfully be cultured on, although they only form weak adhesions. Potentially, a high number of individually weak adhesions might eventually form sufficient and strong adhesion complexes [211]. This might explain why osteoclast differentiation on common 6-well plastic plates was easily successful in our experiments but appeared to be difficult on the soft membranes of the BioFlex® culture plates. Other investigators faced similar problems using flexible membranes as the ones produced by Flexcell® or silicone dishes [212]. Macrophages were cultured successfully on fibronectin-coated culture dishes, a molecule responsible for adhesion and integration of cells to the extracellular matrix [213]. For this study, we decided to use collagen I-coated dishes, as collagen I is the major extracellular matrix protein of bone and therefore should support osteoclast differentiation on the soft Flexwell® membranes. Contrary to expectations, we could not achieve an improved osteoclastogenic differentiation on collagen I-coated plates. Later, a more in depth

literature search indicated an osteoclastogenic inhibition when using collagen I. For example, osteoclast differentiation of murine bone marrow macrophages was reduced on collagen I-coated dishes [214,215]. Furthermore, artificial extracellular matrix (ECM) preparations containing collagen I repressed the differentiation and activation of human osteoclasts [216]. Additionally, collagen I had a mild cytotoxic effect on rat vascular smooth muscle cells and led to a reduced cell attachment to the culture dish surface after exposure to reactive oxygen-producing macrophages [217]. Besides, when plated on collagen I, rat osteoclasts appeared to have a rather round morphology, contrary to the spread phenotype during cultivation on glass plates [218]. Gowen and colleagues studied the attachment of RAW 264.7 macrophages to different molecular forms of collagen I. Macrophages adhered significantly to monomeric, heat-denatured collagen I via scavenger-receptors, but only poorly to the native, fibrillar form of collagen I [35]. Apart from these experimental insights regarding culture dish surfaces, the group of Ikeda observed a density-dependent differentiation of bone marrow macrophages. The cell density on the culture plates at seeding and during differentiation was critical for the number of osteoclasts that appeared after three to four days [219,220]. Therefore, we suggest that various modalities like surface structure and cell seeding influence macrophage phenotype and activity critically and need to be considered in experimental studies. It is thought that substrate stiffness is more important for successful macrophage cultivation or osteoclast differentiation and surface manipulation by coating with ECM molecules might not be able to fully overcome growth restrictions induced by soft surface materials. Another experimental approach to achieve better cell attachment and growth results on collagen I-coated, soft stretch membranes might be the co-culture of osteoclasts and osteoblasts. This could mimic the physiological balance that these cells keep in the bone milieu in vivo and potentially ameliorate osteoclast differentiation. Furthermore, osteoblasts might produce a matrix that is closer to the natural osteoclast substrate in bone.

5.2 Result discussion

Macrophages are cells with various tasks and abilities, ranging from immunological functions to providing the osteoclast precursor pool. They are able to modulate their cell shape and phenotype, dependent upon the surface substrate and the environmental conditions. Macrophages are regulated by numerous molecules including cytokines, chemokines and neurotransmitters and can react to mechanical forces such as tension in the bone or stretch in the lungs. Macrophages are unique in their ability to adjust to a plethora of endogenous and exogenous factors and acquire a range of phenotypes to adjust to their current environment. The sensory neuropeptide, SP, is able to influence osteoclasts and their precursors, the macrophages [61]. Macrophages might also respond to αCGRP as they express the respective receptors [62]. The main interest of this work was how the combination of sensory neuropeptide stimulation and mechanical loading affects macrophage behavior.

5.2.1 Impact of mechanical loading on gene and protein expression of the neuropeptides SP and αCGRP and their receptors in RAW 264.7 macrophages

5.2.1.1 NK1R and SP expression: formation of a negative feedback loop

The mechanosensing potency of NK1R has first been observed by Millward-Sadler et al. in chondrocytes of human articular cartilage [20]. So far, studies have demonstrated that various bone cells, specifically osteocytes [21] and also osteoclasts [161,162], possess the NK1R, but mechanotransduction processes have not been analyzed yet. Our study of gene and protein expression of NK1R and SP after mechanical force application indicate a negative feedback loop between SP and its receptor: after loading, the NK1R gene and protein were upregulated, whilst there was a downregulation of SP gene expression. Opposite to the results of our study, mechanical loading of tenocytes led to an increased SP mRNA and decreased NK1R mRNA expression [23]. Yet consistent with our observations, Backman et al. suggest a negative feedback loop as the regulating mechanism for SP release and production. In accordance to their study, further experiments of our group revealed a reduced NK1R mRNA expression after SP stimulation of unloaded RAW 264.7 macrophages, while SP mRNA expression of stretched murine macrophages was further reduced by picomolar SP concentrations [52]. The altered gene and protein expressions of NK1R

and SP observed in this study demonstrated for the first time an involvement of the tachykinin system in mechanotransduction processes of murine macrophages. A negative feedback loop between NK1R and SP, as previously described in the literature has been confirmed after application of shear stress on RAW 264.7 macrophages.

After SP binding to its receptor, the NK1R receptor is internalized from the cell surface into the cytoplasm and recycled afterwards [221,222]. This internalization is accompanied by cell desensitization towards SP stimulation through modulation by β-arrestin. Furthermore, low concentrations of SP induce a rapid NK1R recruitment to the cell surface, whereas high SP concentrations lead to a prolonged recycling process [46], supporting the hypothesis of a negative feedback loop of the receptor and its ligand. On the other hand, Koh et al. observed a higher NK1R expression following SP stimulation of murine pancreatic cells, suggesting a positive feedback loop [223]. Exercise-induced loading of salmon osteocytes and osteoblasts resulted in increased SP mRNA/ protein and NK1R protein levels [22]. In conclusion, our results partly differ from previous studies presumably due to differences in cell type, loading modality and parameters used in various studies, individual cell reactivity towards mechanical stimuli and complex physiological cellular interplay in vivo. Furthermore, the NK1R-SP-response might be confounded by additional/parallel receptor-ligand interactions. For example, SP might also bind to NK2R and NK3R, though with a much lower affinity [224]. Hence, effects mediated via these receptors also need to be considered when interpreting the results. Additionally, Neurokinins A and B cross-react with NK1R, which might interfere especially in in vivo observations [225].

Results from previous studies indicate that SP has different metabolic effects depending upon cell type and the used peptide concentration. During embryonic development and skeletal growth, SP seems to have anabolic effects, whereas in adult organisms, it promotes catabolic actions, as shown in chondrocytes [17,145]. Bone formation is affected positively when stimulated with a concentration higher than 10^{-8}M, but inhibited with low or no SP stimulation [17]. Current research reports about SP effects on various cell types confirm the assumption of a trophic function of the neuropeptide. In the evaluated studies, apoptosis was unchanged [155] or lowered [158] after stimulation with SP, whereas the proliferation of chondrocytes was enhanced [23,60,155–157,226]. The effect of SP on adhesion was mixed [155,227].

However, the combination of SP stimulation and loading has not been examined in depth so far and little is known about the combined effects of these two conditions. We observed a reduced adhesion and proliferation in unloaded RAW 264.7 macrophages but no effects in loaded cells. It can be concluded that loading seems to alter the reactivity of the tachykinin system resulting in changes in metabolic responses to SP stimulation. Furthermore, altered SP concentration or binding reactivity might have a major impact on experimental outcomes. In the first place, SP is likely to produce a high intra-assay variability due to a less selective receptor binding to the NK1R. Another reason might be digestion via rapid peptidases [228]. In tissues, unbound SP turnover is more rapid than in the central nervous system, mediated by the metalloendopeptidase neprilysin [46,229]. The half-life of SP is dependent on its binding to certain molecules and on its site of action. The SP half-life is prolonged by binding of fibronectin and differs between blood and tissues [46].

In conclusion, we demonstrated that mechanical loading interferes with the gene expression of NK1R and SP by formation of a negative feedback loop. Still, further effects of SP stimulation on macrophages were neglectable and almost undetectable in combination with loading. Therefore, follow-up studies are needed to reveal additional SP effects.

5.2.1.2 Are α-CGRP and its receptors involved in macrophage mechanotransduction?

To our knowledge, there is no observation published that the αCGRP receptor is mechanosensitive or -responsive. It might enhance the mechanosensation of articular chondrocyte nociceptors in rats with surgically induced OA [230]. We observed that the gene expression of αCGRP is influenced by mechanical loading. αCGRP mRNA was not detectable in unloaded RAW 264.7 cells, but expression was induced in loaded cells. Yet, the protein expression of αCGRP, measured by ELISA, remained unaffected indicating that alterations of protein expression require a longer loading duration, other frequency or different neuropeptide concentration.

Additionally, cyclic stretch increased the gene and protein expression of the CRLR subunit but not the co-receptor unit, RAMP1, that is responsible for the receptor specificity for αCGRP. In a study using vascular smooth muscle cells (VSMC), a similar effect was observed [231]. After exposure to hypoxia, the CRLR mRNA was elevated

70

after 3 and 4 h, whilst there was no change in RAMP1 mRNA. Exposing VSMC to chronic hypoxic stress increased both CRLR and RAMP1 mRNA. Similar observations were made by Nikitenko and colleagues who detected an activated CRLR gene transcription under hypoxia in microvascular endothelial cells, whereas the expression of RAMP1, 2 and 3 also remained unaffected by low oxygen levels [232]. Though the experimental conditions differ, it seems that cell stress, whether induced by hypoxia or mechanical loading, has comparable effects on the expression of the CGRP receptor complex. In addition to our short-term loading protocol, a longer mechanical loading period could show how CRLR and RAMP gene expression would develop during chronic mechanical stress. From the studies reported so far, it can be assumed that RAMP1 mRNA and protein expression might be upregulated with increasing duration or force independent of the CRLR subunit, as shown in a condition of chronic stress.

The binding affinity of αCGRP is highest to the CRLR/RAMP1 complex. Besides, αCGRP binds with lower affinity to the receptors formed with RAMP2 and RAMP3 that are most sensitive to adrenomedullin, as well as the amylin receptor subtypes, AMY1 and AMY3 [179]. Considering this complex cross-reactive system, it is difficult to relate αCGRP effects only to the CRLR/RAMP1 receptor, because the influence of other receptor responses cannot be excluded. Regarding in vivo conditions, adrenomedullin and intermedin can evoke a signal when binding to the CRLR/RAMP1 complex but with lower potencies than αCGRP [182]. Additionally, the receptor component protein (RCP) might modulate CRLR/ RAMP1 signaling efficacy in vivo. RCP is responsible for the coupling of CRLR with RAMP1. If the RCP expression is enhanced, the receptor signaling is increased [181]. Since enhanced RCP levels in the spinal cord and an elevated αCGRP sensitivity are reported during the inflammatory stage of osteoarthritis, the participation of RCP in CRLR signaling can be assumed [233]. The effect of loading on the RCP expression is not yet known, but it can be assumed that mechanical stress might also affect RCP level modulations and sensitivity changes of the αCGRP receptor.

This study demonstrated for the first time that the CRLR/ RAMP1 complex participates in mechanotransduction and that macrophages react to mechanical stress with alterations in the αCGRP gene expression.

5.2.2 Impact of mechanical loading on inherent metabolic behavior of RAW 264.7 macrophages in the presence of sensory neuropeptides

The metabolic parameters, adhesion, proliferation and apoptosis are critical indicators for cell activity and viability. Thus, we analyzed how mechanical stress and sensory neuropeptide stimulation affected these parameters.

5.2.2.1 Apoptosis

In our experiments, loading of RAW 264.7 macrophages induced a higher caspase 3/7 mediated apoptosis. Similar observations are described in the literature: Xu et al. stretched osteoclasts, differentiated from RAW 264.7 macrophages, and observed an increased apoptotic rate at low physiological mechanical strain [78]. Osteoclasts on the maxillary bone surface became apoptotic after the application of a tensional force that was not seen on the control bone surface [234]. Noble and colleagues loaded mice ulnae with physiological and pathologically high strains. The apoptosis of osteocytes subjected to lower strains was reduced, while the apoptotic rate of the extensively loaded osteocytes was elevated [191]. Higher apoptosis rates were also shown for fibroblasts subjected to compressive loading [194], alveolar type II cells in rat lungs exposed to intermittent stretch [195] and human chondrocytes from the epiphyseal growth plate loaded with 4000 µ-strain [193] compared to controls. In contrast, mechanical stretching of fibroblast-like synoviocytes either from healthy control tissue or rheumatoid arthritis synovium did not affect apoptosis [199]. In summary, previous examinations on the impact of mechanical force application on apoptosis are consistent with our study but the number of experiments that specifically dealt with loading of macrophages is little. Cells that have been most extensively studied under loading are bone cells (e.g. osteocytes or osteoblasts), chondrocytes and cell types involved in dental structures that are typically exposed to tensile or compressive force. Increased apoptosis of macrophages and osteoclasts could be a protective mechanism to prevent enhanced bone resorption due to mechanically induced micro-damages. On the one hand, micro-damage could be the initiation signal for bone remodeling, accelerated bone turnover and repair of affected sites. On the other hand, overactivation of macrophages might evoke immune responses that are unfavorable in pathologies like OA which includes structural joint damage. Macrophage activity might be controlled by an upregulation of apoptosis to prevent detrimental inflammatory conditions.

The apoptosis of RAW 264.7 cells was not affected significantly by SP and αCGRP stimulation. Similarly, Opolka et al. observed little effect of SP stimulation on the apoptotic rate of mice costal chondrocytes [155]. In contrast, apoptosis of human tenocytes and human mesenteric pre-adipocytes was decreased by SP stimulation [158,159]. It has also been observed that treating vascular smooth muscle cells with 10^{-8}M CGRP prior to oxidative stress exposure reduced the number of apoptotic nuclei [235]. So far, the knowledge about the influence of SP and αCGRP concerning apoptosis of macrophages is very limited. Gherardini et al. examined intracutaneous human macrophages and detected a significantly increased cell number after SP stimulation, but the effect could be attributed to an enhanced differentiation from progenitor cells and not to altered rates of apoptosis or proliferation [236].

Regarding the broad spectrum and various effects of different loading parameters and taking into account the combination of loading and neuropeptide stimulation in this study, the question arises, whether the observed effects in RAW 264.7 macrophages can be considered anabolic or catabolic. Here, the increased apoptosis rate of RAW 264.7 macrophages points to inhibitory processes due to mechanical stress with a reduced cell vitality and metabolic activity. Further addition of SP and αCGRP had little effects on apoptosis leading to the conclusion that both neuropeptides are not involved in apoptotic processes related to mechanical strain.

5.2.2.2 Proliferation

The proliferation rate of the RAW 264.7 macrophages used in our experiments was not significantly altered by mechanical loading and only had a tendency for a reduced proliferation rate. Similarly, when human fibroblast-like synoviocytes from healthy tissues were exposed to stretch, the proliferation was unaffected, whereas in synoviocytes from RA patients proliferation was significantly increased [199]. A higher proliferation in response to loading was also seen in experiments using periosteal fibroblast-like cells, going along with a disorganization of the actin cytoskeleton after loading followed by a subsequent reorganization [192]. Moreover, periodic mechanical stress induced the proliferation of chondrocytes, possibly by an integrin-calmodulin kinase II-Pyk2-ERK 1/2 pathway [6]. Stretching of human bone marrow mesenchymal stem cells (BMSC) at a frequency of 1 Hz presented a high variability [202]. Stretching with a low strain and for short time periods as well as long-time loading caused a significant increase in hBMSC proliferation. In contrast, higher strains for a short time

evoked a decrease. Interestingly, stretched BMSC of either ovariectomized or Sham rats clearly displayed a decreased proliferation rate after three days of loading [198]. Peyton et al. used both constant and intermittent cyclic stretch and observed an overall inhibited proliferation of the examined human microvascular endothelial cells [237]. To summarize, the effects of mechanical loading on proliferation vary in experiments so far and either confirm or contradict our results. The reasons for deviating results might be a variation in loading times and parameters, as well as differences in the proliferative behavior of the cell type or particular macrophage subtype used for the experiments.

Regarding proliferation and neuropeptide influence, we observed a decreased proliferative rate of unloaded RAW 264.7 macrophages after 10^{-8} M SP stimulation. Contrarily, SP increased the proliferation rate in endothelial cells of the rat knee-joint [60] and in mouse chondrocytes using a $10^{-9}/10^{-10}$ M SP concentration [155]. Furthermore, in a study by Backman et al., SP increased cell viability and proliferation of human tenocytes, possibly through an autocrine loop between SP and NK1R [23]. This is consistent with the negative feedback loop of the gene and protein expression of NK1R and SP that we observed and discussed above (see 5.2.1.1). Confirming the results from Backman and colleagues, Zhou et al. observed an elevated proliferation rate in tendon-derived stem cells in response to SP and dose-dependent effects of SP on patella tendons in vivo, whereby low concentrations of SP enhanced tenogenesis, whereas high doses of SP induced tendinopathy [157]. The proliferation of neural stem cells was enhanced by SP in vitro as well as in vivo [156]. Regarding our experiments, SP stimulation did not influence the proliferation of loaded RAW 264.7 macrophages. Yet, combined stimulation using SP and the NK1R antagonist induced a decreased proliferation of loaded cells. This is similar to the effect of loading itself, which led to a reduced proliferation rate and displays an effective blockade of the NK1R through the L733,060 antagonist.

To summarize, the combination of SP stimulation and loading had no significant effect on RAW 264.7 macrophages, whereas the decreased proliferation of unloaded cells after SP stimulation is contrary to other studies. Previous experiments used other cell types rather than macrophages, which might explain the diverging results and points towards an altered neuropeptide signaling in case of macrophages.

Stimulation with 10^{-10} M αCGRP decreased the proliferation rate of the unloaded RAW macrophages. Already in 1994, Owan and his group determined an inhibitory effect of human αCGRP on bone marrow macrophages. The number and also the size of their macrophage colonies in culture were smaller compared to controls [57]. In a study examining the effect of αCGRP stimulation on smooth muscle cells, the proliferation rate was dose-dependently affected by the FCS concentration of the medium. αCGRP had no effect in the presence of 1 % FCS, but 10 % FCS in combination with αCGRP stimulation modulated cell proliferation. αCGRP enhanced growth rates of slow-proliferating smooth muscle cells and inhibited growth rates of a rapidly-proliferating smooth muscle cell population, depicting a dual role of αCGRP signaling [238]. Endothelial cell proliferation in rat knee-joints was elevated under αCGRP influence [60]. In our study, 10^{-10} M αCGRP decreased the proliferation, whereas the higher concentration of 10^{-8} M had no effect. Generally, it is assumed that macrophages might show a better response to micromolar concentrations than to the nanomolar concentrations which we used in these experiments, and as it was shown for SP [239]. Whether this also applies for αCGRP remains unknown and deserves more intense investigation.

5.2.2.3 Adhesion

Experiments examining the influence of loading on adhesion are very few in number. In general, the adhesive mechanisms of macrophages have been studied intensely, but there are no reports about the impact of loading. For example, stretched fibroblasts developed a higher number of focal adhesions than control cells, possibly as a mechanism to correct the increased force on the cell [196]. Cyclic stretch on human periodontal ligament cells enhanced the gene expression of adhesion molecules [240]. Our examinations demonstrated no influence of loading on the adhesion of RAW 264.7 macrophages suggesting a low or no impact of mechanical loading on the molecular processes, which determine adhesive behavior of macrophages. The adhesion of RAW 264.7 macrophages to collagen I seems to be modulated by class A macrophage scavenger-receptors (SR-A) and not by β-integrins, which are the main adhesion receptors for macrophages. The main mediators of macrophage and osteoclast adhesions are the podosomes; dynamic cylindrical attachment structures whose subunits react tissue- and substrate-dependent [27]. Overall, macrophages have shown different adhesion mechanisms to collagen I, are dependent upon the cell

phenotype and tissue-specificity, as well as a varying pool of adhesive receptors. Since subsets of integrins and the above-mentioned scavenger-receptors are unique for each macrophage species [27] they might contribute to the reported variability in macrophage adhesive behavior.

In our study, stimulation with 10^{-8} M SP decreased the adhesion of unloaded macrophages. Addition of 10^{-10} M SP had opposite effects on the adhesion of loaded and unloaded cells; the adhesion rate of unloaded cells was higher, whilst the adhesion of loaded cells was lower compared to respective unstimulated cells. In a study from Levite and colleagues, SP blocked the neuropeptide-induced adhesion of T-cells to fibronectin [227]. In contrast, in murine costal chondrocytes, SP stimulation increased adhesion in a dose-dependent manner [155]. Furthermore, SP increased the focal adhesion formation of keratocytes [241] and the expression of adhesion-associated genes in rat fibroblasts and non-human primate fibroblasts [242].

αCGRP stimulation had little effect in unloaded RAW 264.7 macrophages. In contrast, adhesion rate decreased in loaded macrophages upon addition of either 10^{-10} M αCGRP, the CGRP receptor antagonist CGRP$_{8-37}$ or combined application. In compliance to our results, Sung et al. observed a reduction in the adhesion capability of leukocytes to endothelial cells after αCGRP stimulation [243], whilst a different study demonstrated an increase in T-cell adhesion to fibronectin after stimulation with CGRP [227]. These opposing observations indicate the involvement of more complicated mechanisms in the regulation of adhesion after αCGRP stimulation and imply that only little variations in the study design might lead to opposing results.

Regarding the adhesion of RAW 264.7 macrophages, neuropeptide stimulation and mechanical loading both display inhibitory effects. If this can be considered a benefit or drawback in macrophage physiology remains unclear. For one thing, reduced adhesion could facilitate macrophage mobility and migration, although a lack of adherence might make adequate cell-surface contacts and locomotion impossible. To sum up, adhesive behavior of cells and particularly macrophages is highly variable, and the underlying mechanisms are complex and difficult to understand. Further elucidation of macrophage adhesion might help to understand and interpret experimental outcomes when using macrophages *in vitro* and *in vivo.*

5.2.2.4 Neuropeptide antagonist effects

The effect of the neuropeptide antagonists is still indistinct. In our experiment, antagonist stimulation produced results that are difficult to explain. Often the receptor antagonist neutralized the effect of the competitive ligand insufficiently, when evaluating stimulation with the combination of neuropeptide and its receptor antagonist or stimulation with the antagonist alone.

The effect of CGRP receptor antagonists is based on the lack of the N-terminal of the CGRP molecule interfering with the necessary connection between ligand and receptor domain [179]. The $CGRP_{8-37}$ receptor antagonist is a 30-amino-acid fragment of the αCGRP neuropeptide with a short half-life [60] that seemed to reduce mechanical hypersensitivity after lumbar nerve transection in mice [244]. The CGRP receptor antagonist olcegepant (BIBN4096BS) has already been observed to alleviate migraine pain and reduce neuronal activity of the trigeminus nerve and predominantly block peripheral CGRP receptor-mediated inflammation [171]. In this study, stimulation with the CGRP receptor antagonist $CGRP_{8-37}$ induced a higher adhesion rate of unloaded macrophages. Referring to our outcome, Lerner et al. demonstrated that $CGRP_{8-37}$ lacked an antagonistic effect regarding bone resorption and assumed the presence of receptor subtypes on osteoclasts [162]. Previously, Dennis et al. suggested the existence of two CGRP receptor subtypes, one with high and one with low affinity for $CGRP_{8-37}$ [245]. Intrathecal spinal injection of only the antagonist $CGRP_{8-37}$ also evoked an unexpected effect in rats indicating a potential endogenous CGRP release [246].

The piperidine ether-based L733,060 is a highly effective NK1R antagonist with good blood-brain barrier permeability. It acts stereoselective, so its enantiomer L733,061 does not form a strong binding. Studies with this antagonist reported a blockade of neurogenic inflammation and subsequent plasma extravasation [247], as well as an anti-nociceptive impact in gerbils [248]. These findings suggest a promising role for NK1R and SP antagonists in the treatment of painful inflammatory diseases. In our study, L733,060 often seemed to lack its antagonistic effect and the reasons for that still need to be elucidated. The group of Hamity observed that the efficacy of the NK1R antagonist L733,060 was time-dependent as administration of L-733,060 to rat medulla was highly effective at 15 min but ineffective at 30 min prior to SP treatment [249]. Further experiments would test pre-stimulations using the L-733,060.

5.2.3 Impact of mechanical loading on osteoclastogenic differentiation potential of RAW 264.7 macrophages

Differentiation of macrophages into osteoclasts depends on stimulation of two specific receptors on the macrophage precursor cell: RANK and CSF1R (also c-FMS). When RAW 264.7 cells were subjected to cyclic stretch, we observed an upregulation of RANK mRNA, whereas the CSF1R mRNA expression remained unaffected, potentially suggesting an enhanced osteoclastogenic differentiation potential upon mechanical loading. In compliance, 4-point bending of RAW 264.7 macrophages resulted in strain-dependent RANK mRNA alteration [78]. Using high strain, RANK mRNA expression was increased. In contrast, mechanical stress on rodent femoral heads decreased the RANK/RANKL mRNA expression [250]. In any case, RANK expression seems to be regulated by mechanical loading. Compressive loading of human osteoblasts also evoked a RANKL mRNA and protein increase [251], whilst similar results were achieved by static compression of periodontal ligament cells [252]. In contrast, high loading frequencies reduced the RANKL mRNA expression of murine stromal cells [253], as did simultaneous fluid shear stress and αCGRP stimulation on pre-osteoblastic cells [77]. Application of fluid shear stress on an osteocytic cell line, Ocy 454, altered RANKL mRNA in strain dependent manner [254]. In earlier studies, CSF1R mRNA expression was increased after cyclic stretch [255] and after the release of loading [79]. Reports regarding the influence of mechanical loading on RANK and c-FMS gene expression are very few, whereas numerous studies examined the expression of the ligand RANKL. The increased RANKL gene expression and the potential induction of osteoclastogenesis following mechanical stress contradict various other studies, whereby mechanical loading led to an osteoclastogenic downregulation and cannot be discussed in the context of our study on RAW 264.7 macrophages (see section 4.2.4). In our loading experiments on metabolic behavior, macrophage apoptosis was increased after mechanical loading resulting in the loss of precursor cells for potential osteoclast differentiation. The upregulation of RANK gene expression might be a compensatory mechanism. Still, gene regulation without analysis of subsequent protein regulation does not allow for any solid statements regarding physiological effects.

5.2.4 Impact of mechanical loading on macrophage polarization: induction of M1 activity

Macrophages display a wide range of phenotypes, the main groups being M1 or proinflammatory macrophages versus M2 or anti-inflammatory macrophages. The phenotype plasticity allows macrophages to adapt their function and provide an adequate and controlled immunological reaction. Previously, it was reported that mechanical loading affects macrophage polarization. Depending upon the stretch intensity, both M1 and M2 phenotypes were induced [27]. We observed that a two-day-loading protocol led to an increased gene expression of M1-associated genes like NF-κB, TNF-α, IL-6 and iNOS, representing classically activated macrophages. Therefore, it can be assumed that the mechanical stretch parameters used in our setup preferably induce a proinflammatory macrophage phenotype. Gene expression of M2 macrophage markers remain unaffected. Proinflammatory M1 macrophages provide a protective immune response by releasing cytokines and protecting the body cells from bacteria and viruses by phagocytosis. Alternatively-activated M2 macrophages arise to produce extracellular matrix for tissue repair and operate in an anti-inflammatory manner [29]. The group of Hammerschmidt demonstrated a balance shift towards a proinflammatory immune response after stretching alveolar type II cells or rat lungs [256]. Only a few experiments concerning mechanical stress on macrophages are described in the literature. In accordance with our study, mechanical loading increased the expression of proinflammatory genes such as iNOS, IL-6, IL-1β or TNF-α of macrophages [38,257]. Ballotta et al. observed differential effects after the application of low 7 % strain compared to a higher 12 % stretch. Stretching macrophages with 12% alignment indicated the predominance of pro-inflammatory M1 macrophages, whereas the lower stress increased the M2/M1 ratio, resulting in an elevated anti-inflammatory activity [36]. In conclusion, various studies including our own observations demonstrate the differential impact of varying ranges of mechanical stress on macrophage phenotype development. It cannot clearly be stated if mechanical stress on macrophages has positive or negative effects or if an anti- or proinflammatory response is dose-dependent. Shan et al. loaded RAW 264.7 macrophages for 1, 2 and 4 h with 5 %, 10 % and 15 % strain and observed a strain-independent overall increase of proinflammatory gene expression and cytokine release [257]. In contrast, stretching of skin macrophages induced M2 polarization at a

relatively high strain of 33 % for 7 days [258]. In general, mechanically loaded macrophages showed a higher cytokine release than without loading [37,259]. Numerous other cell types like fibroblasts, human blood monocytes or mesenchymal stem cells reacted to mechanical strain with release of proinflammatory cytokines [10,36,79,197,200,212,260,261]. Our results and previous work indicate an influence of mechanical loading on macrophage phenotype plasticity with polarization depending upon the loaded cell type and loading parameters. The M1 polarization demonstrated in our experiments is in line with the proinflammatory conditions observed in OA pathology [262,263].

Besides, numerous approaches and suggestions exist to update the common macrophage classification since the dichotome differentiation in M1 and M2 only displays one of many macrophage features and is too general for the multiple and diversified appearances and tasks that macrophages can perform.

5.2.5 Impact of mechanical loading on inherent metabolic behavior of BMM from DMM- and Sham mice in the presence of sensory neuropeptides

One hypothesis of this work was that BMM from osteoarthritic animals show different metabolic activity compared to Sham BMMs, since OA is related to an altered mechanotransduction among other features [122,130,264–266]. Initially, we studied apoptosis and proliferation of BMM from Sham- and DMM mice in the context of cyclic stretch and sensory neuropeptide stimulation.

BMM from wildtype mice 8 weeks after DMM surgery exhibited an elevated apoptosis- as well as proliferation rate after cyclic stretch. The increased apoptosis rate of loaded BMM at 8 weeks post DMM surgery in comparison to no apoptosis in loaded BMM at 2 weeks post surgery might suggest a preventive measure to counteract a macrophage-derived overactivation of the immune system and subsequent detrimental inflammatory conditions. Apart from bone matrix degradation, osteoclastogenesis is likewise important for the formation of new bone subsequent to its resorption. A reduced osteoclastogenesis due to a reduced number of precursor macrophages, thus indicates less bone turnover and might cause an insufficient repair of microdamage or development of sclerotic bone, characteristic of late OA subchondral bone changes. Bone homeostasis is strictly dependent upon the balance between catabolic and

anabolic processes. Yet, the combination of an enhanced apoptosis and also proliferation rate of BMM after OA induction indicate the complex interplay of intrinsic cellular mechanisms as a response to mechanical stress applied in vivo (DMM) or in vitro (cyclic stretch). These first experiments allow us to conclude that OA has an impact on BMMs, but at the same time data are not sufficient yet for specific conclusions. Additionally, BMM might contribute to inflammatory reactions in OA [267,268] that also might explain the increased proliferation rate in our experiments. Overall, our study focuses on only one cell type in primed in vitro conditions, which makes it difficult to draw conclusions about in vivo effects.

The stimulation of BMM with neuropeptides and their respective inhibitors resulted in a high intra-assay variability regarding their effects on proliferation and apoptosis. Our results so far allow no deductions regarding neuropeptide effects on BMM from DMM and Sham mice after loading. Previous studies from our group demonstrated a higher proliferation rate of BMM after SP stimulation [61]. Wang et al. observed increased proliferation of BMM after CGRP stimulation and no proliferative effect of SP [166,269]. Further experimental trials examining the effect of neuropeptide stimulations on the adhesion of BMMs might be interesting, since in in vitro experiments on RAW 264.7 macrophages, adhesion and mechanical loading had similar effects. In general, the variability of *in vivo* experiments is higher than of *in vitro* experiments using cell lines, which we can confirm by our observations.

5.2.6 Conclusion

This study demonstrates the participation of SP and αCGRP and their neuropeptide receptors NK1R and CRLR/RAMP1 in the mechanotransduction process of murine macrophages. Our results indicate an autocrine negative feedback regulation of the NK1R/ SP system. The involvement of αCGRP and its receptor CRLR/ RAMP1 in mechanosensation and -regulation was demonstrated for the first time. Further experiments could aim to elucidate if the expression of the RAMP1 subunit is an indicator for chronic stress after long-time loading. Since macrophages are resident cells in most musculoskeletal tissues, they are exposed to mechanical stress and neuropeptide signaling. Therefore, elucidating the impact of mechanoregulation and neuropeptide stimulation on local cellular interactions might help to understand macrophage-related physiological and pathological mechanisms of musculoskeletal tissues. Macrophages displayed increased apoptosis rates after cyclic stretching,

possibly depicting a prevention of macrophage-driven detrimental immune reactions. Mechanical loading altered macrophage adhesive behavior in response to SP and αCGRP stimulation, which might indicate mechano-dependent signaling alterations interfering with migration and mobility. Moreover, the induction of OA appears to interfere with apoptosis and proliferation of bone marrow-derived macrophages in response to mechanical stress, indicating OA-associated altered biomechanical signaling. Cyclic stretching of RAW 264.7 macrophages induced the gene expression of cytokines associated with M1 polarization and increased RANK gene expression, suggesting a pro-inflammatory and pro-osteoclastogenic activity in response to mechanical stress. This partly depicts the eminent role of macrophages and mechanical force in pathophysiological processes as described in subchondral bone alterations during OA pathogenesis. More detailed insight could explore possible treatment options targeting pathological signaling pathways related to mechanotransduction. Future studies examining mechanotransduction of macrophages should aim to elucidate possible receptor isoforms or variations of the NK1R and CRLR/RAMP1, as well as interactions of SP and αCGRP to enlighten still unexplained macrophage responses to neuropeptide stimulations in this specific context.

The limitations of our experiments regarding protein and gene expression of neuropeptides, their receptors, osteoclastogenesis and macrophage polarization markers include the usage of a cell line, the RAW 264.7 macrophages. Cell lines are a satisfying model organism to study mechanistic processes, but immortalized cells might not show an aberrant metabolic behavior compared to primary cells and the in vivo situation. In vitro conditions always simplify the physiological properties and lack the influence of other cell types, the tissue-specific milieu and species-related specialties. Repetitions of our experiments using primary bone marrow macrophages could elucidate the interplay of mechanical stress and sensory neuropeptide stimulation in macrophages in a more physiological setting.

6 Summary

Macrophages as precursor cells of osteoclasts are of importance during bone formation, whose physiologically well-balanced process is altered during osteoarthritis (OA). Mechanosensing within cells is necessary for growth and maturation of joints, whereas pathological stress can cause inflammation and disorders, such as articular cartilage degeneration or subchondral bone sclerosis in OA. The neuropeptides Substance P (SP) and α-calcitonin gene-related peptide (αCGRP), acting on the neurokinin-1 receptor (NK1R) and the calcitonin receptor-like receptor (CRLR)/ receptor activity-modifying protein (RAMP1), are involved in joint physiology and OA-associated degenerative processes and were shown to modulate osteoclastogenesis. Regarding these mechanisms, the topic of this work was to elucidate the combination of both mechanical loading and sensory neuropeptide stimulation on metabolic parameters of murine macrophages.

RAW 264.7 macrophages were subjected to cyclic mechanical stretch. Neuropeptide receptor and neuropeptide gene and protein expression was assayed by PCR analysis and western blotting, respectively. Metabolic behavior of macrophages was analyzed by studying apoptosis, proliferation and adhesion, with and without neuropeptide stimulation after application of cyclic stretch. The expression of macrophage polarization markers and osteoclastogenesis-associated genes was examined after loading. Neuropeptide stimulation experiments were repeated on primary BMM after the surgical induction of OA.

This study demonstrated the involvement of SP and αCGRP and their receptors in macrophage mechanotransduction and -regulation. Mechanoregulation via αCGRP-CRLR/RAMP1 interaction had never been previously addressed. Our results further indicate the regulation of RAMP1 in experimental conditions of mechanically induced stress. In agreement with results from other groups, we observed an autocrine negative feedback mechanism of NK1R/SP signaling.

Furthermore, macrophages exposed to mechanical stress developed a sensitization for caspase 3/7-mediated apoptosis induction and an inhibited adhesion after αCGRP stimulation, pointing towards a preventive mechanism regarding detrimental inflammatory conditions by upregulation of macrophage apoptosis and a reduced macrophage migration. The M1 polarization after loading suggests a proinflammatory

activity of mechanically stressed macrophages. If and how this would affect macrophage activity in vivo remains elusive. Furthermore, we observed that the gene expression of the RANK receptor was enhanced after mechanical loading leading to the assumption of a higher osteoclastogenic differentiation potential of macrophages.

Additionally, the induction of experimental OA appears to alter the mechanotransduction of primary murine BMM, as we observed a higher proliferation rate and an increased sensitivity to apoptosis induction of BMM at 8 weeks post OA surgical induction in comparison to BMM from Sham-operated animals. From that, we conclude that altered cellular biomechanics, induced by OA, affect bone resident macrophage populations. The underlying molecular mechanisms remain unknown so far. Future studies could help to identify regulatory processes involved in the altered cellular reactivity and might contribute to the development of new treatment options that target pathological signaling pathways of macrophage mechanoregulation and neuropeptide sensitivity.

7 Abbreviations

AB   antibody
AC   adenylate cyclase
ACLT   anterior cruciate ligament transection
ADAMTS   A disintegrin and metalloprotease with thrombospondin motifs
APS   ammonium persulfate
AUT   Austria
BCA   bicinchoninic acid
B-ME   β-mercaptoethanol
BMM   bone marrow macrophages
BMP   bone morphogenetic protein
BMSC   bone marrow mesenchymal stem cells
bp   base pairs
BrdU   5-bromo-2'-deoxyuridine
BSA   bovine serum albumin
Ca^{2+} calcium
cAMP   cyclic adenosine monophosphate
cDNA   complementary deoxyribonucleic acid
c-FMS   macrophage colony-stimulating factor
CFU-M   macrophage colony-forming unit
CGRP   calcitonin gene-related peptide
COX   cyclooxygenase
CRLR   calcitonin receptor-like receptor
ctrl   control
DMM   destabilization of the medial meniscus
DNA   desoxyribonucleic acid
dNTP   deoxyribonucleotide triphosphates
DTT   dithiothreitol
ECM   extracellular matrix
EIA   enzyme immuno-assay
ELISA   enzyme-linked immunosorbent assay
ERK   extracellular signal-regulated kinases
FAK   focal adhesion kinases
FCS   fetal calf serum
GAPDH   Glyceraldehyde-3-phosphate dehydrogenase
GER   Germany
GPCR   G-protein coupled receptor
h   hour/ hours
HIF   hypoxia-inducible factor
HRP   horse radish peroxidase
IG   immunglobuline
IL   interleukin
iNOS   inducible nitric oxide synthase
IP   inositoltriphosphate
JNK   c-Jun-N-terminal kinases
KLF   kruppel-like factor
MAPK   mitogen-activated protein kinases
M-CSF   macrophage colony-stimulating factor
MMTL   medial meniscal tear ligament

MIA	monoiodacedate
Min	minutes
MMP	matrix metalloproteinase
MRC-1	mannose receptor
MRI	magnetic resonance imaging
mRNA	messenger ribonucleic acid
MT	meniscal tear
MTX	methotrexate
NF-κB	nuclear factor-kappa-B
NGF	nerve growth factor
NK1R	neurokinin-1 receptor
NO	nitric oxide
NOS	nitric oxide synthase
NSAID	non-steroidal anti-inflammatory drugs
OA	osteoarthritis
OARSI	osteoarthritis research society international
PBS	phosphate-buffered saline
PCR	polymerase chain reaction
PGE$_2$	prostaglandin E$_2$
PKC	protein kinase C
qRT-PCR	quantitate real-time polymerase chain reaction
RA	rheumatoid arthritis
RAMP1	receptor activity-modifying protein 1
RANK	receptor activator of nuclear factor kappa-b
RANKL	receptor activator of nuclear factor kappa-b ligand
RCP	receptor component protein
RIN	RNA integrity number
RIPA	radioimmunoprecipitation assay
RNA	ribonucleic acid
ROS	reactive oxygen species
RQ	relative quantification
Sec	Seconds
SR-A	class A scavenger-receptor
SDS-PAGE	sodium dodecyl sulfate polyacrylamide gel electrophoresis
SP	substance P
TAC	tachykinin
TAE	tris-acetate EDTA
TEMED	tetramethylethylendiamin
TBS	tris-buffered saline
TGF-β	transforming growth factor
TM	temperature maximum
TNF-α	tumor necrosis factor
TRAP	tartrate-resistant acid phosphatase
TRPV	transient receptor potential vanilloid
USA	United States of America
VIP	vasoactive intestinal peptide
VSMC	vascular smooth muscle cells
WT	wildtype
2D/3D	two-dimensional/ three-dimensional

8 References

1. Kurth F, Eyer K, Franco-Obregón A, Dittrich PS. A new mechanobiological era: Microfluidic pathways to apply and sense forces at the cellular level. Current Opinion in Chemical Biology. 2012;16(3-4):400–8. doi: 10.1016/j.cbpa.2012.03.014.

2. Chen Y, Ju L, Rushdi M, Ge C, Zhu C. Receptor-mediated cell mechanosensing. Mol Biol Cell. 2017;28(23):3134–55. doi: 10.1091/mbc.E17-04-0228. PubMed PMID: 28954860.

3. Gusmão CVBd, Belangero WD. HOW DO BONE CELLS SENSE MECHANICAL LOADING? Rev Bras Ortop. 2009;44(4):299–305. doi: 10.1016/S2255-4971(15)30157-9. PubMed PMID: 27022510.

4. Fletcher DA, Mullins RD. Cell mechanics and the cytoskeleton. Nature. 2010;463(7280):485–92. doi: 10.1038/nature08908.

5. Huang H, Kamm RD, Lee RT. Cell mechanics and mechanotransduction: Pathways, probes, and physiology. American Journal of Physiology-Cell Physiology. 2004;287(1):C1-C11. doi: 10.1152/ajpcell.00559.2003.

6. Liang W, Li Z, Wang Z, Zhou J, Song H, Xu S, et al. Periodic Mechanical Stress INDUCES Chondrocyte Proliferation and Matrix Synthesis via CaMKII-Mediated Pyk2 Signaling. Cell Physiol Biochem. 2017;42(1):383–96. doi: 10.1159/000477483. PubMed PMID: 28558386.

7. Winters CJ, Koval O, Murthy S, Allamargot C, Sebag SC, Paschke JD, et al. CaMKII inhibition in type II pneumocytes protects from bleomycin-induced pulmonary fibrosis by preventing Ca 2+ -dependent apoptosis. American Journal of Physiology-Lung Cellular and Molecular Physiology. 2016;310(1):L86-L94. doi: 10.1152/ajplung.00132.2015.

8. Orr AW, Helmke BP, Blackman BR, Schwartz MA. Mechanisms of Mechanotransduction. Developmental Cell. 2006;10(1):11–20. doi: 10.1016/j.devcel.2005.12.006.

9. Hughes-Fulford M. Signal transduction and mechanical stress. Sci STKE. 2004;2004(249):RE12. doi: 10.1126/stke.2492004re12. PubMed PMID: 15353762.

10. Agarwal S, Deschner J, Long P, Verma A, Hofman C, Evans CH, et al. Role of NF-kappaB transcription factors in antiinflammatory and proinflammatory actions of mechanical signals. Arthritis Rheum. 2004;50(11):3541–8. doi: 10.1002/art.20601. PubMed PMID: 15529376.

11. Carvalho RS, Scott JE, Suga DM, Yen EHK. Stimulation of signal transduction pathways in osteoblasts by mechanical strain potentiated by parathyroid hormone. J Bone Miner Res. 1994;9(7):999–1011. doi: 10.1002/jbmr.5650090707.

12. Howard MR, Millward-Sadler SJ, Vasilliou AS, Salter DM, Quinn JP. Mechanical stimulation induces preprotachykinin gene expression in osteoarthritic chondrocytes which is correlated with modulation of the transcription factor neuron restrictive silence factor. Neuropeptides. 2008;42(5-6):681–6. doi: 10.1016/j.npep.2008.09.004. PubMed PMID: 18990442.

13. Griffin TM, Guilak F. The role of mechanical loading in the onset and progression of osteoarthritis. Exerc Sport Sci Rev. 2005;33(4):195–200. PubMed PMID: 16239837.

14. Moyer RF, Ratneswaran A, Beier F, Birmingham TB. Osteoarthritis Year in Review 2014: Mechanics – basic and clinical studies in osteoarthritis. Osteoarthr Cartil. 2014;22(12):1989–2002. doi: 10.1016/j.joca.2014.06.034.

15. Burr DB. Anatomy and physiology of the mineralized tissues: Role in the pathogenesis of osteoarthrosis. Osteoarthr Cartil. 2004;12:20–30. doi: 10.1016/j.joca.2003.09.016.

16. French AS, Torkkeli PH. Mechanoreceptors. In: Squire LR, editor. Encyclopedia of neuroscience. [Amsterdam]: Elsevier; 2009. p. 689–95.

17. Grässel SG. The role of peripheral nerve fibers and their neurotransmitters in cartilage and bone physiology and pathophysiology. Arthritis Res Ther. 2014;16(6):485. PubMed PMID: 25789373.

18. Jones KB, Mollano AV, Morcuende JA, Cooper RR, Saltzman CL. Bone and Brain: A Review of Neural, Hormonal, and Musculoskeletal Connections. Iowa Orthop J. 2004;24:123–32. PubMed PMID: 15296219.

19. Grässel S, Muschter D. Peripheral Nerve Fibers and Their Neurotransmitters in Osteoarthritis Pathology. Int J Mol Sci. 2017;18(5). doi: 10.3390/ijms18050931. PubMed PMID: 28452955.

20. Millward-Sadler SJ, Mackenzie A, Wright MO, Lee H-S, Elliot K, Gerrard L, et al. Tachykinin expression in cartilage and function in human articular chondrocyte mechanotransduction. Arthritis Rheum. 2003;48(1):146–56. doi: 10.1002/art.10711. PubMed PMID: 12528114.

21. Fristad I, Vandevska-Radunovic V, Fjeld K, Wimalawansa SJ, Hals Kvinnsland I. NK1, NK2, NK3 and CGRP1 receptors identified in rat oral soft tissues, and in bone and dental hard tissue cells. Cell Tissue Res. 2003;311(3):383–91. doi: 10.1007/s00441-002-0691-z. PubMed PMID: 12658446.

22. Ytteborg E, Torgersen JS, Pedersen ME, Helland SJ, Grisdale-Helland B, Takle H. Exercise induced mechano-sensing and substance P mediated bone modeling in Atlantic salmon. Bone. 2013;53(1):259–68. doi: 10.1016/j.bone.2012.11.025. PubMed PMID: 23219942.

23. Backman LJ, Fong G, Andersson G, Scott A, Danielson P. Substance P is a mechanoresponsive, autocrine regulator of human tenocyte proliferation. PLoS ONE. 2011;6(11):e27209. doi: 10.1371/journal.pone.0027209. PubMed PMID: 22069500.

24. Heffner MA, Genetos DC, Christiansen BA. Bone adaptation to mechanical loading in a mouse model of reduced peripheral sensory nerve function. PLoS ONE. 2017;12(10):e0187354. doi: 10.1371/journal.pone.0187354. PubMed PMID: 29088267.

25. Sample SJ, Heaton CM, Behan M, Bleedorn JA, Racette MA, Hao Z, et al. Role of calcitonin gene-related peptide in functional adaptation of the skeleton. PLoS ONE. 2014;9(12):e113959. doi: 10.1371/journal.pone.0113959. PubMed PMID: 25536054.

26. Atri C, Guerfali F, Laouini D. Role of Human Macrophage Polarization in Inflammation during Infectious Diseases. Int J Mol Sci. 2018;19(6):1801. doi: 10.3390/ijms19061801.

27. McWhorter FY, Davis CT, Liu WF. Physical and mechanical regulation of macrophage phenotype and function. Cell Mol Life Sci. 2015;72(7):1303–16. doi: 10.1007/s00018-014-1796-8. PubMed PMID: 25504084.

28. Mosser DM, Edwards JP. Exploring the full spectrum of macrophage activation. Nat Rev Immunol. 2008;8(12):958–69. doi: 10.1038/nri2448.

29. Liu Y-C, Zou X-B, Chai Y-F, Yao Y-M. Macrophage Polarization in Inflammatory Diseases. Int. J. Biol. Sci. 2014;10(5):520–9. doi: 10.7150/ijbs.8879.

30. Shapouri-Moghaddam A, Mohammadian S, Vazini H, Taghadosi M, Esmaeili S-A, Mardani F, et al. Macrophage plasticity, polarization, and function in health and disease. J Cell Physiol. 2018;233(9):6425–40. doi: 10.1002/jcp.26429.

31. Stein M, Keshav S, Harris N, Gordon S. Interleukin 4 potently enhances murine macrophage mannose receptor activity: A marker of alternative immunologic macrophage activation. The Journal of Experimental Medicine. 1992;176(1):287–92. doi: 10.1084/jem.176.1.287.

32. Liao X, Sharma N, Kapadia F, Zhou G, Lu Y, Hong H, et al. Krüppel-like factor 4 regulates macrophage polarization. J. Clin. Invest. 2011;121(7):2736–49. doi: 10.1172/JCI45444.

33. Wynn TA, Vannella KM. Macrophages in Tissue Repair, Regeneration, and Fibrosis. Immunity [Internet]. 2016;44(3):450–62. Available from: http://www.sciencedirect.com/science/article/pii/S107476131630053X.

34. Murray PJ. Macrophage Polarization. Annu Rev Physiol. 2017;79:541–66. doi: 10.1146/annurev-physiol-022516-034339. PubMed PMID: 27813830.

35. Gowen BB, Borg TK, Ghaffar A, Mayer EP. Selective adhesion of macrophages to denatured forms of type I collagen is mediated by scavenger receptors. Matrix Biology. 2000;19(1):61–71. doi: 10.1016/S0945-053X(99)00052-9.

36. Ballotta V, Driessen-Mol A, Bouten CVC, Baaijens FPT. Strain-dependent modulation of macrophage polarization within scaffolds. Biomaterials. 2014;35(18):4919–28. doi: 10.1016/j.biomaterials.2014.03.002. PubMed PMID: 24661551.

37. Pugin J, Dunn I, Jolliet P, Tassaux D, Magnenat JL, Nicod LP, et al. Activation of human macrophages by mechanical ventilation in vitro. Am J Physiol. 1998;275(6):L1040-50. doi: 10.1152/ajplung.1998.275.6.L1040. PubMed PMID: 9843840.

38. Wehner S, Buchholz BM, Schuchtrup S, Rocke A, Schaefer N, Lysson M, et al. Mechanical strain and TLR4 synergistically induce cell-specific inflammatory gene expression in intestinal smooth muscle cells and peritoneal macrophages.

Am J Physiol Gastrointest Liver Physiol. 2010;299(5):G1187-97.
doi: 10.1152/ajpgi.00452.2009. PubMed PMID: 20829523.

39. Adams S, Wuescher LM, Worth R, Yildirim-Ayan E. Mechano-Immunomodulation: Mechanoresponsive Changes in Macrophage Activity and Polarization. Annals of biomedical engineering [Internet]. 2019;47(11). Available from: https://pubmed.ncbi.nlm.nih.gov/31218484/.

40. Hotchkiss KM, Clark NM, Olivares-Navarrete R. Macrophage response to hydrophilic biomaterials regulates MSC recruitment and T-helper cell populations. Biomaterials [Internet]. 2018;182. Available from: https://pubmed.ncbi.nlm.nih.gov/30138783/.

41. Rosenson-Schloss RS, Vitolo JL, Moghe PV. Flow-mediated cell stress induction in adherent leukocytes is accompanied by modulation of morphology and phagocytic function. Medical & biological engineering & computing [Internet]. 1999;37(2). Available from: https://pubmed.ncbi.nlm.nih.gov/10396832/.

42. Mattana J, Sankaran RT, Singhal PC. Increased applied pressure enhances the uptake of IgG complexes by macrophages. Pathobiology. 1996;64(1):40–5. doi: 10.1159/000164004. PubMed PMID: 8856794.

43. Mattana J, Sankaran RT, Singhal PC. Repetitive mechanical strain suppresses macrophage uptake of immunoglobulin G complexes and enhances cyclic adenosine monophosphate synthesis. The American Journal of Pathology. 1995;147(2):529–40. PubMed PMID: 7543737.

44. Yaraee R, Ebtekar M, Ahmadiani A, Sabahi F. Neuropeptides (SP and CGRP) augment pro-inflammatory cytokine production in HSV-infected macrophages. Int Immunopharmacol. 2003;3(13-14):1883–7. doi: 10.1016/S1567-5769(03)00201-7.

45. Sun J, Ramnath RD, Tamizhselvi R, Bhatia M. Role of protein kinase C and phosphoinositide 3-kinase-Akt in substance P-induced proinflammatory pathways in mouse macrophages. FASEB J. 2009;23(4):997–1010. doi: 10.1096/fj.08-121756. PubMed PMID: 19029199.

46. Suvas S. Role of Substance P Neuropeptide in Inflammation, Wound Healing, and Tissue Homeostasis. J Immunol. 2017;199(5):1543–52. doi: 10.4049/jimmunol.1601751. PubMed PMID: 28827386.

47. Chauhan VS, Sterka DG, Gray DL, Bost KL, Marriott I. Neurogenic Exacerbation of Microglial and Astrocyte Responses to Neisseria meningitidis and Borrelia

burgdorferi. J Immunol. 2008;180(12):8241–9.
doi: 10.4049/jimmunol.180.12.8241.

48. Foldenauer MEB, McClellan SA, Barrett RP, Zhang Y, Hazlett LD. Substance P Affects Growth Factors in Pseudomonas aeruginosa–Infected Mouse Cornea. Cornea. 2012;31(10):1176–88. doi: 10.1097/ICO.0b013e31824d6ffd.

49. Montana G, Lampiasi N, Mukhopadhyay P. Substance P Induces HO-1 Expression in RAW 264.7 Cells Promoting Switch towards M2-Like Macrophages. PLoS ONE. 2016;11(12):e0167420.
doi: 10.1371/journal.pone.0167420.

50. Leal EC, Carvalho E, Tellechea A, Kafanas A, Tecilazich F, Kearney C, et al. Substance P Promotes Wound Healing in Diabetes by Modulating Inflammation and Macrophage Phenotype. The American Journal of Pathology. 2015;185(6):1638–48. doi: 10.1016/j.ajpath.2015.02.011.

51. Murris-Espin M, Pinelli E, Pipy B, Leophonte P, Didier A. Substance P and alveolar macrophages: Effects on oxidative metabolism and eicosanoid production. Allergy. 1995;50(4):334–9. doi: 10.1111/j.1398-9995.1995.tb01157.x. PubMed PMID: 7573817.

52. Muschter D, Beiderbeck A-S, Späth T, Kirschneck C, Schröder A, Grässel S. Sensory Neuropeptides and their Receptors Participate in Mechano-Regulation of Murine Macrophages. Int J Mol Sci. 2019;20(3). doi: 10.3390/ijms20030503. PubMed PMID: 30682804.

53. Chancellor-Freeland C, Zhu GF, Kage R, Di Beller, Leeman SE, Black PH. Substance P and stress-induced changes in macrophages. Ann N Y Acad Sci [Internet]. 1995;771. Available from: https://pubmed.ncbi.nlm.nih.gov/8597423/.

54. James DE, Nijkamp FP. Neuroendocrine and immune interactions with airway macrophages. Inflammation research : official journal of the European Histamine Research Society … [et al.] [Internet]. 2000;49(6). Available from: https://pubmed.ncbi.nlm.nih.gov/10939615/.

55. Nong YH, Titus RG, Ribeiro JM, Remold HG. Peptides encoded by the calcitonin gene inhibit macrophage function. J Immunol. 1989;143(1):45–9. PubMed PMID: 2543703.

56. Yaraee R, Ebtekar M, Ahmadiani A, Sabahi F. Effect of neuropeptides (SP and CGRP) on antigen presentation by macrophages. Immunopharmacol

Immunotoxicol. 2005;27(3):395–404. doi: 10.1080/08923970500240974.
PubMed PMID: 16237951.

57. Owan I, Ibaraki K. The role of calcitonin gene-related peptide (CGRP) in macrophages: The presence of functional receptors and effects on proliferation and differentiation into osteoclast-like cells. Bone and Mineral. 1994;24(2):151–64. doi: 10.1016/S0169-6009(08)80152-3.

58. Pittner RA. Lack of effect of calcitonin gene-related peptide and amylin on major markers of glucose metabolism in hepatocytes. European Journal of Pharmacology [Internet]. 1997;325(2-3). Available from: https://pubmed.ncbi.nlm.nih.gov/9163566/.

59. Ahmed AA, Wahbi AH, Nordlin K. Neuropeptides modulate a murine monocyte/macrophage cell line capacity for phagocytosis and killing of Leishmania major parasites. Immunopharmacol Immunotoxicol. 2001;23(3):397–409. doi: 10.1081/iph-100107339. PubMed PMID: 11694030.

60. Mapp PI, McWilliams DF, Turley MJ, Hargin E, Walsh DA. A role for the sensory neuropeptide calcitonin gene-related peptide in endothelial cell proliferation in vivo. Br J Pharmacol. 2012;166(4):1261–71. doi: 10.1111/j.1476-5381.2012.01848.x. PubMed PMID: 22233274.

61. Niedermair T, Schirner S, Seebröker R, Straub RH, Grässel S. Substance P modulates bone remodeling properties of murine osteoblasts and osteoclasts. Sci Rep. 2018;8(1):9199. doi: 10.1038/s41598-018-27432-y. PubMed PMID: 29907830.

62. Fernandez S, Knopf MA, Bjork SK, McGillis JP. Bone marrow-derived macrophages express functional CGRP receptors and respond to CGRP by increasing transcription of c-fos and IL-6 mRNA. Cell Immunol. 2001;209(2):140–8. doi: 10.1006/cimm.2001.1795. PubMed PMID: 11446746.

63. Duan J-X, Zhou Y, Zhou A-Y, Guan X-X, Liu T, Yang H-H, et al. Calcitonin gene-related peptide exerts anti-inflammatory property through regulating murine macrophages polarization in vitro. Mol Immunol. 2017;91:105–13. doi: 10.1016/j.molimm.2017.08.020. PubMed PMID: 28892747.

64. Berger A, Tran AH, Paige CJ. Co-regulated decrease of Neurokinin-1 receptor and Hemokinin-1 gene expression in monocytes and macrophages after activation with pro-inflammatory cytokines. J Neuroimmunol. 2007;187(1-2):83–93. doi: 10.1016/j.jneuroim.2007.04.019.

65. Boyle WJ, Simonet WS, Lacey DL. Osteoclast differentiation and activation. Nature. 2003;423(6937):337–42. doi: 10.1038/nature01658. PubMed PMID: 12748652.

66. Raggatt LJ, Partridge NC. Cellular and Molecular Mechanisms of Bone Remodeling. J. Biol. Chem. 2010;285(33):25103–8. doi: 10.1074/jbc.R109.041087.

67. Gruber R. Molecular and cellular basis of bone resorption. Wien Med Wochenschr. 2015;165(3-4):48–53. doi: 10.1007/s10354-014-0310-0.

68. Georgess D, Machuca-Gayet I, Blangy A, Jurdic P. Podosome organization drives osteoclast-mediated bone resorption. Cell Adh Migr. 2014;8(3):192–204. doi: 10.4161/cam.27840.

69. Negishi-Koga T, Takayanagi H. Ca 2+ -NFATc1 signaling is an essential axis of osteoclast differentiation. Immunological Reviews. 2009;231(1):241–56. doi: 10.1111/j.1600-065X.2009.00821.x.

70. Cho E-S, Lee K-S, Son Y-O, Jang Y-S, Lee S-Y, Kwak S-Y, et al. Compressive mechanical force augments osteoclastogenesis by bone marrow macrophages through activation of c-Fms-mediated signaling. J Cell Biochem. 2010;111(5):1260–9. doi: 10.1002/jcb.22849. PubMed PMID: 20803546.

71. Hayakawa T, Yoshimura Y, Kikuiri T, Matsuno M, Hasegawa T, Fukushima K, et al. Optimal compressive force accelerates osteoclastogenesis in RAW264.7 cells. Mol Med Rep. 2015;12(4):5879–85. doi: 10.3892/mmr.2015.4141. PubMed PMID: 26238100.

72. Kameyama S, Yoshimura Y, Kameyama T, Kikuiri T, Matsuno M, Deyama Y, et al. Short-term mechanical stress inhibits osteoclastogenesis via suppression of DC-STAMP in RAW264.7 cells. Int J Mol Med. 2013;31(2):292–8. doi: 10.3892/ijmm.2012.1220. PubMed PMID: 23292096.

73. Kurata K, Uemura T, Nemoto A, Tateishi T, Murakami T, Higaki H, et al. Mechanical strain effect on bone-resorbing activity and messenger RNA expressions of marker enzymes in isolated osteoclast culture. J Bone Miner Res. 2001;16(4):722–30. doi: 10.1359/jbmr.2001.16.4.722. PubMed PMID: 11316000.

74. Ma Q, Ma Z, Liang M, Luo F, Xu J, Dou C, et al. The role of physical forces in osteoclastogenesis. J Cell Physiol. 2018;234(8):12498–507. doi: 10.1002/jcp.28108.

75. Li X, Yang J, Liu D, Li J, Niu K, Feng S, et al. Knee loading inhibits osteoclast lineage in a mouse model of osteoarthritis. Sci Rep. 2016;6:24668. doi: 10.1038/srep24668. PubMed PMID: 27087498.

76. Guo Y, Wang Y, Liu Y, Wang H, Guo C, Zhang X. Effect of the same mechanical loading on osteogenesis and osteoclastogenesis in vitro. Chin J Traumatol. 2015;18(3):150–6. PubMed PMID: 26643241.

77. Yoo Y-M, Kwag JH, Kim KH, Kim CH. Effects of neuropeptides and mechanical loading on bone cell resorption in vitro. Int J Mol Sci. 2014;15(4):5874–83. doi: 10.3390/ijms15045874. PubMed PMID: 24717410.

78. Xu X-Y, Guo C, Yan Y-X, Guo Y, Li R-X, Song M, et al. Differential effects of mechanical strain on osteoclastogenesis and osteoclast-related gene expression in RAW264.7 cells. Mol Med Rep. 2012;6(2):409–15. doi: 10.3892/mmr.2012.908. PubMed PMID: 22580758.

79. Shibata K, Yoshimura Y, Kikuiri T, Hasegawa T, Taniguchi Y, Deyama Y, et al. Effect of the release from mechanical stress on osteoclastogenesis in RAW264.7 cells. Int J Mol Med. 2011;28(1):73–9. doi: 10.3892/ijmm.2011.675. PubMed PMID: 21491081.

80. Rhoades B. OARSI White Paper_OA Serious Disease 121416 (1). 2016.

81. Walsh DA, Mapp PI, Kelly S. Calcitonin gene-related peptide in the joint: Contributions to pain and inflammation. Br J Clin Pharmacol. 2015;80(5):965–78. doi: 10.1111/bcp.12669. PubMed PMID: 25923821.

82. Cucchiarini M, Girolamo L de, Filardo G, Oliveira JM, Orth P, Pape D, et al. Basic science of osteoarthritis. J Exp Orthop. 2016;3(1):22. doi: 10.1186/s40634-016-0060-6. PubMed PMID: 27624438.

83. Kingsbury SR, Gross HJ, Isherwood G, Conaghan PG. Osteoarthritis in Europe: Impact on health status, work productivity and use of pharmacotherapies in five European countries. Rheumatology (Oxford). 2014;53(5):937–47. doi: 10.1093/rheumatology/ket463. PubMed PMID: 24489012.

84. Cox LGE, van Donkelaar CC, van Rietbergen B, Emans PJ, Ito K. Decreased bone tissue mineralization can partly explain subchondral sclerosis observed in osteoarthritis. Bone. 2012;50(5):1152–61. doi: 10.1016/j.bone.2012.01.024. PubMed PMID: 22342798.

85. Anetzberger H, Mayer A, Glaser C, Lorenz S, Birkenmaier C, Müller-Gerbl M. Meniscectomy leads to early changes in the mineralization distribution of

subchondral bone plate. Knee Surg Sports Traumatol Arthrosc. 2014;22(1):112–9. doi: 10.1007/s00167-012-2297-7. PubMed PMID: 23160848.

86. Witt KL, Vilensky JA. The anatomy of osteoarthritic joint pain. Clin Anat. 2014;27(3):451–4. doi: 10.1002/ca.22120. PubMed PMID: 22730047.

87. Pan J, Wang B, Li W, Zhou X, Scherr T, Yang Y, et al. Elevated cross-talk between subchondral bone and cartilage in osteoarthritic joints. Bone. 2012;51(2):212–7. doi: 10.1016/j.bone.2011.11.030. PubMed PMID: 22197997.

88. Suri S, Gill SE, Massena de Camin S, McWilliams DF, Wilson D, Walsh DA. Neurovascular invasion at the osteochondral junction and in osteophytes in osteoarthritis. Ann Rheum Dis. 2007;66(11):1423–8. doi: 10.1136/ard.2006.063354.

89. Funck-Brentano T, Cohen-Solal M. Subchondral bone and osteoarthritis. Curr Opin Rheumatol. 2015;27(4):420–6. doi: 10.1097/BOR.0000000000000181. PubMed PMID: 26002035.

90. Roemer FW, Guermazi A, Javaid MK, Lynch JA, Niu J, Zhang Y, et al. Change in MRI-detected subchondral bone marrow lesions is associated with cartilage loss: The MOST Study. A longitudinal multicentre study of knee osteoarthritis. Ann Rheum Dis. 2009;68(9):1461–5. doi: 10.1136/ard.2008.096834.

91. Zhang Y, Nevitt M, Niu J, Lewis C, Torner J, Guermazi A, et al. Fluctuation of knee pain and changes in bone marrow lesions, effusions, and synovitis on magnetic resonance imaging. Arthritis & Rheumatism. 2011;63(3):691–9. doi: 10.1002/art.30148.

92. Li G, Yin J, Gao J, Cheng TS, Pavlos NJ, Zhang C, et al. Subchondral bone in osteoarthritis: Insight into risk factors and microstructural changes. Arthritis Res Ther. 2013;15(6):223. doi: 10.1186/ar4405. PubMed PMID: 24321104.

93. Goldring MB, Goldring SR. Articular cartilage and subchondral bone in the pathogenesis of osteoarthritis. Ann N Y Acad Sci. 2010;1192(1):230–7. doi: 10.1111/j.1749-6632.2009.05240.x.

94. Buckland-Wright JC. Early radiographic features in patients with anterior cruciate ligament rupture. Ann Rheum Dis. 2000;59(8):641–6. doi: 10.1136/ard.59.8.641.

95. Yuan XL, Meng HY, Wang YC, Peng J, Guo QY, Wang AY, et al. Bone-cartilage interface crosstalk in osteoarthritis: Potential pathways and future therapeutic strategies. Osteoarthr Cartil. 2014;22(8):1077–89. doi: 10.1016/j.joca.2014.05.023. PubMed PMID: 24928319.

96. Madry H, van Dijk CN, Mueller-Gerbl M. The basic science of the subchondral bone. Knee Surg Sports Traumatol Arthrosc. 2010;18(4):419–33. doi: 10.1007/s00167-010-1054-z.

97. Rik J. Lories, Silvia Monteagudo. Review Article: Is Wnt Signaling an Attractive Target for the Treatment of Osteoarthritis? Rheumatol Ther [Internet]. 2020;7(2):259–70. Available from: https://link.springer.com/article/10.1007/s40744-020-00205-8#Fig2.

98. Cope PJ, Ourradi K, Li Y, Sharif M. Models of osteoarthritis: The good, the bad and the promising. Osteoarthr Cartil. 2019;27(2):230–9. doi: 10.1016/j.joca.2018.09.016. PubMed PMID: 30391394.

99. McCoy AM. Animal Models of Osteoarthritis: Comparisons and Key Considerations. Vet Pathol. 2015;52(5):803–18. doi: 10.1177/0300985815588611. PubMed PMID: 26063173.

100. Lorenz J, Grässel S. Experimental osteoarthritis models in mice. Methods in molecular biology (Clifton, N.J.) [Internet]. 2014;1194. Available from: https://pubmed.ncbi.nlm.nih.gov/25064117/.

101. McNulty MA, Loeser RF, Davey C, Callahan MF, Ferguson CM, Carlson CS. Histopathology of naturally occurring and surgically induced osteoarthritis in mice. Osteoarthr Cartil. 2012;20(8):949–56. doi: 10.1016/j.joca.2012.05.001. PubMed PMID: 22595226.

102. Chen Y, Jiang W, Yong H, He M, Yang Y, Deng Z, et al. Macrophages in osteoarthritis: Pathophysiology and therapeutics. Am J Transl Res. 2020;12(1):261–8. PubMed PMID: 32051751.

103. Chen Z, Ma Y, Li X, Deng Z, Zheng M, Zheng Q. The Immune Cell Landscape in Different Anatomical Structures of Knee in Osteoarthritis: A Gene Expression-Based Study. Biomed Res Int. 2020;2020. doi: 10.1155/2020/9647072. PubMed PMID: 32258161.

104. Sinder BP, Pettit AR, McCauley LK. Macrophages: Their Emerging Roles in Bone. J Bone Miner Res. 2015;30(12):2140–9. doi: 10.1002/jbmr.2735.

105. Gaffney L, Warren P, Wrona EA, Fisher MB, Freytes DO. Macrophages' Role in Tissue Disease and Regeneration. Results and problems in cell differentiation [Internet]. 2017;62. Available from: https://pubmed.ncbi.nlm.nih.gov/28455712/.

106. Leung A, Gregory NS, Allen L-AH, Sluka KA. Regular physical activity prevents chronic pain by altering resident muscle macrophage phenotype and

increasing interleukin-10 in mice. Pain [Internet]. 2016;157(1):70–9. Available from: http://dx.doi.org/10.1097/j.pain.0000000000000312.

107.   Chang MK, Raggatt L-J, Alexander KA, Kuliwaba JS, Fazzalari NL, Schroder K, et al. Osteal Tissue Macrophages Are Intercalated throughout Human and Mouse Bone Lining Tissues and Regulate Osteoblast Function In Vitro and In Vivo. J Immunol. 2008;181(2):1232–44. doi: 10.4049/jimmunol.181.2.1232.

108.   Horwood NJ. Macrophage Polarization and Bone Formation: A review. Clinic Rev Allerg Immunol. 2016;51(1):79–86. doi: 10.1007/s12016-015-8519-2.

109.   Kraus VB, McDaniel G, Huebner JL, Stabler TV, Pieper CF, Shipes SW, et al. Direct in vivo evidence of activated macrophages in human osteoarthritis. Osteoarthr Cartil. 2016;24(9):1613–21. doi: 10.1016/j.joca.2016.04.010. PubMed PMID: 27084348.

110.   Weber A, Chan PMB, Wen C. Do immune cells lead the way in subchondral bone disturbance in osteoarthritis? Progress in Biophysics and Molecular Biology. 2019;148:21–31. doi: 10.1016/j.pbiomolbio.2017.12.004.

111.   Geurts J, Patel A, Hirschmann MT, Pagenstert GI, Müller-Gerbl M, Valderrabano V, et al. Elevated marrow inflammatory cells and osteoclasts in subchondral osteosclerosis in human knee osteoarthritis. J. Orthop. Res. 2016;34(2):262–9. doi: 10.1002/jor.23009.

112.   Wu C-L, McNeill J, Goon K, Little D, Kimmerling K, Huebner J, et al. Conditional Macrophage Depletion Increases Inflammation and Does Not Inhibit the Development of Osteoarthritis in Obese Macrophage Fas-Induced Apoptosis-Transgenic Mice. Arthritis & Rheumatology. 2017;69(9):1772–83. doi: 10.1002/art.40161.

113.   Berenbaum F. Osteoarthritis as an inflammatory disease (osteoarthritis is not osteoarthrosis!:). Osteoarthr Cartil. 2013;21(1):16–21. doi: 10.1016/j.joca.2012.11.012.

114.   Nair A, Kanda V, Bush-Joseph C, Verma N, Chubinskaya S, Mikecz K, et al. Synovial fluid from patients with early osteoarthritis modulates fibroblast-like synoviocyte responses to Toll-like receptor 4 and Toll-like receptor 2 ligands via soluble CD14. Arthritis & Rheumatism. 2012;64(7):2268–77. doi: 10.1002/art.34495.

115. Zhen G, Wen C, Jia X, Li Y, Crane JL, Mears SC, et al. Inhibition of TGF-β signaling in mesenchymal stem cells of subchondral bone attenuates osteoarthritis. Nat Med. 2013;19(6):704–12. doi: 10.1038/nm.3143.

116. Utomo L, van OGJ, Bayon Y, Verhaar JA, Bastiaansen-Jenniskens YM. Guiding synovial inflammation by macrophage phenotype modulation: An in vitro study towards a therapy for osteoarthritis. Osteoarthr Cartil [Internet]. 2016;24(9). Available from: https://pubmed.ncbi.nlm.nih.gov/27095417/.

117. Kulkarni K, Karssiens T, Kumar V, Pandit H. Obesity and osteoarthritis. Maturitas [Internet]. 2016;89. Available from: https://pubmed.ncbi.nlm.nih.gov/27180156/.

118. Tanamas S, Hanna FS, Cicuttini FM, Wluka AE, Berry P, Urquhart DM. Does knee malalignment increase the risk of development and progression of knee osteoarthritis? A systematic review. Arthritis Rheum. 2009;61(4):459–67. doi: 10.1002/art.24336. PubMed PMID: 19333985.

119. Roos EM. Joint injury causes knee osteoarthritis in young adults. Curr Opin Rheumatol. 2005;17(2):195–200. doi: 10.1097/01.bor.0000151406.64393.00. PubMed PMID: 15711235.

120. Bader DL, Salter DM, Chowdhury TT. Biomechanical Influence of Cartilage Homeostasis in Health and Disease. Arthritis. 2011;2011. doi: 10.1155/2011/979032. PubMed PMID: 22046527.

121. Guilak F. Biomechanical factors in osteoarthritis. Best Pract Res Clin Rheumatol. 2011;25(6):815–23. doi: 10.1016/j.berh.2011.11.013. PubMed PMID: 22265263.

122. Zhao Z, Li Y, Wang M, Zhao S, Zhao Z, Fang J. Mechanotransduction pathways in the regulation of cartilage chondrocyte homoeostasis. J Cell Mol Med. 2020;24(10):5408–19. doi: 10.1111/jcmm.15204.

123. Sanchez-Adams J, Leddy HA, McNulty AL, O'Conor CJ, Guilak F. The mechanobiology of articular cartilage: Bearing the burden of osteoarthritis. Curr Rheumatol Rep. 2014;16(10):451. doi: 10.1007/s11926-014-0451-6. PubMed PMID: 25182679.

124. Thompson CL, Chapple JP, Knight MM. Primary cilia disassembly down-regulates mechanosensitive hedgehog signalling: A feedback mechanism controlling ADAMTS-5 expression in chondrocytes. Osteoarthr Cartil. 2014;22(3):490–8. doi: 10.1016/j.joca.2013.12.016.

125. Murphy G, Lee M. What are the roles of metalloproteinases in cartilage and bone damage? Ann Rheum Dis. 2005;64(Suppl 4):iv44-7. doi: 10.1136/ard.2005.042465. PubMed PMID: 16239386.

126. Malemud CJ. Inhibition of MMPs and ADAM/ADAMTS. Biochem Pharmacol. 2019;165:33–40. doi: 10.1016/j.bcp.2019.02.033. PubMed PMID: 30826330.

127. Donell S. Subchondral bone remodelling in osteoarthritis. EFORT Open Reviews. 2019;4(6):221–9. doi: 10.1302/2058-5241.4.180102.

128. Saito T, Fukai A, Mabuchi A, Ikeda T, Yano F, Ohba S, et al. Transcriptional regulation of endochondral ossification by HIF-2α during skeletal growth and osteoarthritis development. Nat Med. 2010;16(6):678–86. doi: 10.1038/nm.2146.

129. Yang S, Kim J, Ryu J-H, Oh H, Chun C-H, Kim BJ, et al. Hypoxia-inducible factor-2α is a catabolic regulator of osteoarthritic cartilage destruction. Nat Med. 2010;16(6):687–93. doi: 10.1038/nm.2153.

130. O'Conor CJ, Leddy HA, Benefield HC, Liedtke WB, Guilak F. TRPV4-mediated mechanotransduction regulates the metabolic response of chondrocytes to dynamic loading. Proceedings of the National Academy of Sciences. 2014;111(4):1316–21. doi: 10.1073/pnas.1319569111.

131. Burr DB, Radin EL. Microfractures and microcracks in subchondral bone: Are they relevant to osteoarthrosis? Rheumatic Disease Clinics of North America. 2003;29(4):675–85. doi: 10.1016/S0889-857X(03)00061-9.

132. Zhen G, Cao X. Targeting TGFβ signaling in subchondral bone and articular cartilage homeostasis. Trends Pharmacol Sci. 2014;35(5):227–36. doi: 10.1016/j.tips.2014.03.005.

133. Blaney Davidson EN, van der Kraan PM, van den Berg WB. TGF-β and osteoarthritis. Osteoarthr Cartil. 2007;15(6):597–604. doi: 10.1016/j.joca.2007.02.005.

134. Hukkanen M, Konttinen YT, Rees RG, Santavirta S, Terenghi G, Polak JM. Distribution of nerve endings and sensory neuropeptides in rat synovium, meniscus and bone. Int J Tissue React. 1992;14(1):1–10. PubMed PMID: 1383167.

135. Saito T, Koshino T. Distribution of neuropeptides in synovium of the knee with osteoarthritis. Clin Orthop Relat Res. 2000(376):172–82. PubMed PMID: 10906873.

136.	Felson DT. The sources of pain in knee osteoarthritis. Curr Opin Rheumatol. 2005;17(5):624–8. doi: 10.1097/01.bor.0000172800.49120.97.

137.	Eitner A, Pester J, Nietzsche S, Hofmann GO, Schaible H-G. The innervation of synovium of human osteoarthritic joints in comparison with normal rat and sheep synovium. Osteoarthr Cartil. 2013;21(9):1383–91. doi: 10.1016/j.joca.2013.06.018. PubMed PMID: 23973153.

138.	Buma P, Verschuren C, Versleyen D, van der Kraan P, Oestreicher AB. Calcitonin gene-related peptide, substance P and GAP-43/B-50 immunoreactivity in the normal and arthrotic knee joint of the mouse. Histochemistry. 1992;98(5):327–39. PubMed PMID: 1283163.

139.	Murakami K, Nakagawa H, Nishimura K, Matsuo S. Changes in peptidergic fiber density in the synovium of mice with collagenase-induced acute arthritis. Can J Physiol Pharmacol. 2015;93(6):435–41. doi: 10.1139/cjpp-2014-0446. PubMed PMID: 25909759.

140.	Mapp PI, Kidd BL, Gibson SJ, Terry JM, Revell PA, Ibrahim NB, et al. Substance P-, calcitonin gene-related peptide- and C-flanking peptide of neuropeptide Y-immunoreactive fibres are present in normal synovium but depleted in patients with rheumatoid arthritis. Neuroscience. 1990;37(1):143–53. PubMed PMID: 1700840.

141.	Saxler G, Löer F, Skumavc M, Pförtner J, Hanesch U. Localization of SP- and CGRP-immunopositive nerve fibers in the hip joint of patients with painful osteoarthritis and of patients with painless failed total hip arthroplasties. Eur J Pain. 2007;11(1):67–74. doi: 10.1016/j.ejpain.2005.12.011. PubMed PMID: 16460974.

142.	Ashraf S, Wibberley H, Mapp PI, Hill R, Wilson D, Walsh DA. Increased vascular penetration and nerve growth in the meniscus: A potential source of pain in osteoarthritis. Ann Rheum Dis. 2011;70(3):523–9. doi: 10.1136/ard.2010.137844.

143.	Dong T, Chang H, Zhang F, Chen W, Zhu Y, Wu T, et al. Calcitonin gene-related peptide can be selected as a predictive biomarker on progression and prognosis of knee osteoarthritis. Int Orthop. 2015;39(6):1237–43. doi: 10.1007/s00264-015-2744-4. PubMed PMID: 25813459.

144.	Wang H, Zhang X, He J-Y, Zheng X-F, Li D, Li Z, et al. Increasing expression of substance P and calcitonin gene-related peptide in synovial tissue and fluid

contribute to the progress of arthritis in developmental dysplasia of the hip. Arthritis Res Ther. 2015;17(1):4. doi: 10.1186/s13075-014-0513-1.

145. Inoue H, Shimoyama Y, Hirabayashi K, Kajigaya H, Yamamoto S, Oda H, et al. Production of neuropeptide substance P by synovial fibroblasts from patients with rheumatoid arthritis and osteoarthritis. Neurosci Lett. 2001;303(3):149–52. doi: 10.1016/S0304-3940(01)01713-X.

146. Lane NE, Schnitzer TJ, Birbara CA, Mokhtarani M, Shelton DL, Smith MD, et al. Tanezumab for the treatment of pain from osteoarthritis of the knee. N Engl J Med. 2010;363(16):1521–31. doi: 10.1056/NEJMoa0901510. PubMed PMID: 20942668.

147. Tiseo PJ, Kivitz AJ, Ervin JE, Ren H, Mellis SJ. Fasinumab (REGN475), an antibody against nerve growth factor for the treatment of pain: Results from a double-blind, placebo-controlled exploratory study in osteoarthritis of the knee. Pain. 2014;155(7):1245–52. doi: 10.1016/j.pain.2014.03.018. PubMed PMID: 24686255.

148. Grässel S, Muschter D. Recent advances in the treatment of osteoarthritis. F1000Res. 2020;9:325. doi: 10.12688/f1000research.22115.1.

149. CHANG MM, LEEMAN SE, NIALL HD. Amino-acid Sequence of Substance P. Nature New Biology. 1971;232(29):86–7. doi: 10.1038/newbio232086a0.

150. Otsuka M, Yoshioka K. Neurotransmitter functions of mammalian tachykinins. Physiol Rev. 1993;73(2):229–308. doi: 10.1152/physrev.1993.73.2.229. PubMed PMID: 7682720.

151. Harrison S. Substance P. The International Journal of Biochemistry & Cell Biology. 2001;33(6):555–76. doi: 10.1016/S1357-2725(01)00031-0.

152. Oku R, Satoh M, Takagi H. Release of substance P from the spinal dorsal horn is enhanced in polyarthritic rats. Neurosci Lett. 1987;74(3):315–9. PubMed PMID: 2436112.

153. Schaible HG, Jarrott B, Hope PJ, Duggan AW. Release of immunoreactive substance P in the spinal cord during development of acute arthritis in the knee joint of the cat: A study with antibody microprobes. Brain Res. 1990;529(1-2):214–23. PubMed PMID: 1704282.

154. Lembeck F, Holzer P. Substance P as neurogenic mediator of antidromic vasodilation and neurogenic plasma extravasation. Naunyn Schmiedebergs Arch Pharmacol. 1979;310(2):175–83. PubMed PMID: 93706.

155.   Opolka A, Straub RH, Pasoldt A, Grifka J, Grässel S. Substance P and norepinephrine modulate murine chondrocyte proliferation and apoptosis. Arthritis Rheum. 2012;64(3):729–39. doi: 10.1002/art.33449. PubMed PMID: 22042746.

156.   Kim K-T, Kim H-J, Cho D-C, Bae J-S, Park S-W. Substance P stimulates proliferation of spinal neural stem cells in spinal cord injury via the mitogen-activated protein kinase signaling pathway. Spine J. 2015;15(9):2055–65. doi: 10.1016/j.spinee.2015.04.032. PubMed PMID: 25921821.

157.   Zhou Y, Zhou B, Tang K. The effects of substance p on tendinopathy are dose-dependent: An in vitro and in vivo model study. J Nutr Health Aging. 2015;19(5):555–61. doi: 10.1007/s12603-014-0576-3. PubMed PMID: 25923486.

158.   Backman LJ, Eriksson DE, Danielson P. Substance P reduces TNF-α-induced apoptosis in human tenocytes through NK-1 receptor stimulation. Br J Sports Med. 2014;48(19):1414–20. doi: 10.1136/bjsports-2013-092438. PubMed PMID: 23996004.

159.   Gross K, Karagiannides I, Thomou T, Koon HW, Bowe C, Kim H, et al. Substance P promotes expansion of human mesenteric preadipocytes through proliferative and antiapoptotic pathways. Am J Physiol Gastrointest Liver Physiol. 2009;296(5):G1012-9. doi: 10.1152/ajpgi.90351.2008. PubMed PMID: 19282377.

160.   DeFea KA, Vaughn ZD, O'Bryan EM, Nishijima D, Dery O, Bunnett NW. The proliferative and antiapoptotic effects of substance P are facilitated by formation of a beta -arrestin-dependent scaffolding complex. Proceedings of the National Academy of Sciences. 2000;97(20):11086–91. doi: 10.1073/pnas.190276697.

161.   Goto T, Yamaza T, Kido MA, Tanaka T. Light- and electron-microscopic study of the distribution of axons containing substance P and the localization of neurokinin-1 receptor in bone. Cell Tissue Res. 1998;293(1):87–93. PubMed PMID: 9634600.

162.   Lerner UH. Neuropeptidergic regulation of bone resorption and bone formation. J Musculoskelet Neuronal Interact. 2002;2(5):440–7. PubMed PMID: 15758412.

163.   Sohn SJ. Substance P upregulates osteoclastogenesis by activating nuclear factor kappa B in osteoclast precursors. Acta Otolaryngol. 2005;125(2):130–3. PubMed PMID: 15880941.

164.	Mori T, Ogata T, Okumura H, Shibata T, Nakamura Y, Kataoka K. Substance P regulates the function of rabbit cultured osteoclast; increase of intracellular free calcium concentration and enhancement of bone resorption. Biochem Biophys Res Commun. 1999;262(2):418–22. doi: 10.1006/bbrc.1999.1220. PubMed PMID: 10462490.

165.	Shih C, Bernard GW. Neurogenic Substance P Stimulates Osteogenesis In Vitro. Peptides. 1997;18(2):323–6. doi: 10.1016/S0196-9781(96)00280-X.

166.	Wang L, Zhao R, Shi X, Wei T, Halloran BP, Clark DJ, et al. Substance P stimulates bone marrow stromal cell osteogenic activity, osteoclast differentiation, and resorption activity in vitro. Bone. 2009;45(2):309–20. doi: 10.1016/j.bone.2009.04.203. PubMed PMID: 19379851.

167.	Jiang MH, Lim JE, Chi GF, Ahn W, Zhang M, Chung E, et al. Substance P reduces apoptotic cell death possibly by modulating the immune response at the early stage after spinal cord injury. Neuroreport. 2013;24(15):846–51. doi: 10.1097/WNR.0b013e3283650e3d. PubMed PMID: 23995292.

168.	Hao S, Meng J, Zhang Y, Liu J, Nie X, Wu F, et al. Macrophage phenotypic mechanomodulation of enhancing bone regeneration by superparamagnetic scaffold upon magnetization. Biomaterials [Internet]. 2017;140. Available from: https://pubmed.ncbi.nlm.nih.gov/28623721/.

169.	Brain SD, Williams TJ, Tippins JR, Morris HR, MacIntyre I. Calcitonin gene-related peptide is a potent vasodilator. Nature. 1985;313(5997):54–6. PubMed PMID: 3917554.

170.	Fernihough J, Gentry C, Bevan S, Winter J. Regulation of calcitonin gene-related peptide and TRPV1 in a rat model of osteoarthritis. Neurosci Lett. 2005;388(2):75–80. doi: 10.1016/j.neulet.2005.06.044. PubMed PMID: 16039054.

171.	Hirsch S, Corradini L, Just S, Arndt K, Doods H. The CGRP receptor antagonist BIBN4096BS peripherally alleviates inflammatory pain in rats. Pain. 2013;154(5):700–7. doi: 10.1016/j.pain.2013.01.002. PubMed PMID: 23473785.

172.	Ishida K, Kawamata T, Tanaka S, Shindo T, Kawamata M. Calcitonin gene-related peptide is involved in inflammatory pain but not in postoperative pain. Anesthesiology. 2014;121(5):1068–79. doi: 10.1097/ALN.0000000000000364. PubMed PMID: 24992521.

173.   Assas BM, Pennock JI, Miyan JA. Calcitonin gene-related peptide is a key neurotransmitter in the neuro-immune axis. Front Neurosci. 2014;8:23. doi: 10.3389/fnins.2014.00023. PubMed PMID: 24592205.

174.   Granholm S, Lundberg P, Lerner UH. Expression of the calcitonin receptor, calcitonin receptor-like receptor, and receptor activity modifying proteins during osteoclast differentiation. J Cell Biochem. 2008;104(3):920–33. doi: 10.1002/jcb.21674. PubMed PMID: 18384073.

175.   Schinke T, Liese S, Priemel M, Haberland M, Schilling AF, Catala-Lehnen P, et al. Decreased bone formation and osteopenia in mice lacking alpha-calcitonin gene-related peptide. J Bone Miner Res. 2004;19(12):2049–56. doi: 10.1359/JBMR.040915. PubMed PMID: 15537449.

176.   Brain SD, Grant AD. Vascular actions of calcitonin gene-related peptide and adrenomedullin. Physiol Rev. 2004;84(3):903–34. doi: 10.1152/physrev.00037.2003. PubMed PMID: 15269340.

177.   Benschop RJ, Collins EC, Darling RJ, Allan BW, Leung D, Conner EM, et al. Development of a novel antibody to calcitonin gene-related peptide for the treatment of osteoarthritis-related pain. Osteoarthr Cartil. 2014;22(4):578–85. doi: 10.1016/j.joca.2014.01.009. PubMed PMID: 24508775.

178.   Hoare SRJ. Mechanisms of peptide and nonpeptide ligand binding to Class B G-protein-coupled receptors. Drug Discov Today. 2005;10(6):417–27. doi: 10.1016/S1359-6446(05)03370-2. PubMed PMID: 15808821.

179.   Lee S-M, Hay DL, Pioszak AA. Calcitonin and Amylin Receptor Peptide Interaction Mechanisms: INSIGHTS INTO PEPTIDE-BINDING MODES AND ALLOSTERIC MODULATION OF THE CALCITONIN RECEPTOR BY RECEPTOR ACTIVITY-MODIFYING PROTEINS. J Biol Chem. 2016;291(16):8686–700. doi: 10.1074/jbc.M115.713628. PubMed PMID: 26895962.

180.   Watkins HA, Walker CS, Ly KN, Bailey RJ, Barwell J, Poyner DR, et al. Receptor activity-modifying protein-dependent effects of mutations in the calcitonin receptor-like receptor: Implications for adrenomedullin and calcitonin gene-related peptide pharmacology. Br J Pharmacol. 2014;171(3):772–88. doi: 10.1111/bph.12508. PubMed PMID: 24199627.

181.   Dickerson IM. Role of CGRP-Receptor Component Protein (RCP) in CLR/RAMP Function.

182. Weston C, Winfield I, Harris M, Hodgson R, Shah A, Dowell SJ, et al. Receptor Activity-modifying Protein-directed G Protein Signaling Specificity for the Calcitonin Gene-related Peptide Family of Receptors. J Biol Chem. 2016;291(42):21925–44. doi: 10.1074/jbc.M116.751362. PubMed PMID: 27566546.

183. D'Souza SM, MacIntyre I, Girgis SI, Mundy GR. Human synthetic calcitonin gene-related peptide inhibits bone resorption in vitro. Endocrinology. 1986;119(1):58–61. doi: 10.1210/endo-119-1-58. PubMed PMID: 3487444.

184. Yamamoto I, Kitamura N, Aoki J, Shigeno C, Hino M, Asonuma K, et al. Human calcitonin gene-related peptide possesses weak inhibitory potency of bone resorption in vitro. Calcif Tissue Int. 1986;38(6):339–41. PubMed PMID: 3089556.

185. Zaidi M, Fuller K, Bevis PJ, GainesDas RE, Chambers TJ, MacIntyre I. Calcitonin gene-related peptide inhibits osteoclastic bone resorption: A comparative study. Calcif Tissue Int. 1987;40(3):149–54. PubMed PMID: 3105845.

186. Cornish J, Callon KE, Bava U, Kamona SA, Cooper GJS, Reid IR. Effects of calcitonin, amylin, and calcitonin gene-related peptide on osteoclast development. Bone. 2001;29(2):162–8. doi: 10.1016/S8756-3282(01)00494-X.

187. He H, Chai J, Zhang S, Ding L, Yan P, Du W, et al. CGRP may regulate bone metabolism through stimulating osteoblast differentiation and inhibiting osteoclast formation. Mol Med Rep. 2016;13(5):3977–84. doi: 10.3892/mmr.2016.5023. PubMed PMID: 27035229.

188. Valentijn K, Gutow AP, Troiano N, Gundberg C, Gilligan JP, Vignery A. Effects of calcitonin gene-related peptide on bone turnover in ovariectomized rats. Bone. 1997;21(3):269–74. PubMed PMID: 9276092.

189. Pfaffl MW. A new mathematical model for relative quantification in real-time RT-PCR. Nucleic acids research [Internet]. 2001;29(9). Available from: https://pubmed.ncbi.nlm.nih.gov/11328886/.

190. Wall ME, Weinhold PS, Siu T, Brown TD, Banes AJ. Comparison of cellular strain with applied substrate strain in vitro. J Biomech. 2007;40(1):173–81. doi: 10.1016/j.jbiomech.2005.10.032. PubMed PMID: 16403503.

191. Noble BS, Peet N, Stevens HY, Brabbs A, Mosley JR, Reilly GC, et al. Mechanical loading: Biphasic osteocyte survival and targeting of osteoclasts for

bone destruction in rat cortical bone. Am J Physiol , Cell Physiol. 2003;284(4):C934-43. doi: 10.1152/ajpcell.00234.2002. PubMed PMID: 12477665.

192.   Sakai D, Kii I, Nakagawa K, Matsumoto HN, Takahashi M, Yoshida S, et al. Remodeling of actin cytoskeleton in mouse periosteal cells under mechanical loading induces periosteal cell proliferation during bone formation. PLoS ONE. 2011;6(9):e24847. doi: 10.1371/journal.pone.0024847. PubMed PMID: 21935480.

193.   Sun K, Liu F, Wang J, Guo Z, Ji Z, Yao M. The effect of mechanical stretch stress on the differentiation and apoptosis of human growth plate chondrocytes. In Vitro Cell Dev Biol Anim. 2017;53(2):141–8. doi: 10.1007/s11626-016-0090-5. PubMed PMID: 27605110.

194.   Kanazawa T, Nakagami G, Minematsu T, Yamane T, Huang L, Mugita Y, et al. Biological responses of three-dimensional cultured fibroblasts by sustained compressive loading include apoptosis and survival activity. PLoS ONE. 2014;9(8):e104676. doi: 10.1371/journal.pone.0104676. PubMed PMID: 25102054.

195.   Edwards YS, Sutherland LM, Power JHT, Nicholas TE, Murray AW. Cyclic stretch induces both apoptosis and secretion in rat alveolar type II cells. FEBS Letters. 1999;448(1):127–30. doi: 10.1016/S0014-5793(99)00357-9.

196.   Boccafoschi F, Bosetti M, Sandra PM, Leigheb M, Cannas M. Effects of mechanical stress on cell adhesion: A possible mechanism for morphological changes. Cell Adh Migr. 2010;4(1):19–25. PubMed PMID: 19829055.

197.   Inoh H, Ishiguro N, Sawazaki S-I, Amma H, Miyazu M, Iwata H, et al. Uni-axial cyclic stretch induces the activation of transcription factor nuclear factor kappaB in human fibroblast cells. FASEB J. 2002;16(3):405–7. doi: 10.1096/fj.01-0354fje. PubMed PMID: 11790721.

198.   Wu Y, Zhang P, Dai Q, Yang X, Fu R, Jiang L, et al. Effect of mechanical stretch on the proliferation and differentiation of BMSCs from ovariectomized rats. Mol Cell Biochem. 2013;382(1-2):273–82. doi: 10.1007/s11010-013-1744-1. PubMed PMID: 23842623.

199.   Yan Y, Singh GK, Zhang F, Wang P, Liu W, Zhong L, et al. Comparative study of normal and rheumatoid arthritis fibroblast-like synoviocytes proliferation under cyclic mechanical stretch: Role of prostaglandin E2. Connect Tissue Res.

2012;53(3):246–54. doi: 10.3109/03008207.2011.632828. PubMed
PMID: 22149896.

200.   Sumanasinghe RD, Pfeiler TW, Monteiro-Riviere NA, Loboa EG. Expression
of proinflammatory cytokines by human mesenchymal stem cells in response to
cyclic tensile strain. J Cell Physiol. 2009;219(1):77–83. doi: 10.1002/jcp.21653.
PubMed PMID: 19089992.

201.   Saminathan A, Vinoth KJ, Wescott DC, Pinkerton MN, Milne TJ, Cao T, et al.
The effect of cyclic mechanical strain on the expression of adhesion-related
genes by periodontal ligament cells in two-dimensional culture. J Periodont Res.
2012;47(2):212–21. doi: 10.1111/j.1600-0765.2011.01423.x. PubMed
PMID: 22010885.

202.   Song G, Ju Y, Soyama H, Ohashi T, Sato M. Regulation of cyclic longitudinal
mechanical stretch on proliferation of human bone marrow mesenchymal stem
cells. Mol Cell Biomech. 2007;4(4):201–10. PubMed PMID: 18437917.

203.   Wiesner C, Le-Cabec V, El Azzouzi K, Maridonneau-Parini I, Linder S.
Podosomes in space: Macrophage migration and matrix degradation in 2D and
3D settings. Cell Adh Migr. 2014;8(3):179–91. doi: 10.4161/cam.28116. PubMed
PMID: 24713854.

204.   Vadiakas GP, Banes AJ. Verapamil decreases cyclic load-induced calcium
incorporation in ROS 17/2.8 osteosarcoma cell cultures. Matrix. 1992;12(6):439–
47. doi: 10.1016/S0934-8832(11)80088-0.

205.   Rubin CT, Lanyon LE. Regulation of bone formation by applied dynamic loads.
J Bone Joint Surg Am. 1984;66(3):397–402. PubMed PMID: 6699056.

206.   Turner CH, Forwood, Rho JY, Yoshikawa T. Mechanical loading thresholds for
lamellar and woven bone formation. J Bone Miner Res [Internet]. 1994;9(1).
Available from: https://pubmed.ncbi.nlm.nih.gov/8154314/.

207.   Michael Delaine-Smith R, Javaheri B, Helen Edwards J, Vazquez M, Rumney
RMH. Preclinical models for in vitro mechanical loading of bone-derived cells.
Bonekey Rep. 2015;4. doi: 10.1038/bonekey.2015.97. PubMed
PMID: 26331007.

208.   Mikuni-Takagaki Y, Suzuki Y, Kawase T, Saito S. Distinct responses of
different populations of bone cells to mechanical stress. Endocrinology.
1996;137(5):2028–35. doi: 10.1210/endo.137.5.8612544. PubMed
PMID: 8612544.

209. You L, Cowin SC, Schaffler MB, Weinbaum S. A model for strain amplification in the actin cytoskeleton of osteocytes due to fluid drag on pericellular matrix. J Biomech. 2001;34(11):1375–86. doi: 10.1016/S0021-9290(01)00107-5.

210. Adlerz KM, Aranda-Espinoza H, Hayenga HN. Substrate elasticity regulates the behavior of human monocyte-derived macrophages. Eur Biophys J. 2016;45(4):301–9. doi: 10.1007/s00249-015-1096-8. PubMed PMID: 26613613.

211. Pixley FJ. Macrophage Migration and Its Regulation by CSF-1. Int J Cell Biol. 2012;2012:501962. doi: 10.1155/2012/501962. PubMed PMID: 22505929.

212. Pratsinis H, Papadopoulou A, Neidlinger-Wilke C, Brayda-Bruno M, Wilke H-J, Kletsas D. Cyclic tensile stress of human annulus fibrosus cells induces MAPK activation: Involvement in proinflammatory gene expression. Osteoarthr Cartil. 2016;24(4):679–87. doi: 10.1016/j.joca.2015.11.022. PubMed PMID: 26687822.

213. Murray MY, Birkland TP, Howe JD, Rowan AD, Fidock M, Parks WC, et al. Macrophage migration and invasion is regulated by MMP10 expression. PLoS ONE. 2013;8(5):e63555. doi: 10.1371/journal.pone.0063555. PubMed PMID: 23691065.

214. Boraschi-Diaz I, Mort JS, Brömme D, Senis YA, Mazharian A, Komarova SV. Collagen type I degradation fragments act through the collagen receptor LAIR-1 to provide a negative feedback for osteoclast formation. Bone. 2018;117:23–30. doi: 10.1016/j.bone.2018.09.006. PubMed PMID: 30217615.

215. Agis H, Magdalenko M, Stögerer K, Watzek G, Gruber R. Collagen barrier membranes decrease osteoclastogenesis in murine bone marrow cultures. Clin Oral Implants Res. 2010;21(6):656–61. doi: 10.1111/j.1600-0501.2009.01888.x. PubMed PMID: 20337667.

216. Ren X, Zhou Q, Foulad D, Dewey MJ, Bischoff D, Miller TA, et al. Nanoparticulate mineralized collagen glycosaminoglycan materials directly and indirectly inhibit osteoclastogenesis and osteoclast activation. J Tissue Eng Regen Med. 2019;13(5):823–34. doi: 10.1002/term.2834. PubMed PMID: 30803152.

217. Bacáková L, Herget J, Wilhelm J. Influence of macrophages and macrophage-modified collagen I on the adhesion and proliferation of vascular smooth muscle cells in culture. Physiol Res. 1999;48(5):341–51. PubMed PMID: 10625223.

218. Arkett SA, Dixon SJ, Sims SM. Substrate influences rat osteoclast morphology and expression of potassium conductances. J Physiol (Lond). 1992;458:633–53. doi: 10.1113/jphysiol.1992.sp019438. PubMed PMID: 1338794.

219. Motiur Rahman M, Takeshita S, Matsuoka K, Kaneko K, Naoe Y, Sakaue-Sawano A, et al. Proliferation-coupled osteoclast differentiation by RANKL: Cell density as a determinant of osteoclast formation. Bone. 2015;81:392–9. doi: 10.1016/j.bone.2015.08.008.

220. Ikeda K, Takeshita S. The role of osteoclast differentiation and function in skeletal homeostasis. J Biochem. 2016;159(1):1–8. doi: 10.1093/jb/mvv112.

221. Hökfelt T, Pernow B, Wahren J. Substance P: A pioneer amongst neuropeptides. J Intern Med. 2001;249(1):27–40. PubMed PMID: 11168782.

222. Mantyh PW, DeMaster E, Malhotra A, Ghilardi JR, Rogers SD, Mantyh CR, et al. Receptor endocytosis and dendrite reshaping in spinal neurons after somatosensory stimulation. Science. 1995;268(5217):1629–32. doi: 10.1126/science.7539937. PubMed PMID: 7539937.

223. Koh Y-H, Moochhala S, Bhatia M. Activation of neurokinin-1 receptors up-regulates substance P and neurokinin-1 receptor expression in murine pancreatic acinar cells. J Cell Mol Med. 2012;16(7):1582–92. doi: 10.1111/j.1582-4934.2011.01475.x. PubMed PMID: 22040127.

224. Goto T, Tanaka T. Tachykinins and tachykinin receptors in bone. Microsc Res Tech. 2002;58(2):91–7. doi: 10.1002/jemt.10123. PubMed PMID: 12203708.

225. Liu D, Jiang L-S, Dai L-Y. Substance P and its receptors in bone metabolism. Neuropeptides. 2007;41(5):271–83. doi: 10.1016/j.npep.2007.05.003. PubMed PMID: 17655927.

226. Liu H-J, Yan H, Yan J, Li H, Chen L, Han L-R, et al. Substance P Promotes the Proliferation, but Inhibits Differentiation and Mineralization of Osteoblasts from Rats with Spinal Cord Injury via RANKL/OPG System. PLoS ONE. 2016;11(10):e0165063. doi: 10.1371/journal.pone.0165063. PubMed PMID: 27764190.

227. Levite M, Cahalon L, Hershkoviz R, Steinman L, Lider O. Neuropeptides, via specific receptors, regulate T cell adhesion to fibronectin. J Immunol. 1998;160(2):993–1000. PubMed PMID: 9551939.

228. Cumberbatch MJ, Chizh BA, MaxHeadley P. Modulation of excitatory amino acid responses by tachykinins and selective tachykinin receptor agonists in the

rat spinal cord. Br J Pharmacol. 1995;115(6):1005–12. doi: 10.1111/j.1476-5381.1995.tb15911.x.

229. Erdös EG, Skidgel RA. Neutral endopeptidase 24.11 (enkephalinase) and related regulators of peptide hormones. FASEB J. 1989;3(2):145–51. PubMed PMID: 2521610.

230. Bullock CM, Wookey P, Bennett A, Mobasheri A, Dickerson I, Kelly S. Peripheral calcitonin gene-related peptide receptor activation and mechanical sensitization of the joint in rat models of osteoarthritis pain. Arthritis & rheumatology (Hoboken, N.J.). 2014;66(8):2188–200. doi: 10.1002/art.38656. PubMed PMID: 24719311.

231. Cueille C, Birot O, Bigard X, Hagner S, Garel J-M. Post-transcriptional regulation of CRLR expression during hypoxia. Biochem Biophys Res Commun. 2005;326(1):23–9. doi: 10.1016/j.bbrc.2004.10.205. PubMed PMID: 15567147.

232. Nikitenko LL, Smith DM, Bicknell R, Rees MCP. Transcriptional regulation of the CRLR gene in human microvascular endothelial cells by hypoxia. FASEB J. 2003;17(11):1499–501. doi: 10.1096/fj.02-0993fje. PubMed PMID: 12824306.

233. Bullock CM, Kelly S. Calcitonin gene-related peptide receptor antagonists: Beyond migraine pain--a possible analgesic strategy for osteoarthritis? Curr Pain Headache Rep. 2013;17(11):375. doi: 10.1007/s11916-013-0375-2. PubMed PMID: 24068339.

234. Kobayashi Y, Hashimoto F, Miyamoto H, Kanaoka K, Miyazaki-Kawashita Y, Nakashima T, et al. Force-induced osteoclast apoptosis in vivo is accompanied by elevation in transforming growth factor beta and osteoprotegerin expression. J Bone Miner Res. 2000;15(10):1924–34. doi: 10.1359/jbmr.2000.15.10.1924. PubMed PMID: 11028444.

235. Schaeffer C, Thomassin L, Rochette L, Connat JL. Apoptosis induced in vascular smooth muscle cells by oxidative stress is partly prevented by pretreatment with CGRP. Ann N Y Acad Sci. 2003;1010:733–7. PubMed PMID: 15033819.

236. Gherardini J, Uchida Y, Hardman JA, Chéret J, Mace K, Bertolini M, et al. Tissue-resident macrophages can be generated de novo in adult human skin from resident progenitor cells during substance P-mediated neurogenic inflammation ex vivo. PLoS ONE. 2020;15(1):e0227817. doi: 10.1371/journal.pone.0227817.

237. Peyton KJ, Liu X-m, Durante W. Prolonged Cyclic Strain Inhibits Human Endothelial Cell Growth. Front Biosci (Elite Ed). 2016;8:205–12. PubMed PMID: 26709656.

238. Connat JL, Schnüriger V, Zanone R, Schaeffer C, Gaillard M, Faivre B, et al. The neuropeptide calcitonin gene-related peptide differently modulates proliferation and differentiation of smooth muscle cells in culture depending on the cell type. Regul Pept. 2001;101(1-3):169–78. PubMed PMID: 11495693.

239. Spitsin S, Meshki J, Winters A, Tuluc F, Benton TD, Douglas SD. Substance P-mediated chemokine production promotes monocyte migration. J Leukoc Biol. 2017;101(4):967–73. doi: 10.1189/jlb.1AB0416-188RR. PubMed PMID: 28366881.

240. Ma J, Zhao D, Wu Y, Xu C, Zhang F. Cyclic stretch induced gene expression of extracellular matrix and adhesion molecules in human periodontal ligament cells. Arch Oral Biol. 2015;60(3):447–55. doi: 10.1016/j.archoralbio.2014.11.019. PubMed PMID: 25541636.

241. Słoniecka M, Le Roux S, Zhou Q, Danielson P. Substance P Enhances Keratocyte Migration and Neutrophil Recruitment through Interleukin-8. Mol Pharmacol. 2016;89(2):215–25. doi: 10.1124/mol.115.101014. PubMed PMID: 26646648.

242. Meléndez GC, Manteufel EJ, Dehlin HM, Register TC, Levick SP. Non-human primate and rat cardiac fibroblasts show similar extracellular matrix-related and cellular adhesion gene responses to substance P. Heart Lung Circ. 2015;24(4):395–403. doi: 10.1016/j.hlc.2014.11.015. PubMed PMID: 25550118.

243. Sung CP, Arleth AJ, Aiyar N, Bhatnagar PK, Lysko PG, Feuerstein G. CGRP stimulates the adhesion of leukocytes to vascular endothelial cells. Peptides. 1992;13(3):429–34. PubMed PMID: 1326102.

244. Malon JT, Cao L. Calcitonin gene-related peptide contributes to peripheral nerve injury-induced mechanical hypersensitivity through CCL5 and p38 pathways. J Neuroimmunol. 2016;297:68–75. doi: 10.1016/j.jneuroim.2016.05.003. PubMed PMID: 27397078.

245. T Dennis, A Fournier, A Cadieux, F Pomerleau, F B Jolicoeur, S St Pierre, et al. hCGRP8-37, a calcitonin gene-related peptide antagonist revealing calcitonin gene-related peptide receptor heterogeneity in brain and periphery. J Pharmacol Exp Ther. 1990;254(1):123–8. PubMed PMID: 2164085.

246. Marquez de Prado B, Hammond DL, Russo AF. Genetic Enhancement of Calcitonin Gene-Related Peptide-Induced Central Sensitization to Mechanical Stimuli in Mice. The Journal of Pain. 2009;10(9):992–1000. doi: 10.1016/j.jpain.2009.03.018.

247. Seabrook GR, Shepheard SL, Williamson DJ, Tyrer P, Rigby M, Cascieri MA, et al. L-733,060, a novel tachykinin NK1 receptor antagonist; effects in [Ca2+]i mobilisation, cardiovascular and dural extravasation assays. European Journal of Pharmacology. 1996;317(1):129–35. doi: 10.1016/S0014-2999(96)00706-6.

248. Rupniak NMJ, Carlson E, Boyce S, Webb JK, Hill RG. Enantioselective inhibition of the formalin paw late phase by the NK1 receptor antagonist L-733,060 in gerbils. Pain. 1996;67(1):189–95. doi: 10.1016/0304-3959(96)03109-0.

249. Hamity MV, White SR, Hammond DL. Effects of neurokinin-1 receptor agonism and antagonism in the rostral ventromedial medulla of rats with acute or persistent inflammatory nociception. Neuroscience. 2010;165(3):902–13. doi: 10.1016/j.neuroscience.2009.10.064.

250. Fu D, Qin K, Yang S, Lu J, Lian H, Zhao D. Proper mechanical stress promotes femoral head recovery from steroid-induced osteonecrosis in rats through the OPG/RANK/RANKL system. BMC Musculoskelet Disord. 2020;21(1):45. doi: 10.1186/s12891-020-03301-6.

251. Grimm S, Walter C, Pabst A, Goldschmitt J, Wehrbein H, Jacobs C. Effect of compressive loading and incubation with clodronate on the RANKL/OPG system of human osteoblasts. J Orofac Orthop. 2015;76(6):531–42. doi: 10.1007/s00056-015-0316-2. PubMed PMID: 26446504.

252. Jianru YI, MeiLe LI, Yang Y, Zheng W, Yu LI, Zhao Z. Static compression regulates OPG expression in periodontal ligament cells via the CAMK II pathway. J Appl Oral Sci. 2015;23(6):549–54. doi: 10.1590/1678-775720150156. PubMed PMID: 26814456.

253. Kim CH, Kim KH, Jacobs CR. Effects of high frequency loading on RANKL and OPG mRNA expression in ST-2 murine stromal cells. BMC Musculoskelet Disord. 2009;10:109. doi: 10.1186/1471-2474-10-109. PubMed PMID: 19728893.

254. Spatz JM, Wein MN, Gooi JH, Qu Y, Garr JL, Liu S, et al. The Wnt Inhibitor Sclerostin Is Up-regulated by Mechanical Unloading in Osteocytes in Vitro. J. Biol. Chem. 2015;290(27):16744–58. doi: 10.1074/jbc.M114.628313.

255. Yang J-H, Sakamoto H, Xu EC, Lee RT. Biomechanical Regulation of Human Monocyte/Macrophage Molecular Function. The American Journal of Pathology. 2000;156(5):1797–804. doi: 10.1016/S0002-9440(10)65051-1.

256. Hammerschmidt S, Kuhn H, Sack U, Schlenska A, Gessner C, Gillissen A, et al. Mechanical stretch alters alveolar type II cell mediator release toward a proinflammatory pattern. Am J Respir Cell Mol Biol. 2005;33(2):203–10. doi: 10.1165/rcmb.2005-0067OC. PubMed PMID: 15947422.

257. Shan S, Fang B, Zhang Y, Wang C, Zhou J, Niu C, et al. Mechanical stretch promotes tumoricidal M1 polarization via the FAK/NF-κB signaling pathway. FASEB J. 2019;33(12):13254–66. doi: 10.1096/fj.201900799RR. PubMed PMID: 31539281.

258. Chu S-Y, Chou C-H, Huang H-D, Yen M-H, Hong H-C, Chao P-H, et al. Mechanical stretch induces hair regeneration through the alternative activation of macrophages. Nat Commun. 2019;10(1):1524. doi: 10.1038/s41467-019-09402-8. PubMed PMID: 30944305.

259. Dixon D-L, Barr HA, Bersten AD, Doyle IR. Intracellular storage of surfactant and proinflammatory cytokines in co-cultured alveolar epithelium and macrophages in response to increasing CO_2 and cyclic cell stretch. Exp Lung Res. 2008;34(1):37–47. doi: 10.1080/01902140701807928. PubMed PMID: 18205076.

260. Kumar A, Lnu S, Malya R, Barron D, Moore J, Corry DB, et al. Mechanical stretch activates nuclear factor-kappaB, activator protein-1, and mitogen-activated protein kinases in lung parenchyma: Implications in asthma. FASEB J. 2003;17(13):1800–11. doi: 10.1096/fj.02-1148com. PubMed PMID: 14519659.

261. Lee S-K, Min K-S, Kim Y, Jeong G-S, Lee S-H, Lee H-J, et al. Mechanical stress activates proinflammatory cytokines and antioxidant defense enzymes in human dental pulp cells. J Endod. 2008;34(11):1364–9. doi: 10.1016/j.joen.2008.08.024. PubMed PMID: 18928848.

262. Kalaitzoglou E, Griffin TM, Humphrey MB. Innate Immune Responses and Osteoarthritis. Curr Rheumatol Rep. 2017;19(8):45. doi: 10.1007/s11926-017-0672-6. PubMed PMID: 28718060.

263. Wang P, Guan PP, Guo C, Zhu F, Konstantopoulos K, Wang ZY. Fluid shear stress-induced osteoarthritis: Roles of cyclooxygenase-2 and its metabolic products in inducing the expression of proinflammatory cytokines and matrix metalloproteinases. FASEB J [Internet]. 2013;27(12). Available from: https://pubmed.ncbi.nlm.nih.gov/23964078/.

264. Kim J-H, Lee G, Won Y, Lee M, Kwak J-S, Chun C-H, et al. Matrix cross-linking–mediated mechanotransduction promotes posttraumatic osteoarthritis. Proceedings of the National Academy of Sciences. 2015;112(30):9424–9. doi: 10.1073/pnas.1505700112.

265. Spyropoulou A, Karamesinis K, Basdra EK. Mechanotransduction pathways in bone pathobiology. Biochimica et Biophysica Acta (BBA) - Molecular Basis of Disease. 2015;1852(9):1700–8. doi: 10.1016/j.bbadis.2015.05.010.

266. Chery DR, Han B, Li Q, Zhou Y, Heo S-J, Kwok B, et al. Early changes in cartilage pericellular matrix micromechanobiology portend the onset of post-traumatic osteoarthritis. Acta Biomaterialia. 2020;111:267–78. doi: 10.1016/j.actbio.2020.05.005.

267. Manferdini C, Paolella F, Gabusi E, Silvestri Y, Gambari L, Cattini L, et al. From osteoarthritic synovium to synovial-derived cells characterization: Synovial macrophages are key effector cells. Arthritis Res Ther. 2016;18(1):1697. doi: 10.1186/s13075-016-0983-4.

268. Bondeson J, Wainwright SD, Lauder S, Amos N, Hughes CE. The role of synovial macrophages and macrophage-produced cytokines in driving aggrecanases, matrix metalloproteinases, and other destructive and inflammatory responses in osteoarthritis. Arthritis Res Ther. 2006;8(6):R187. doi: 10.1186/ar2099.

269. Wang L, Shi X, Zhao R, Halloran BP, Clark DJ, Jacobs CR, et al. Calcitonin-gene-related peptide stimulates stromal cell osteogenic differentiation and inhibits RANKL induced NF-kappaB activation, osteoclastogenesis and bone resorption. Bone. 2010;46(5):1369–79. doi: 10.1016/j.bone.2009.11.029. PubMed PMID: 19962460.

9 Publication

Muschter D*, Beiderbeck A-S*, Späth T, Kirschneck C, Schröder A, Grässel S. Sensory Neuropeptides and their Receptors Participate in Mechano-Regulation of Murine Macrophages. Int J Mol Sci. 2019;20(3). doi: 10.3390/ijms20030503. PubMed PMID: 30682804.

* shared first authorship

10 Declaration of authorship

I, Anna-Sophie Beiderbeck, born on January 6, 1994 in Regensburg, hereby declare that the thesis submitted is my own unaided work.

I have not used any sources other than those listed in the bibliography and identified as references. In particular, I have not enlisted the non gratuitous assistance of consulting services.

I further declare that I have not submitted this thesis at any other institution in order to obtain a degree.

Ich, Anna-Sophie Beiderbeck, geboren am 06.01.1994 in Regensburg, erkläre hiermit, dass ich die vorliegende Arbeit ohne unzulässige Hilfe Dritter und ohne Benutzung anderer als der angegebenen Hilfsmittel angefertigt habe.

Die aus anderen Quellen direkt oder indirekt übernommenen Daten und Konzepte sind unter Angabe der Quelle gekennzeichnet. Insbesondere habe ich nicht die entgeltliche Hilfe von Vermittlungs- bzw. Beratungsdiensten (Promotionsberater oder andere Personen) in Anspruch genommen.

Die Arbeit wurde bisher weder im In- noch im Ausland in gleicher oder ähnlicher Form einer anderen Prüfungsbehörde vorgelegt.

place, date/ Ort, Datum   signature of doctoral candidate/
                                      Unterschrift des Promovenden

11 Acknowledgments

12 Curriculum Vitae